SCATTERING OF SH-WAVES BY CYLINDERS OF ARBITRARY CROSS-SECTION -- SOLUTION BY THE BOUNDARY INTEGRAL EQUATION METHOD

by

NABİ ÖZGÜÇ

Submitted to the Faculty of Engineering
in partial fulfillment of
the requirements for the degree of

MASTER OF SCIENCE
in
MECHANICAL ENGINEERING

Boğaziçi University
1981

ABSTRACT

The scattering of steady-state anti-plane shear waves (SH waves) from arbitrarily shaped inclusions in an infinite medium is described by means of integral equations expressed in terms of displacement fields. The problem is examined for the two dimensional case where an inclusion fixed in space like a cavity or a rigid body with material constants different from the surrounding medium is taken as the scatterer.The resulting singular integral equations are solved numerically. Both near and far-field solutions pertaining to circular,elliptical and rectangular cross sections are obtained.All the results are presented in graphical form and are found to be in good agreement compared with the known exact solutions.

ÖZET

Skaler kayma dalgalarının (SH dalgaları) sonsuz uzaydaki lâlettayin kesitli şekillerden saçılmaları, yerdeğiştirme alanının integral denklem halinde ifadesiyle tarif edilmiştir.Problem iki boyutta,boşluk,veya malzeme sabitleri içinde bulundukları ortamdan farklı, hareket etmeyen rijit iç cisimler için incelenmiştir. Ortaya çıkan tekil integral denklemler sayısal olarak çözülmüştür.Dairesel,eliptik ve dörtgenel kesitli şekiller için yakın ve uzak bölge çözümleri elde edilmiştir. Bütün sonuçlar,şekiller halinde gösterilmiş ve bilinen kesin çözümlerle uyuştuğu görülmüştür.

TABLE OF CONTENTS

LIST OF SYMBOLS

C	wave propagation speed
h_j	length of the j-th interval
$G, G(\underline{r},\underline{r}')$	Green's function
$K(\underline{r},\underline{r}')$	kernel of the integral equation
J_o, J_1	Bessel functions of the first kind
Y_o, Y_1	Bessel functions of the second kind
H_o, H_1	zeroth and first order Hankel functions of the first kind
k	wave number
$\underline{n}'$	outer normal to the boundary
$\underline{r}$	position vector of the observation point
$\underline{r}'$	position vector of the source point
$\underline{r}'_{J+}$, $\underline{r}'_{J-}$	position vectors of the end points of the j-th interval
$\underline{r}'_J$	position vector of the j-th nodal point
$\underline{r}'_{J_1}, \ldots, \underline{r}'_{J_4}$	position vectors of the integration points associated with the Gaussian integration
$\hat{r}$	distance between the source and observing points
$\hat{r}_{J_1 \ell}, \ldots, \hat{r}_{J_4 \ell}$	distance between the l-th nodal and the 1-st,...,4-th integration point on the j-th interval
S	boundary of the cross section of an infinite cylinder
n	number of interval points
U	displacement

$U^{(i)}, U^{(s)}, U^{(t)}$	displacement due to the incident, scattered, and total field respectively
$U'^{(i)}, U'^{(s)}, U'^{(t)}$	displacement at the boundary due to the incident, scattered, and total field respectively
x'	x coordinate of the points on the boundary
λ, μ	Lamé constants
ρ	mass density
σ_n	normal stress
$\sigma'^{(i)}, \sigma'^{(s)}, \sigma'^{(t)}$	stress at the boundary due to the incident, scattered, and total field respectively
Δ_J	j-th interval
w	circular frequency
$w_1, \ldots, w_4$	weighting coefficients associated with the Gaussian integration
θ, θ'	angles that $\underline{r}$ and $\underline{r}'$ make with the x-axis respectively
λ	wavelength

CHAPTER I

INTRODUCTION

In an unbounded homogeneous medium, waves propagate without interruption at a constant speed and along a fixed path. However, with the insertion of an obstacle in the medium, the path of the propagation is changed, and the obstacle, when excited by the otherwise undisturbed incident wave, acts as a secondary source emitting waves outward from itself. The deviation of the waves from their original paths is known as diffraction, and the radiation of the secondary waves from the obstacle is called scattering. In an elastic medium, the obstacle may be in the form of a cavity, or a rigid body with elastic moduli and density different from that of the medium.

Scattering theory is used in many branches of physics and mechanics. The diffraction of waves is certainly important in seismology and oil technology and has recently come to be appreciated in connection with the non-destructive evaluation of materials, NDE. In NDE, the scattered waveform is used to identify the shape and the size of the scatterer which can be a void, an inclusion or a crack. This is known as the inverse problem.

In this work, the method of integral equations is used in solving the diffraction problem for the exterior region. From a theoretical point of view, this method is more direct and basic than other methods such as normal modes, as it is based on the Helmholtz and Kirchoff's mathematical interpretation of Huygen's principle[5,9]. Helmholtz and Kirchoff

integral formulas yield mathematically the disturbance at time "t" if the wave velocity "c" and the wave form at time "t_o" are known.

In the usual treatment of the elastodynamic problems one has to find the solution to the equation of motion satisfying certain conditions known as boundary and initial conditions.However,in the method of integral equation,the equation of motion,using the Helmholtz-Kirchoff formula is transformed into an integral equation which relates the wave field at any point inside the medium to the known quantities on the boundary,hence incorporating the boundary conditions directly.According to Huygen's principle the points on the boundary of a scatterer,upon the impinging of an incident wave,act like secondary sources emitting the scattered waves.Therefore,once the wave field on the boundary is known one can precisely determine the scattered field making use of these integral equations.

Previous studies of wave scattering have been usually carried out using the method of separation of variables. The method,however restricts the shape of the scatterer to simple geometries such that they can be expressed conveniently in separable coordinates.This restriction may be removed by the integral equation formulation;however such an approach does not facilitate the analytical solution,that is the problem formulated in terms of integral equations should be solved by using numerical techniques. One such effective procedure is to approximate the integrals by a finite sum and then calculate the unknown quantities at many discrete points by solving a system of algebraic equations [2,3]. To cite a related example : the scattering of steady acoustic waves,formulated as an integ-

ral equation, in terms of the velocity potential was solved by Banaugh and Goldsmith[4] using finite difference methods where the boundary is described parametrically.

The key feature of the method lies in the fact that o only the surface of the body is to be discretized. An additional advantage of this procedure is the reduction of the dimensionality of the problem by one. Hence the complete integral formulation with its numerical approximation has the distinct advantage that the method is not restricted to geometric configurations to which the method of separetion of variables may be applied.

In the formulation that follows, the integral representation for the displacement is taken as the starting point[5,6]. This choice leads respectively to Fredholm integral equations of the second and first kinds for the cavity and rigid inclusion problems. These integral equations are solved in the spirit of the aforementioned numerical approximation. The solutions provide the unprescribed values ($U^{(s)}$ for the cavity and $\partial U^{(s)}/\partial n'$ for the rigid inclusion, where $U^{(s)}$ is the displacement due to the scattered field and $\underline{n}'$ is the outer normal to the boundary). The substitution of these values in the integral representation for the scattered field enables one to calculate $U^{(s)}$ at any point in space. Also the numerical differentiation of $U^{(s)}$ with respect to θ, the polar angle, yields the tangential stress on the boundary in the case of a cavity.

In this work, we present the near and far-field results for a cavity and a rigid inclusion. Chapter 2 reviews the elasticity equations mainly for anti-plane strain case along with SH waves. In chapter 3, the integral equation

representation for the scattering problem is developed and the numerical method employed is discussed.In chapter 4,the formulation of the problem for various cases is given and some specific problems are solved.Results pertaining to circular,elliptical and rectangular geometries are presented in graphical form.

CHAPTER 2

EQUATIONS OF LINEAR ELASTICITY

This chapter briefly discusses the reduction of the Navier's equation to a scalar wave equation in the case of anti-plane strain and describes the nature of the associated waves.

In the absence of body forces, the linearized equations of motion in terms of the displacements (Navier's equation) for a homogeneous, isotropic elastic medium are[1],

$$(\lambda+\mu)\,\nabla(\nabla\cdot\underline{U})+\mu\nabla^2\underline{U}=\rho\frac{\partial^2 U}{\partial t^2} \tag{2.1}$$

where λ and μ are the Lame's constants, and ρ the mass density of the medium.

The solution to the scattering problem requires the solution of the above equation which is valid over a region V, satisfying the boundary conditions in terms of displacements and/or tractions prescribed over a discontinuity surface of either a solid inclusion or a cavity (Fig.2-1).

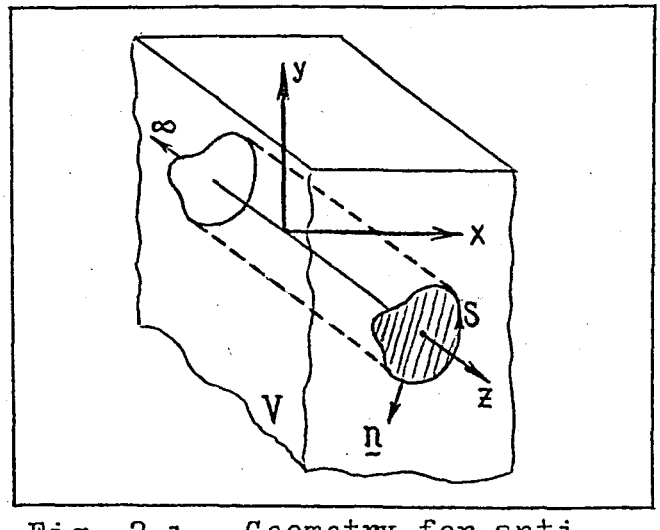

Fig. 2-1 Geometry for anti-plane strain

In two dimensional problems, components of the stress tensor are independent of one of the coordinates, say z, along which the cross sectional area of the body is constant (Fig. 2-1) .A deformation described by a displacement field of the form , [1] ,

$$U_x(x,y,t) = U_y(x,y,t) = 0$$
$$U_z = U_z(x,y,t)$$

is called an anti-plane shear deformation, where U_x , U_y and U_z, referring to the usual cartesian coordinates x,y,z , are the components of the displacement vector $\underline{U}$. Denoting the only non-zero component U_z of $\underline{U}$ by U, Eq.(2.1) takes the form

$$\nabla^2 U(x,y,t) = \frac{1}{c^2}\frac{\partial^2 U(x,y,t)}{\partial t^2} \tag{2.2}$$

where $c = \sqrt{\frac{\mu}{\rho}}$ is the velocity of propagation of the wave.

In the case of anti-plane strain, the only non-vanishing components of the stress tensor are σ_{xz} and σ_{yz} , and from the Hooke's law

$$\underline{\underline{\sigma}} = \lambda(\nabla\cdot\underline{U})\,\underline{\underline{I}} + \mu(\nabla\underline{U} + \underline{U}\nabla)$$

they can be easily determined to be

$$\sigma_{xz} = \mu\frac{\partial U}{\partial x} \quad , \quad \sigma_{yz} = \mu\frac{\partial U}{\partial y} \quad .$$

Considering only harmonic waves with a circular frequency of w, the displacement and stress fields can be written as

$$U(x,y,t) = U(x,y,w)\,e^{-iwt}$$
$$\sigma(x,y,t) = \sigma(x,y,w)\,e^{-iwt} \tag{2.3}$$

To simplify the writing we will suppress the time factor e^{-iwt} in the rest of this work. Substituting Eq.(2.3) into Eq.(2.2) we get

$$\nabla^2 U + k^2 U = 0 \tag{2.4}$$

where $k = \frac{w}{c}$ is the wave number. Eq.(2.4) is known as the Helmholtz equation.

Under the conditions of anti-plane strain, the dilatation, $\nabla \cdot \underline{U}$, is zero, and the waves are only of rotational (s waves) type. Since the displacement is always papallel to the axis of the scatterer, z-axis, which for convenience can be taken as lying in a horizontal plane, waves of anti-plane strain are also known as SH waves. The boundary conditions assoüiated with Eq.(2.4) are

$$\frac{\partial U}{\partial n} = 0 \tag{2.5}$$

for a cavity, and

$$U = 0 \tag{2.6}$$

for a rigid inclusion.

CHAPTER 3

FORMULATION OF THE INTEGRAL EQUATIONS

Application of the separation of variables method to the scattering problems is limited by the geometry of the scatterer since the equations of motion are not separable in all coordinates.However,this restriction can be removed by the use of the integral equation method where the governing equations of motion are transformed into integral equations using the Helmholtz's formulas.Since the integrals involved are defined over the boundaries of the scatterer,the method incorporates the boundary conditions automatically.

In this chapter a derivation of the Helmholtz's interior and exterior formulas and their application to the scattering of SH waves by prismatic cylinders of arbitrary cross section will be presented.We will also outline the numerical procedure employed in solving the resulting integral equations.

3.1 HELMHOLTZ FORMULAS

The Green's identity for two functions U and G defined in a region V bounded by the surface A is [8]

$$\iiint_V (U\nabla^2 G - G\nabla^2 U)\,dV = \iint_A (U \frac{\partial G}{\partial n} - G \frac{\partial U}{\partial n})\,dA \qquad (3.1)$$

where $\frac{\partial}{\partial n}$ denotes differentiation along the outward normal $\underline{n}$ to the surface A.

Consider the case where the functions $U(\underline{r})$ and $G(\underline{r},\underline{r}')$

satisfying the following Helmholtz equations respectively

$$\nabla^2 U(\underline{r}) + k^2 U(\underline{r}) = 0 \tag{3.2}$$

$$(\nabla^2 + k^2)G(\underline{r},\underline{r}') = (\nabla^2 + k^2)G(\underline{r}',\underline{r}) = -\delta(\underline{r} - \underline{r}') \tag{3.3}$$

where $\underline{r}(x,y,z)$ and $\underline{r}'(x',y',z')$ are the position vectors of the "observation" or "receiver",and "source" points respectively, ∇^2 is the Laplacian operator with respect to the "observation coordinates" x,y,z and $\delta(\underline{r} - \underline{r}')$ is the Delta-Dirac function.

Multiplying Eq.(3.2) by $G(\underline{r},\underline{r}')$,Eq.(3.3) by $U(\underline{r})$ and subtracting we get

$$G\nabla^2 U - U\nabla^2 G = U\,\delta(\underline{r} - \underline{r}') \tag{3.4}$$

If Eq.(3.4) is integrated over the volume V bounded by the surface A (Fig.3-1) we obtain

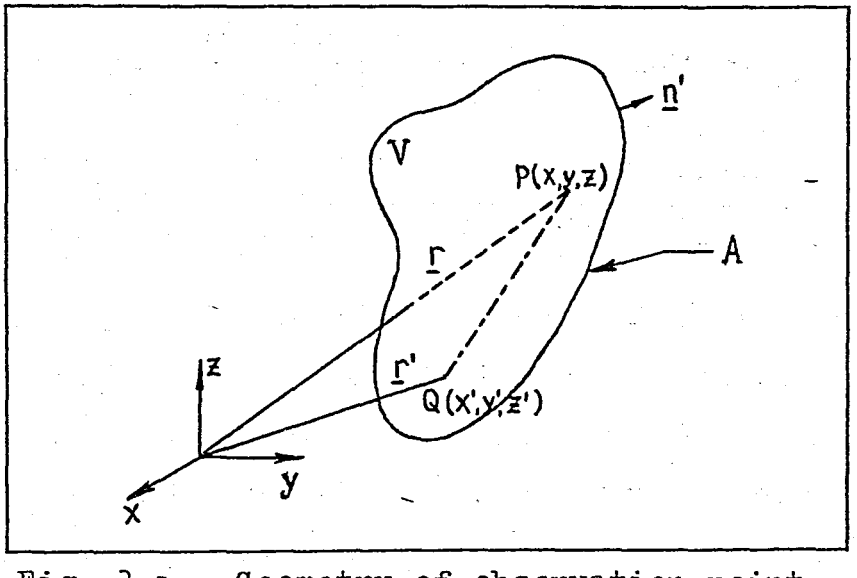

Fig. 3-1 Geometry of observation point $P(\underline{r})$ and source point $Q(\underline{r}')$ for interior problem

$$\iiint_V \left[G(\underline{r},\underline{r}')\nabla'^2 U(\underline{r}') - U(\underline{r}')\nabla'^2 G(\underline{r},\underline{r}')\right] dV' = \iiint_V U(\underline{r}')\,\delta(\underline{r}-\underline{r}')\,dV'$$

where the integration is with respect to the source coor-

dinates. Employing the Green's identity in the above equation we get

$$\iint_A \left[G(\underline{r},\underline{r}') \frac{\partial U(\underline{r}')}{\partial n'} - U(\underline{r}') \frac{\partial G(\underline{r},\underline{r}')}{\partial n'} \right] dA' = \iiint_V U(\underline{r}')\, \delta(\underline{r}-\underline{r}')\, dA' \qquad (3.5)$$

Using the following property of the delta function

$$\iiint_V f(\underline{r}')\, \delta(\underline{r} - \underline{r}')\, dV' = \begin{cases} 0 & \underline{r} \text{ outside } V \\ f(\underline{r}) & \underline{r} \text{ inside } V \end{cases}$$

in Eq.(3.5) we have

$$\iint_A \left[G(\underline{r},\underline{r}') \frac{\partial U(\underline{r}')}{\partial n'} - U(\underline{r}') \frac{\partial G(\underline{r},\underline{r}')}{\partial n'} \right] dA' = \begin{cases} 0 & \underline{r} \text{ outside } A \\ U(\underline{r}) & \underline{r} \text{ inside } A \end{cases} \qquad (3.6)$$

The function $G(\underline{r},\underline{r}')$ is known as the Green's function for the steady-state wave equation, Eq.(3.3). In the three-dimensional case the Green's function has the form [8]

$$G(\underline{r},\underline{r}') = \frac{e^{ik|\underline{r}-\underline{r}'|}}{4\pi|\underline{r}-\underline{r}'|} = \frac{e^{ik\hat{r}}}{4\pi\hat{r}} = G(\underline{r},\underline{r}')$$

for an unbounded region where

$$\hat{r} = |\underline{r} - \underline{r}'| = \sqrt{(x-x')^2 + (y-y')^2 + (z-z')^2}$$

Equation (3.6) is known as the Helmholtz first(interior) formula and is applicable in the case when all the singularities of the function $U(\underline{r})$ lie outside the surface A. If on the other hand, all the singularities of $U(\underline{r})$ lie within a closed surface A, we can apply the Green's identity to the region V bounded internally by A and externally by another closed surface B, such as a sphere centered at the origin and with a large radius R, (Fig.3-2). The surface in Eq.(3.1) is now composed of A + B. Following the same line of reasoning leading to Eq.(3.6) we get

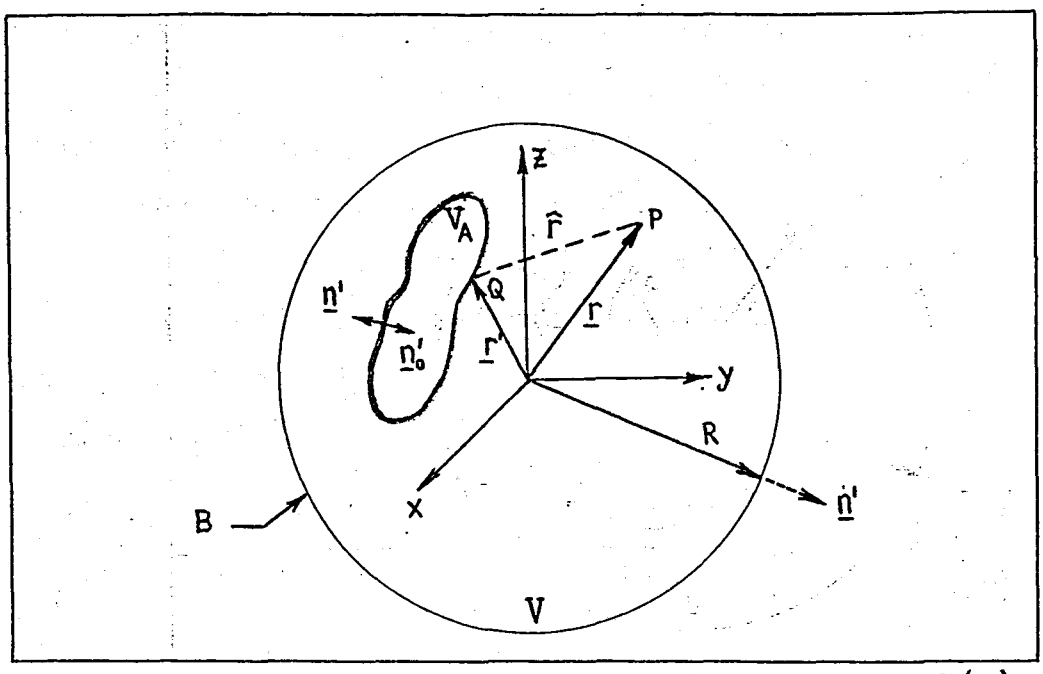

Fig. 3-2 Geometry for the observation point $P(\underline{r})$ and source point $Q(\underline{r}')$ for the exterior problem

$$\iint_{A+B}\left[G(\underline{r},\underline{r}')\frac{\partial U(\underline{r}')}{\partial n'} - U(\underline{r}')\frac{\partial G(\underline{r},\underline{r}')}{\partial n'}\right] dA' = \begin{cases} 0 & \underline{r} \text{ outside } V \\ U(\underline{r}) & \underline{r} \text{ inside } V \end{cases} \tag{3.7}$$

On the large surface B, $\underline{r}' = \underline{R}$ and $\dfrac{\partial}{\partial n'} = \dfrac{\partial}{\partial R}$, also

$dA = R^2 \sin\theta \, d\theta \, d\phi$. Thus the integral in Eq.(3.7), over the surface B, becomes

$$\iint_B\left[G\frac{\partial U}{\partial R} - U\frac{\partial G}{\partial R}\right] dA' = \frac{1}{4\pi}\int_0^{\pi}\int_0^{2\pi} e^{ikR}\left[r'\left(\frac{\partial U}{\partial r'} - ikU\right) + U\right]_{r'=R} \sin\theta d\theta d\phi$$

In the limit as R approaches to infinity this integral vanishes if, for any finite value M,

$$\begin{aligned} |rU| &< M, \quad \text{as } r \longrightarrow \infty \\ r\left(\frac{\partial U}{\partial r} - ikU\right) &\longrightarrow 0, \quad \text{as } r \longrightarrow \infty \end{aligned} \tag{3.8}$$

for all values of angular coordinates θ and ϕ. Equations (3.8) are known as the Sommerfeld radiation conditions

which the Helmholtz equation in unbounded regions must satisfy for the uniqueness of its solution. On physical grounds radiation conditions guarantee that there is no backward radiation from infinity.

Thus, for a function $U(\underline{r})$ being regular in V, and satisfying the radiation conditions given above, its value at an observing point is given by the surface integral over the source point as

$$\iint_A \left[G(\underline{r},\underline{r}') \frac{\partial U(\underline{r}')}{\partial n_o'} - U(\underline{r}') \frac{\partial G(\underline{r},\underline{r}')}{\partial n_o'} \right] dA' = \begin{cases} 0 & \underline{r} \text{ outside } V \\ U(\underline{r}) & \underline{r} \text{ inside } V \end{cases}$$

As shown in Fig.3-2, the unit normal $\underline{n}_o'$ is away from the region V, and is an inward normal to the closed surface A. If an outer normal $\underline{n}'$ to A is used, we have

$$\iint_A \left[U(\underline{r}') \frac{\partial G(\underline{r},\underline{r}')}{\partial n'} - G(\underline{r},\underline{r}') \frac{\partial U(\underline{r}')}{\partial n'} \right] dA' = \begin{cases} U(\underline{r}) & \underline{r} \text{ outside } A \\ 0 & \underline{r} \text{ inside } A \end{cases} \tag{3.9}$$

This is the Helmholtz second(exterior) formula.

If the surface A is a cylindrical surface with its generics parallel to the z-axis, and if $U(\underline{r}')$ and $\partial U(\underline{r}')/\partial n'$ are independent of the coordinate z, the waves $U(\underline{r})$ in the region V are also independent of z and the problem reduces to a two dimensional one for which the Green's function is given by [8]

$$G(\underline{r},\underline{r}') = \frac{i}{4} H_o^{(1)}(k|\underline{r}-\underline{r}'|) = \frac{i}{4} H_o^{(1)}(k\hat{r}) \tag{3.10}$$

where $\underline{r}(x,y)$ and $\underline{r}'(x',y')$ are the position vectors of the observing point and source point respectively. $H_o^{(1)}(k\hat{r})$ is the zeroth order Hankel function of the first kind and $i=\sqrt{-1}$.

For two dimensional interior problems, in view of Eq. (3.10), Eq. (3.6) can be written as

$$\frac{i}{4}\int_S \left[H_o^{(1)}(k\hat{r}) \frac{\partial U(\underline{r}')}{\partial n'} - U(\underline{r}') \frac{\partial H_o^{(1)}(k\hat{r})}{\partial n'} \right] ds' = \begin{cases} U(\underline{r}) & \underline{r} \text{ inside } S \\ 0 & \underline{r} \text{ outside } S \end{cases} \tag{3.11}$$

where S is a closed curve, the circumference of the cross section of the cylinder, with element length ds', and $\frac{\partial}{\partial n'}$ is the derivative along the outer normal to curve S. Similarly, the exterior formula, Eq. (3.9), reads

$$\frac{i}{4}\int_S \left[U(\underline{r}') \frac{\partial H_o^{(1)}(k\hat{r})}{\partial n'} - H_o^{(1)}(k\hat{r}) \frac{\partial U(\underline{r}')}{\partial n'} \right] ds' = \begin{cases} U(\underline{r}) & \underline{r} \text{ outside } S \\ 0 & \underline{r} \text{ inside } S \end{cases} \tag{3.12}$$

where U satisfies the following radiation conditions [1]

$$\begin{aligned} &\sqrt{r}\, U \longrightarrow 0, && \text{as } r \longrightarrow \infty \\ &\sqrt{r}\, \left(\frac{\partial U}{\partial r} - ikU \right) \longrightarrow 0, && \text{as } r \longrightarrow \infty \end{aligned} \tag{3.13}$$

Equations (3.11) and (3.12) are also known as Weber's interior and exterior formulas respectively.

3.2 INTEGRAL EQUATION REPRESENTATIONS

The total wave field, $U^{(t)}$, in a medium is composed of two parts; the incident wave, $U^{(i)}$, and the scattered wave, $U^{(s)}$ i.e.,

$$U^{(t)} = U^{(i)} + U^{(s)} \tag{3.14}$$

where each wave function satisfies the Helmholtz formulas (3.11) or (3.12).

Applying Weber's exterior formula, Eq. (3.12), to scat-

tered waves, $U^{(s)}$, which represents physically the waves radiated by secondary sources on S, we have

$$\frac{i}{4}\int_S \left[U^{(s)}(\underline{r}') \frac{\partial H_o^{(1)}(k\hat{r})}{\partial n'} - H_o^{(1)}(k\hat{r}) \frac{\partial U^{(s)}(\underline{r}')}{\partial n'} \right] ds' = U^{(s)}(\underline{r}), \quad \underline{r} \text{ outside S.} \tag{3.15}$$

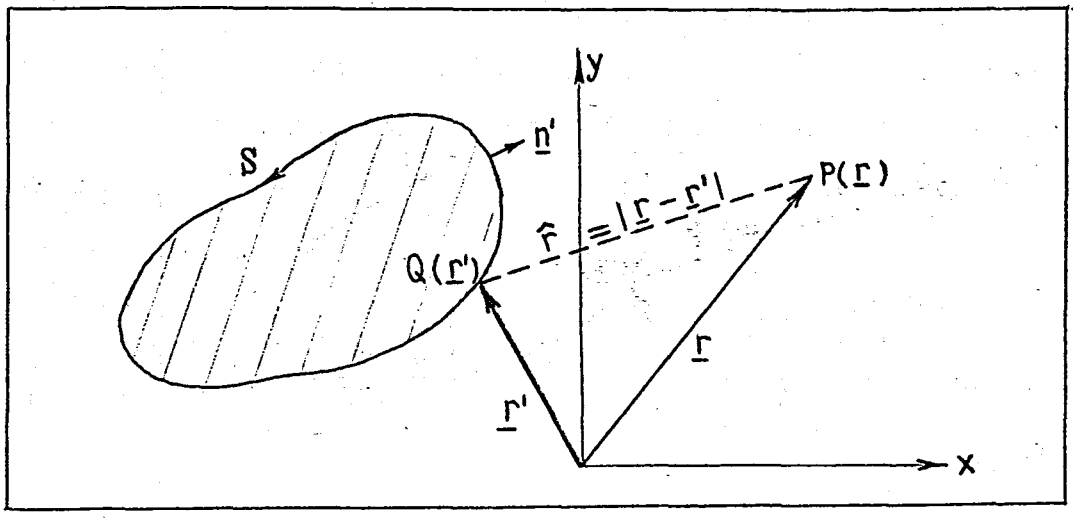

Fig. 3-3 Geometry of observation and source points for two dimensional exterior problem

The equation above states that tha scattered wave field outside the region S, the boundary of the scatterer, can be obtained by a line integration over the curve S once the values of $U^{(s)}(\underline{r}')$ and $\partial U^{(s)}(\underline{r}')/\partial n'$ are known. However, $U^{(s)}(\underline{r}')$ and $\dfrac{\partial U^{(s)}(\underline{r}')}{\partial n'}$ are in general unknown for a given problem. To find $U^{(s)}$ and its normal derivative on the boundary, we let the observation point $P(\underline{r})$ approach the source point $Q(\underline{r}')$ (Fig.3-3). With $\underline{r} \rightarrow \underline{r}'$ Eq.(3.15) reduces to an integral equation for $U^{(s)}(\underline{r}')$ or $\dfrac{\partial U^{(s)}(\underline{r}')}{\partial n'}$.

Since $\dfrac{\partial G(\underline{r},\underline{r}')}{\partial n'}$ is discontinuous on S, one should go through a limiting procedure (Appendix A) to obtain

$$\frac{1}{2}\, U^{(s)}(\underline{r}') = \frac{i}{4}\int_S \left[U^{(s)}(\underline{r}')\, \frac{\partial H_o^{(1)}(k\hat{r})}{\partial n'} - H_o^{(1)}(k\hat{r})\, \frac{\partial U^{(s)}(\underline{r}')}{\partial n'} \right] ds' \tag{3.16}$$

showing that $U^{(s)}$ and $\dfrac{\partial U^{(s)}}{\partial n'}$ are not independent of each other on S.

The boundary conditions are usually prescribed in terms of $U^{(t)}$ or $\partial U^{(t)}/\partial n'$; thus integral equations for the total wave becomes more convenient. For such a representation, we note that the incident field has no singularity inside the boundary S hence, it satisfies the Weber's interior formula (3.11)

$$\frac{i}{4}\int_S \left[H_o^{(1)}(k\hat{r})\, \frac{\partial U^{(i)}(\underline{r}')}{\partial n'} - U^{(i)}(\underline{r}')\, \frac{\partial H_o^{(1)}(k\hat{r})}{\partial n'} \right] ds' = 0 \,, \quad \underline{r} \text{ outside S.}$$

Adding this to Eq.(3.15) and using Eq.(3.14) we get

$$U^{(i)}(\underline{r}) + \frac{i}{4}\int_S \left[U^{(t)}(\underline{r}')\, \frac{\partial H_o^{(1)}(k\hat{r})}{\partial n'} - H_o^{(1)}(k\hat{r})\, \frac{\partial U^{(t)}(\underline{r}')}{\partial n'} \right] ds' = U^{(t)}(\underline{r}) \,, \quad \underline{r} \text{ outside S.} \tag{3.17}$$

If we now let $\underline{r}$ approach $\underline{r}'$, taking the limit as before we obtain

$$\frac{1}{2}\, U^{(t)}(\underline{r}') = U^{(i)}(\underline{r}') + \frac{i}{4}\int_S \left[U^{(t)}(\underline{r}')\, \frac{\partial H_o^{(1)}(k\hat{r})}{\partial n'} - H_o^{(1)}(k\hat{r})\, \frac{\partial U^{(t)}(\underline{r}')}{\partial n'} \right] ds' \tag{3.18}$$

Solutions to Eq.(3.16) and Eq.(3.18) yield $U^{(s)}$ or $U^{(t)}$ on the boundary S, from which the values of the corresponding

quantities outside of S can be obtained using Eq.(3.15) or Eq.(3.17) .

In connection with the above integral representations, two boundary conditions are of great importance. One is that the total field, $U^{(t)}$ (total displacement) on S vanishes, or what is equivalent $U^{(s)} = -U^{(i)}$. This is known as the Dirichlet's condition representing a rigid inclusion (fixed) in space subject to incident SH-waves. Thus, from Eq.(3.18) with $U^{(t)} = 0$, we get

$$U^{(i)}(\underline{r}') = \frac{i}{4}\int_S H_o^{(1)}(k\hat{r}) \frac{\partial U^{(t)}(\underline{r}')}{\partial n'} ds' \tag{3.19}$$

The second boundary condition, known as the Neumann condition, is that the normal derivative of $U^{(t)}$, normal stress, vanishes on S, or equivalently $\frac{\partial U^{(s)}}{\partial n'} = \frac{\partial U^{(i)}}{\partial n'}$.

This is the case of a stress-free boundary, i.e. a cavity subject to incident SH-waves. Eq.(3.18) with $\frac{\partial U^{(t)}}{\partial n'} = 0$ yields

$$U^{(i)}(\underline{r}') = \frac{1}{2} U^{(t)}(\underline{r}') - \frac{i}{4}\int_S U^{(t)}(\underline{r}') \frac{\partial H_o^{(1)}(k\hat{r})}{\partial n'} ds' \tag{3.20}$$

Having obtained the integral equations for the field variables, $U^{(i)}$, $U^{(s)}$ and $U^{(t)}$, in the following section we will outline the method employed to solve them numerically.

3.3 GENERAL PROCEDURE FOR THE SOLUTION OF INTEGRAL EQUATIONS

Boundary value problems formulated in terms of integral equations are concerned with integrals of the form

$$\phi(\underline{r}) = \int_S K(\underline{r},\underline{r}')U(\underline{r}')\,ds' \tag{3.21}$$

where S is a closed contour, and $\underline{r},\underline{r}'$ are vector variables specifying points in the plane and on the contour respectively. The function $K(\underline{r},\underline{r}')$ is a known kernel while $U(\underline{r}')$ is the unknown.

The first step in the numerical solution of Eq.(3.21) is the subdivision of the boundary S into n smooth intervals. Denoting the j-th interval by Δ_J we have

$$S = \Delta_1 + \Delta_2 + \cdots + \Delta_n .$$

The subdivision points are numbered in such a way that the subscript of Δ increases when the boundary is described so as to keep the domain on its left. These sections are simply intervals of plane curves and we refer to the end points of subdivision as "interval points".

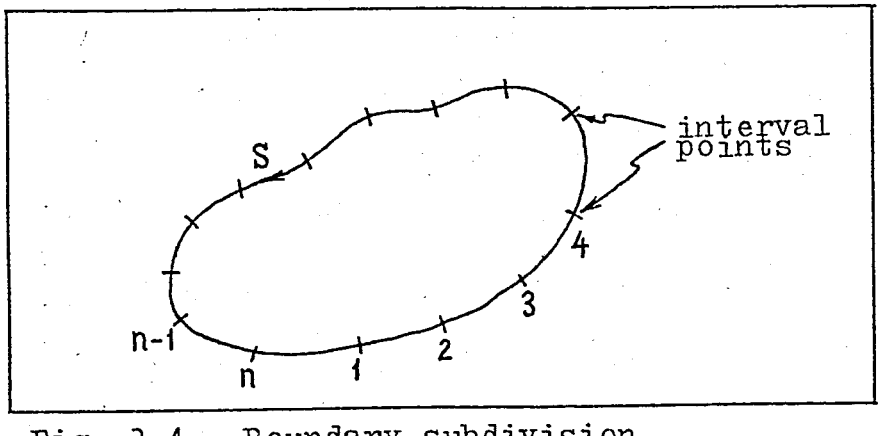

Fig. 3-4 Boundary subdivision

Having chosen the interval points on a given boundary S, we must next select the nodal points, the points where the unknown values are considered. If the interval Δ_J of S is a straight line, its mid-point is taken to be the nodal point for that interval (Fig.3-5a) where the length of the interval is

$$h_J = \left| \underline{r}'_{J+} - \underline{r}'_{J-} \right| \tag{3.22}$$

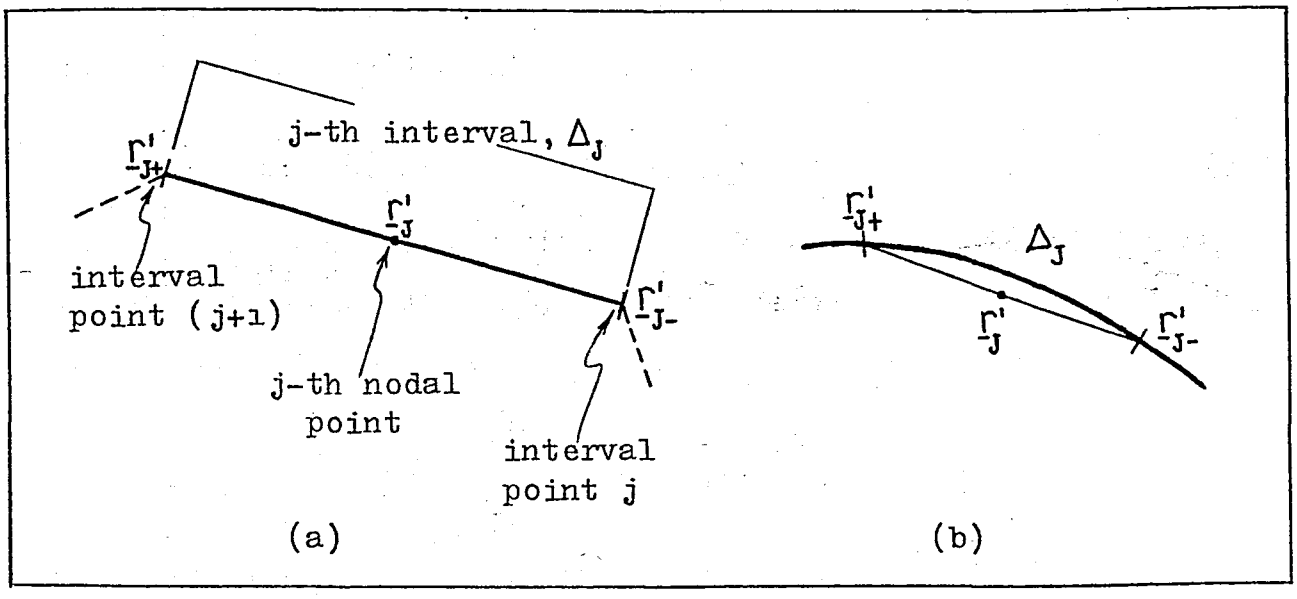

Fig. 3-5 Nodal point definition

When the interval Δ_J is not a straight line we approximate it by a chord joining the end points of the j-th interval and the nodal point is taken as the mid-point of this chord (Fig.3-5b). In this case Eq.(3.22) becomes an approximation to the interval length.

Having divided the boundary into n suitably small sections, $\Delta_1, \Delta_2, \ldots \Delta_n$, the function $U(\underline{r}')$ in Eq.(3.21) is approximated as follows

$$\tilde{U}(\underline{r}') = U_J, \quad \underline{r}' \in \Delta_J \quad ; \quad j = 1,2,3,\ldots,n$$

where U_J's are some constants. Correspondingly, we approximate Eq.(3.21) by

$$\tilde{\phi}(\underline{r}) = \int_S K(\underline{r},\underline{r}')\tilde{U}(\underline{r}')\, ds'$$

which we write in the form

$$\tilde{\phi}(\underline{r}) = \sum_{J=1}^{n} U_J \int_{\Delta_J} K(\underline{r},\underline{r}')\, ds' \qquad (3.23)$$

where $\int_{\Delta_J}$ denotes integration over the j-th interval, Δ_J, of S.

Consider now the case where the function U satisfies an integral equation of the form

$$f(\underline{r}) = \alpha U(\underline{r}) + \int_S K(\underline{r},\underline{r}')U(\underline{r}')\, ds' \ , \quad \underline{r} \in S \tag{3.24}$$

where K is a known kernel, α is a known constant and f is a given function. If $U(\underline{r}')$ is approximated as described above, we obtain by virtue of Eq.(3.23)

$$f(\underline{r}) = \alpha\tilde{U}(\underline{r}) + \sum_{J=1}^{n} U_J \int_{\Delta_J} K(\underline{r},\underline{r}')\, ds' \ , \quad \underline{r} \in S.$$

To solve this equation, one may use the method of "collocation". Applying the equation at one particular point $\underline{r}'_i$ (which is called a nodal point) in each interval Δ_i of S we obtain

$$f_i = \alpha U_i + \sum_{J=1}^{n} U_J \int_{\Delta_J} K(\underline{r}'_i,\underline{r}')\, ds' \tag{3.25}$$

$$\underline{r}_i \in \Delta_i \ , \qquad i = 1,2,3,\ldots,n$$

where $f_i = f(\underline{r}'_i)$ (equivalently $f_i = f(\underline{r}_i)$ when $\underline{r} \in S$).

In this way, we approximate the integral equation (3.24) by a system of n simultaneous linear algebraic equations, Eq.(3.25), in terms of the unknown constants U_J, the approximate displacement at the nodal point of the interval in question. What remains is the evaluation of the integrals in Eq.(3.25). For this, the simplest quadrature formula over the interval Δ_J of length (or approximate length) h_J is

$$\int_{\Delta_J} K(\underline{r},\underline{r}')\, ds' = K(\underline{r},\underline{r}'_J)h_J \ , \quad \underline{r} \in S \tag{3.26}$$

where $\underline{r}'_J$ is the nodal point within the interval. A more accurate result can be obtained by using a four-point Gaussian quadrature

$$\int_{\Delta_J} K(\underline{r},\underline{r}')ds' \simeq \frac{h_J}{2}\left[w_1 K(\underline{r},\underline{r}'_{J_1}) + w_2 K(\underline{r},\underline{r}'_{J_2}) + w_3 K(\underline{r},\underline{r}'_{J_3}) + w_4 K(\underline{r},\underline{r}'_{J_4})\right] \quad , \underline{r} \in S \tag{3.27}$$

where $w_1, \ldots, w_4$ are the weighting coefficients and $\underline{r}'_{J_1}, \ldots, \underline{r}'_{J_4}$ are the integration points on Δ_J. The values of w and the corresponding integration points are given in Appendix B.

Having set up the integral equations for the scattering problem, we will apply these to specific problems as explained in the following chapter.

CHAPTER 4

NUMERICAL EXAMPLES

This chapter is devoted to the applications of the integral equation method described in the previous chapter. The examples presented include various types of cylindrical scatterers such as rigid inclusions or cavities with elliptical, circular and rectangular cross sections. Some of these solutions will be compared with the known exact and approximate solutions [4,5]. Extension of the method to other scatterers with arbitrary cross sections is straightforward.

Both the "near-field" and "far-field" cases are examined. As a consequence of the formulation of the integral equations, first the solution to the former is obtained; namely the solution of the field variables on the boundary. The near-field solution is then used to get the far-field solution.

Consider a circular cylindrical inclusion in an infinitely extended solid as shown in Fig.4-1. The cylinder can be a rigid inclusion or a cavity. An incident SH wave defined by

$$U_x^{(i)} = U_y^{(i)} = 0$$

$$U_z^{(i)} = U^{(i)}(x,y,t) = e^{ikx} \qquad (4.1)$$

propagates in the positive x-direction with constant velocity c, frequency w, and wavelength $\lambda = k/2\pi$. Such waves can be generated by tangential forces distributed over a large plane located far from the cylinder. Upon impinging on the surface of the cylinder, part of the incident wave is reflected.

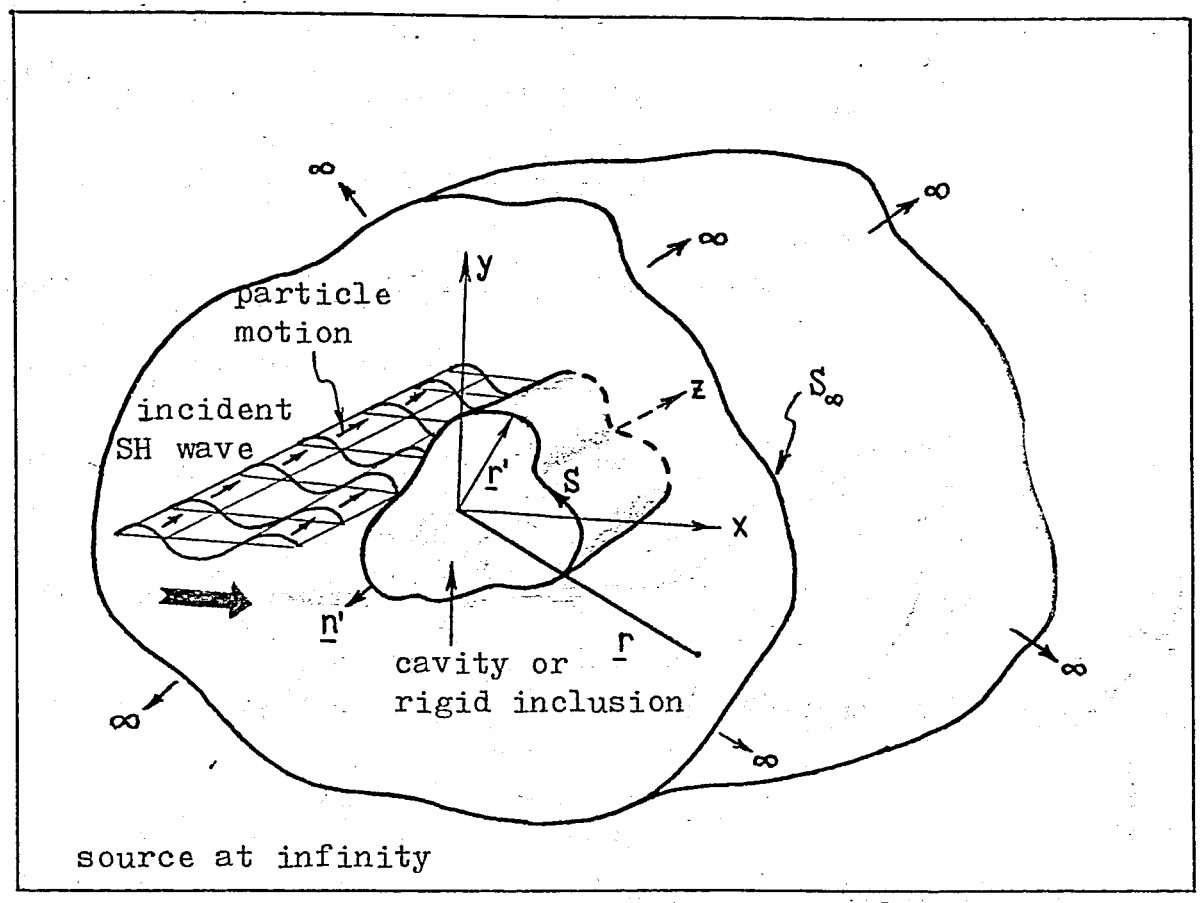

Fig. 4-1 Geometry for the scattering problem

The scattered wave is also an SH wave and is represented by

$$U_x^{(s)} = U_y^{(s)} = 0 \quad , \qquad U_z^{(s)} = U^{(s)}(x,y,t) \ .$$

$U^{(s)}$ is to be found from the solution of the wave equation (2.4) expressed in integral form.

4.1 NEAR-FIELD SOLUTIONS

4.1.1 SCATTERING BY A CAVITY

For a cavity, as stated earlier, the normal derivative of $U^{(t)}$ vanishes on the boundary, i.e. $\frac{\partial U^{(t)}}{\partial n'} = 0$, giving rise to the following integral equation, Eq.(3.20)

$$U^{(i)}(\underline{r}') = \frac{1}{2} U^{(t)}(\underline{r}') - \frac{i}{4} \int_S U^{(t)}(\underline{r}') \frac{\partial H_0^{(1)}(k\hat{r})}{\partial n'} ds' \ . \qquad (4.2)$$

We assume plane waves of the form e^{ikx} so that $U^{(i)}(\underline{r}') = e^{ikx'}$, and utilizing the relation

$$\frac{d}{dz} H_o^{(1)}(y) = -H_1^{(1)}(y) \frac{dy}{dz} ,$$

where $H_m^{(1)}(y) = J_m(y) + iY_m(y)$,

Eq.(4.2) can be written as

$$e^{ikx'} = \frac{1}{2} U^{(t)}(\underline{r}') + \frac{ik}{4} \int_S U^{(t)}(\underline{r}') H_1^{(1)}(k\hat{r}) \frac{\partial \hat{r}}{\partial n'} ds' \qquad (4.3)$$

Using the results of section 3.3, Eq.(4.3) becomes

$$e^{ikx_\ell'} = \frac{1}{2} U_\ell'^{(t)} + \frac{ik}{4} \sum_{J=1}^{n} U_J'^{(t)} \int_{\Delta_J} H_1^{(1)}(k\hat{r}) \frac{\partial \hat{r}}{\partial n'} ds' \qquad (4.4)$$

where $U'^{(t)} = U^{(t)}(\underline{r}')$, $\ell = 1,2,3,\ldots,n$.

(From now on, field variables with " ' " will denote the corresponding values on the boundary). Approximating the integrals in Eq.(4.4) by a four-point Gaussian quadrature, Eq.(3.27), we have

$$e^{ikx_\ell'} = \frac{1}{2} U_\ell'^{(t)} + \frac{ik}{4} \sum_{J=1}^{n} \sum_{i=1}^{4} U_J'^{(t)} \frac{h_J}{2} \left[w_i H_1^{(1)}(k\hat{r}_{J_i\ell}) \left(\frac{\partial \hat{r}}{\partial n'}\right)_{J_i\ell} \right] \qquad (4.5)$$

$$\ell = 1,2,3,\ldots,n .$$

where h_J is the length of the j-th interval, $\hat{r}_{J_i\ell}$ is the distance from the ℓ-th nodal point to the i-th integration point on the j-th interval, $(\partial\hat{r}/\partial n')_{J_i\ell}$ is the cosine of the angle between the vector $\underline{r}_{J_i\ell}$ and the perpendicular to the j-th interval at the i-th integration point.

For the derivation and the numerical approximation of the normal derivatives see Appendix C. The above quantities are further clarified in the figures below.

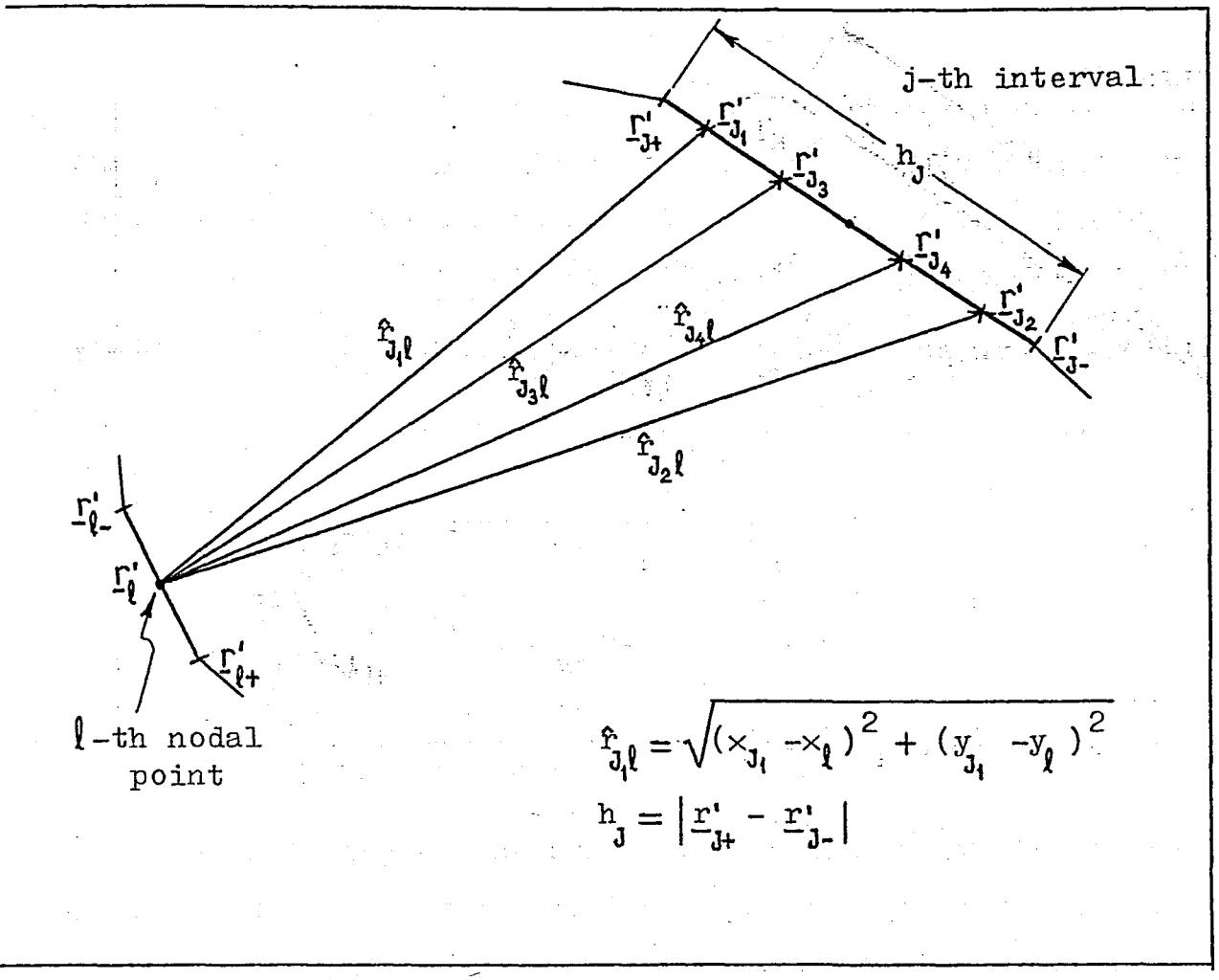

Fig. 4-2 Geometrical definitions

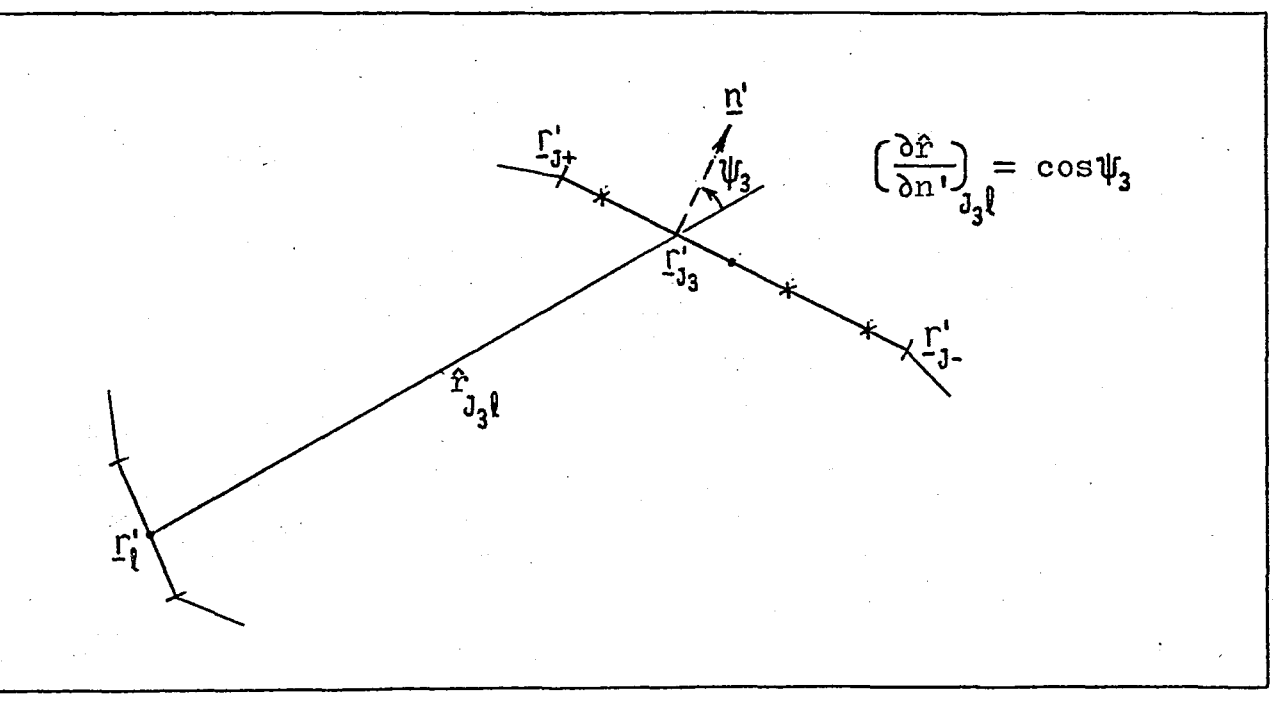

Fig. 4-3 Definition of $\frac{\partial \hat{r}}{\partial n'}$

Note that the integral in Eq.(4.4) seem to have a singularity when $j = \ell$. However, the integrand over the j-th segment of the contour is zero due to the fact that the vector $\hat{r}_{\ell;\ell}$ is orthogonal (see Fig.4-4) to the normal $\underline{n}'$ yielding $\left(\frac{\partial \hat{r}}{\partial n'}\right)_{\ell;\ell} = 0$. Hence the term when $j = \ell$ has no contribution and can simply be excluded from the summation in Eq.(4.5).

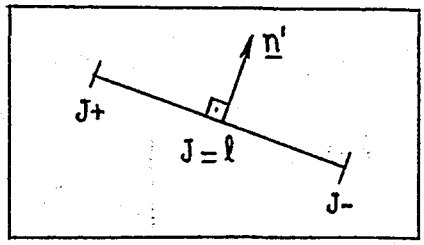

Fig. 4-4

The solution of the system of equations given by (4.5) yields the total displacement at the boundary of the cavity. If desired, scattered displacement field may then be found from the relation

$$U'^{(t)} = U'^{(i)} + U'^{(s)}$$

where $U'^{(i)} = U^{(i)}(\underline{r}')$, $U'^{(s)} = U^{(s)}(\underline{r}')$.

4.1.1-1 ELLİPTİCAL AND CİRCULAR CAVİTY

In the case of an elliptical cross section, the boundary is divided into n intervals such that each interval subtends a central angle of $2\pi/n$. To determine the interval points, use is made of the polar representation of the ellipse given by

$$r = \frac{ab}{\sqrt{a^2 \sin^2 \theta' + b^2 \cos^2 \theta'}}$$

from which conversion to rectangular coordinates is straightforward.

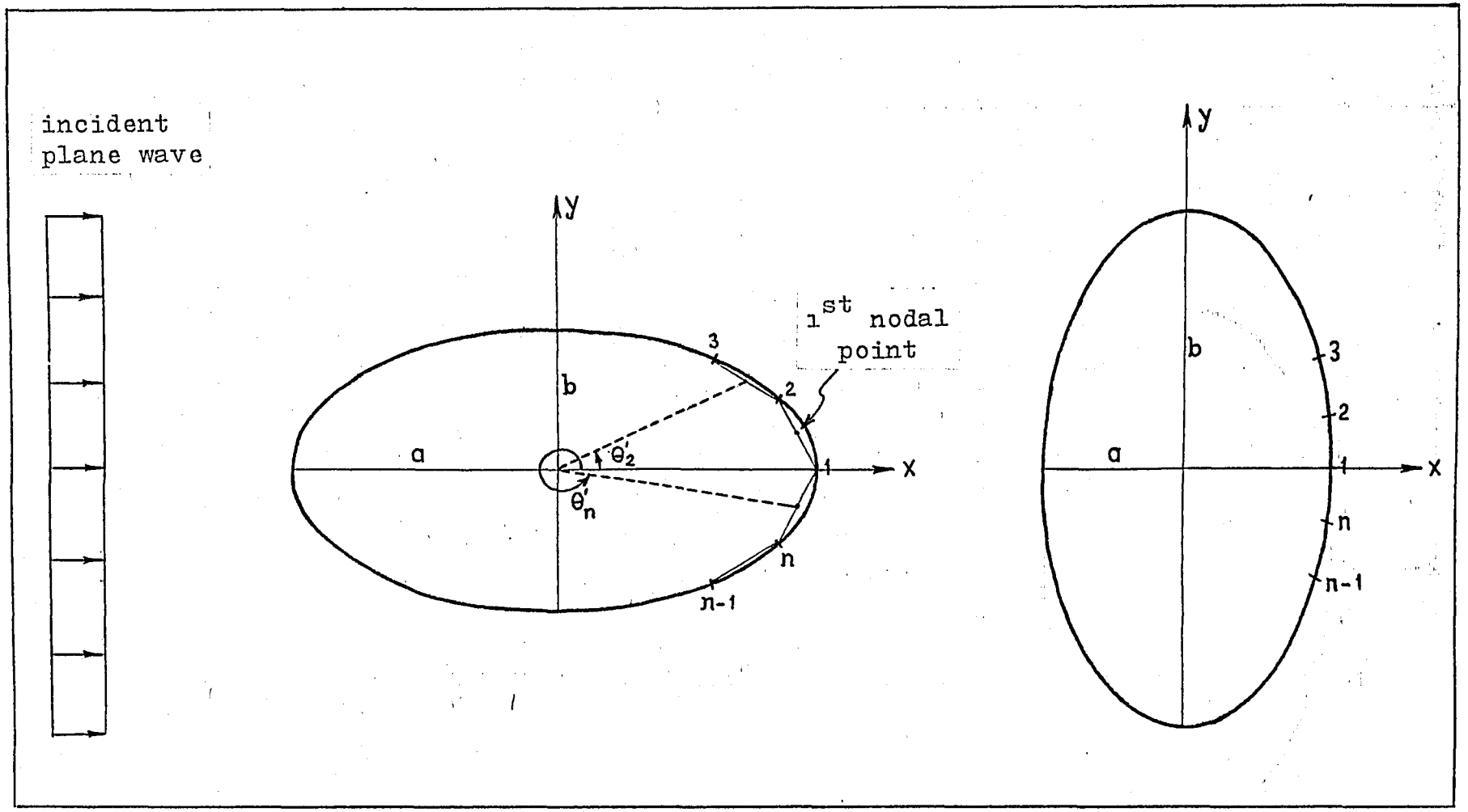

Fig. 4-5 Boundary geometry

Recalling Eq.(4.5), modified to exclude the term when $j = \ell$, we have

$$e^{ikx_\ell'} = \frac{1}{2}U_\ell'^{(t)} + \frac{ik}{4}\sum_{\substack{J=1\\J\neq\ell}}^{n}\sum_{i=1}^{4} U_J'^{(t)}\,\frac{h_J}{2}\left[w_i H_1^{(1)}(k\hat{r}_{J_i\ell})\left(\frac{\partial\hat{r}}{\partial n'}\right)_{J_i\ell}\right] \qquad \ell = 1,2,3,\ldots,n \tag{4.6}$$

which is the set of equations, when solved yields the total displacement on the boundary of the elliptical cavity.

Eq.(4.6) can be written in matrix form as

$$\begin{bmatrix} \frac{1}{2} & \alpha_{12} & \cdots & \alpha_{1n} \\ \vdots & \frac{1}{2} & & \vdots \\ \vdots & & \ddots & \vdots \\ \alpha_{n1} & \cdots & \cdots & \frac{1}{2} \end{bmatrix} \begin{bmatrix} U_1'^{(t)} \\ U_2'^{(t)} \\ \vdots \\ U_n'^{(t)} \end{bmatrix} = \begin{bmatrix} e^{ikx_1'} \\ e^{ikx_2'} \\ \vdots \\ e^{ikx_n'} \end{bmatrix} \tag{4.6'}$$

where x_ℓ' refers to the x-coordinate of the ℓ-th nodal point, $U_\ell'^{(t)}$ is the total displacement at the ℓ-th nodal point, and

$$\alpha_{J\ell} = \frac{ik}{4}\sum_{i=1}^{4}\frac{h_J}{2}\left[w_i H_1^{(1)}(k\hat{r}_{J_i\ell})\left(\frac{\partial\hat{r}}{\partial n'}\right)_{J_i\ell}\right]$$

Due to the geometrical symmetry of the scatterer with respect to the horizontal axis, x-axis, the off-diagonal elements, $\alpha_{J\ell}$ are symmetric. Also the displacement field, $U'^{(t)}$, obtained from Eq.(4.6') has a polar symmetry with respect to the x-axis.

The circular cavity case follows the same line of reasoning with the major axis length set equal to that of minor. The tangential stress is obtained by the numerical differentiation of $U'^{(s)}$ values with respect to θ'. For this, the following "least squares polynomial" is used

$$\frac{dU(\theta'_k)}{d\theta'} \simeq \frac{1}{10D}\left(-2U_{k-2} - U_{k-1} + U_{k+1} + 2U_{k+2}\right)$$

where $D = \theta'_k - \theta'_{k-1}$.

The displacement at the boundary, for various cases are shown in Fig.1 for a circular cavity and in Fig. 6 for an elliptical cavity. Fig. 2 displays the tangential stress for a circular cavity.

4.1.1-2 RECTANGULAR CAVITY

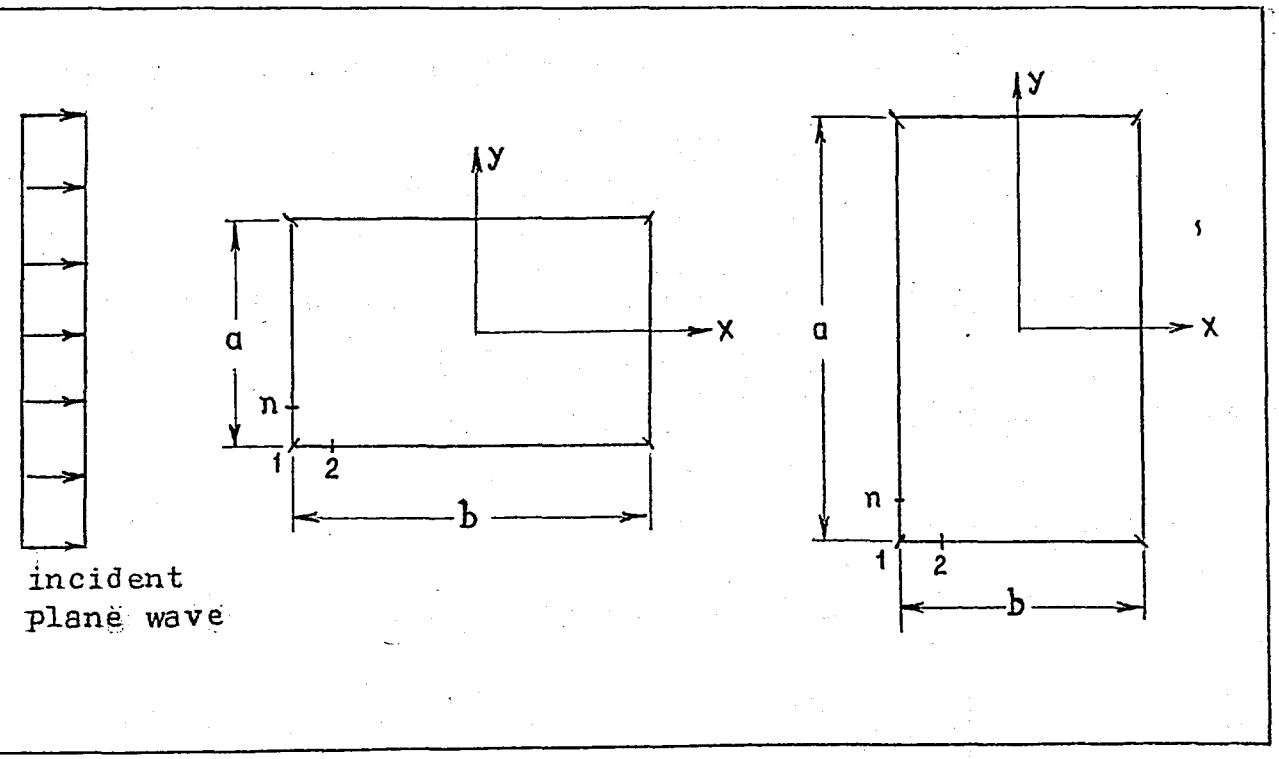

Fig. 4-6 Boundary geometry

The numerical procedure involved in this problem is virtually no more different from that of the elliptical case. The corners do not pose any mathematical difficulty since they are chosen as the interval points which are excluded from the evaluation of the integrals as a result of the use of Gaussian quadrature. The results for the displacement at the boundary are presented in Fig. 10.

4.1.2 SCATTERING BY A RIGID INCLUSION

For a rigid inclusion the boundary condition is that the total displacement, $U'^{(t)}$ vanishes, i.e. $U'^{(s)} = -U'^{(i)}$. The integral equation corresponding to this case is given by Eq.(3.19)

$$U^{(i)}(\underline{r}') = \frac{i}{4} \int_S H_o^{(1)}(k\hat{r}) \frac{\partial U^{(t)}(\underline{r}')}{\partial n'} ds' .$$

Assuming an incident plane wave of the form e^{ikx}, we have

$$e^{ikx'} = \frac{i}{4} \int_S \frac{\partial U^{(t)}(\underline{r}')}{\partial n'} H_o^{(1)}(k\hat{r}) ds' . \tag{4.7}$$

Again with reference to section 3.3, we write Eq.(4.7) as

$$e^{ikx_\ell'} = \frac{i}{4} \sum_{J=1}^{n} \left[\frac{\partial U^{(t)}(\underline{r}')}{\partial n'} \right]_J \int_{\Delta_J} H_o^{(1)}(k\hat{r}) ds' \tag{4.8}$$

where $\frac{\partial U'^{(t)}}{\partial n'}$ represents the total normal stress on the boundary. Using Gaussian integration formula we get

$$e^{ikx_\ell'} = \frac{i}{4} \sum_{J=1}^{n} \sum_{i=1}^{4} \left[\frac{\partial U'^{(t)}}{\partial n'} \right]_J \frac{h_J}{2} \left[w_i \, H_o^{(1)}(k\hat{r}_{J_i\ell}) \right] \tag{4.9}$$

where $\ell = 1,2,3,\ldots,n$.

Hence, the solution of Eq.'s (4.9) yields the total normal stress on the boundary of the rigid inclusion. Scattered normal stress may then be calculated from the relation

$$\frac{\partial U'^{(t)}}{\partial n'} = \frac{\partial U'^{(i)}}{\partial n'} + \frac{\partial U'^{(s)}}{\partial n'}$$

For $U'^{(i)} = U^{(i)}(\underline{r}') = e^{ikx'} = e^{ikr'\cos\theta'}$,

$$\frac{\partial U'^{(i)}}{\partial n'} = ike^{ikx'} \cos\theta' \frac{\partial r'}{\partial n'}$$

where θ' is the angle $\underline{r}'$ makes with the positive x-axis.

4.1.2-1 ELLIPTICAL AND CIRCULAR RIGID INCLUSION

Scattering related to near-field is governed by Eq.(4.9) where boundary subdivision is as explained in section 4.1.1-1. However, in Eq.(4.8) the imaginary part of $H_0^{(1)}(k\hat{r}), Y_0(k\hat{r})$, has a singularity when $j = \ell$. Thus the terms for $j=\ell$ should be excluded from the summation and approximated by other means (see Appendix D). Hence Eq.(4.9) takes the form

$$e^{ikx_\ell'} = \frac{i}{4} \sum_{\substack{J=1 \\ J\neq\ell}}^{n} \sum_{i=1}^{4} \left[\frac{\partial U'^{(t)}}{\partial n'}\right]_J \frac{h_J}{2} \left[w_i H_0^{(1)}(k\hat{r}_{J_i\ell})\right] + \left(\frac{\partial U'^{(t)}}{\partial n'}\right)_\ell \left\{ -\frac{1}{\pi} \ln\left[\frac{k(h_\ell/2)}{2} - 0.4228\right] \frac{h_\ell}{2} + \frac{i}{2}\frac{h_\ell}{2} \right\} \tag{4.10}$$

The above equation yields the total normal stress on the boundary from which the scattered normal stress may be found in a straightforward manner as was explained in section 4.1.2 .

As before, the circular rigid inclusion case can be obtained from the elliptical formulation by letting the two axes become equal.

Normal stress at the boundary are shown in Fig.'s 4 and 8 for a rigid circular inclusion and a rigid elliptical inclusion respectively.

4.2 FAR-FIELD SOLUTIONS

The general integral representation for the scattered field is given by (see Eq. 3.15)

$$U^{(s)}(\underline{r}) = \int_S \frac{\partial G}{\partial n'} U^{(s)}(\underline{r}')\, ds' - \int_S G \frac{\partial U^{(s)}(\underline{r}')}{\partial n'}\, ds'. \quad (4.11)$$

As seen $U^{(s)}(\underline{r})$ at any point outside s is completely determined if $U^{(s)}$ and $\partial U^{(s)}/\partial n$ on the boundary are known. One of these quantities is specified by the prescribed boundary condition, $\partial U'^{(s)}/\partial n'$ for the cavity and $U'^{(s)}$ for a rigid inclusion, while the other is provided by the solution of the problem as described in the previous section. Thus, substitution of $U'^{(s)}$ or $\partial U'^{(s)}/\partial n'$ for the respective problem into Eq.(4.11) gives a complete solution for the scattered displacement, $U^{(s)}$, at any point $\underline{r}$.

4.2.1 CAVITY

Denoting the total, scattered and the incident stresses by $\sigma_n^{(t)}$, $\sigma_n^{(s)}$, $\sigma_n^{(i)}$ respectively, the boundary condition for a cavity is

$$\sigma_n'^{(t)} = 0 = \sigma_n'^{(s)} + \sigma_n'^{(i)} .$$

Hence, $\sigma_{n'}^{(s)} = -\sigma_{n'}^{(i)}$.

For an incident plane wave $U'^{(i)} = e^{ikx'} = e^{ikr'\cos\theta'}$ we have

$$\sigma_{n'}^{(i)} = ike^{ikx'}\cos\theta' \frac{\partial r'}{\partial n'} .$$

Thus,

$$\sigma_{n'}^{(s)} = - ike^{ikx'}\cos\theta' \frac{\partial r'}{\partial n'} = \frac{\partial U'^{(s)}}{\partial n'} \tag{4.12}$$

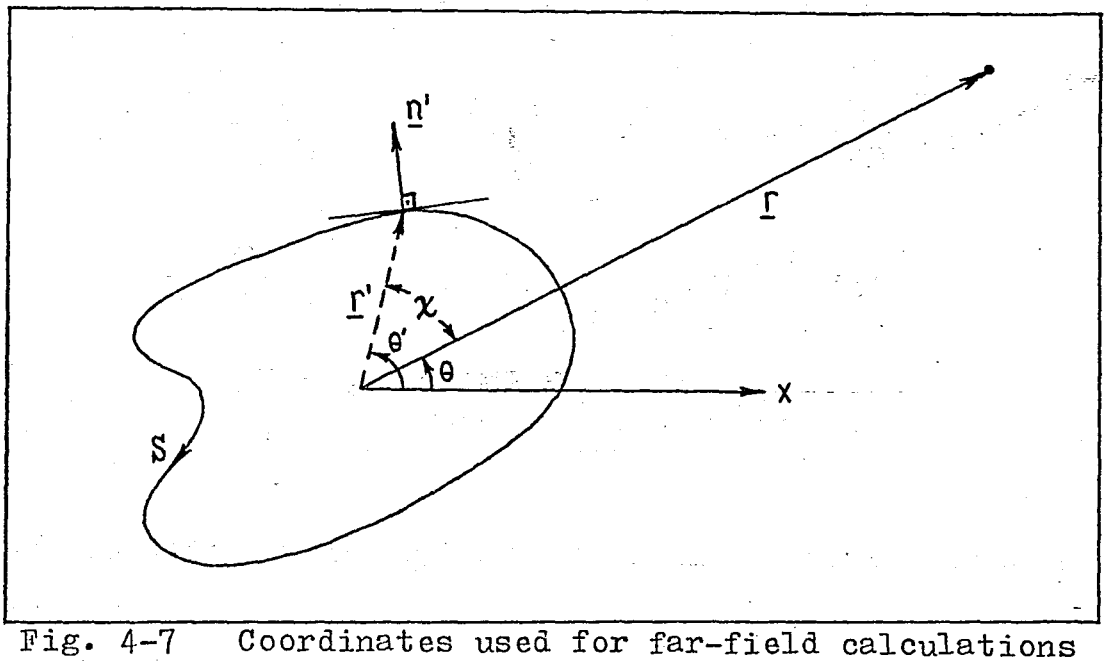

Fig. 4-7 Coordinates used for far-field calculations

When $\underline{r}$ is far away from the obstacle, referring to Fig.4-7, one can write

$$\hat{r} \simeq |\underline{r}| - |\underline{r}'| \cos\chi = r - r' \cos\chi$$

$$\frac{\partial \hat{r}}{\partial n'} = \frac{\partial \hat{r}}{\partial r'} \frac{\partial r'}{\partial n'} , \qquad \frac{\partial \hat{r}}{\partial r'} = - \cos\chi$$

Therefore,

$$\frac{\partial \hat{r}}{\partial n'} = - \cos\chi \frac{\partial r'}{\partial n'} . \tag{4.13}$$

Returning back to Eq.(4.11), and substituting the values of $\sigma_n'^{(s)}$ from Eq.(4.12), and $\partial\hat{r}/\partial n'$ from Eq.(4.13) we get

$$U^{(s)}(\underline{r}) = \int_S -\frac{ik}{4} H_1^{(1)}(k\hat{r}) \frac{\partial \hat{r}}{\partial n'} U'^{(s)} \, ds' - \int_S \frac{i}{4} H_0^{(1)}(k\hat{r}) \, \sigma_n'^{(s)} \, ds' \tag{4.14}$$

$$= \frac{ik}{4} \int_S H_1^{(1)}(k\hat{r}) \left[\cos\chi \frac{\partial r'}{\partial n'} \right] U'^{(s)} \, ds' - \frac{i}{4} \int_S H_0^{(1)}(k\hat{r}) \left[-ike^{ik\times'} \cos\theta' \frac{\partial r'}{\partial n'} \right] ds'$$

$$= \frac{ik}{4} \int_S \cos\chi \, H_1^{(1)}(k\hat{r}) \frac{\partial r'}{\partial n'} U'^{(s)} \, ds' - \frac{k}{4} \int_S e^{ik\times'} \cos\theta' \, H_0^{(1)}(k\hat{r}) \frac{\partial r'}{\partial n'} \, ds' . \tag{4.14'}$$

For any field point $\underline{r}_\ell$ far away from the scatterer we can then write

$$U^{(s)}(\underline{r}_\ell) \simeq \frac{ik}{4} \sum_{J=1}^{n} \left[\cos\chi_{J\ell} \, H_1^{(1)}(k\hat{r}_{J\ell}) \frac{\partial r_J'}{\partial n'} U^{(s)}(\underline{r}_J') \right] h_J - \frac{k}{4} \sum_{J=1}^{n} \left[e^{ik\times_J'} \cos\theta_J' \, H_0^{(1)}(k\hat{r}_{J\ell}) \frac{\partial r_J'}{\partial n'} \right] h_J$$

$$\simeq \frac{k}{4} \sum_{J=1}^{n} \left[\cos\chi_{J\ell} \, iH_1^{(1)}(k\hat{r}_{J\ell}) \, U^{(s)}(\underline{r}_J') - e^{ik\times_J'} \cos\theta_J' \, H_0^{(1)}(k\hat{r}_{J\ell}) \right] \frac{\partial r_J'}{\partial n'} h_J \tag{4.15}$$

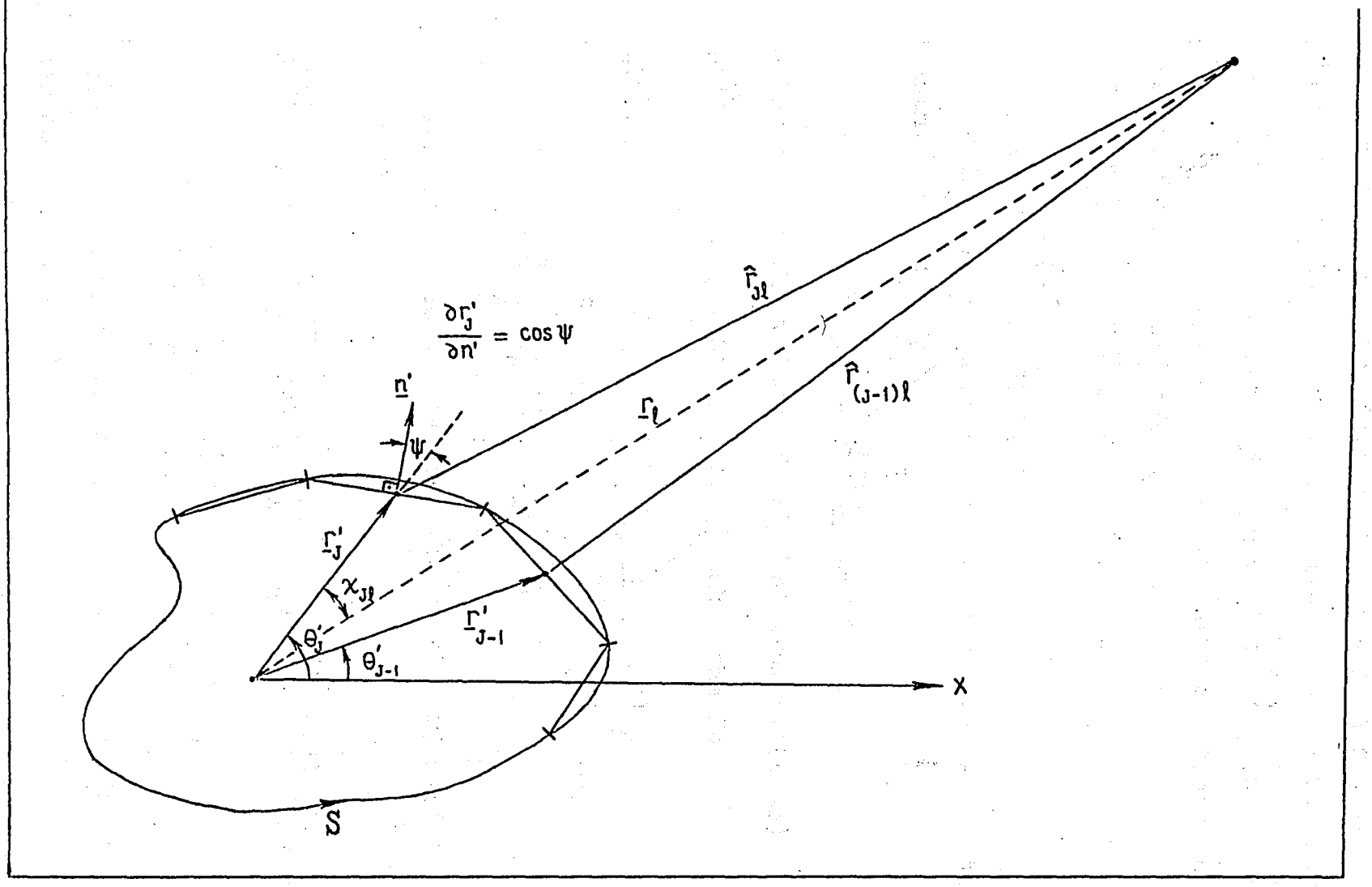

Fig. 4-8 Geometrical definitions

where the integrals are approximated by the so-called mid-ordinate rule for integration (see Eq.3.26).The relevant geometric quantities are illustrated in Fig.4-8 .

Having the near-field results ($U'^{(t)}$, thus $U'^{(s)}$) for circular,elliptical and rectangular cavities,the corresponding far-field solutions obtained from Eq.(4.15) are illustrated in Fig.'s 3 , 7 and 11 .

4.2.2 RIGID INCLUSION

Using the boundary condition corresponding to the pertinent case,we have

$$U'^{(s)} = -U'^{(i)} = -e^{ikx'} \quad . \tag{4.16}$$

Substituting the values of $\partial\hat{r}/\partial n'$ from Eq.(4.13),and $U'^{(s)}$ from Eq.(4.16), Eq.(4.14) takes the form

$$\begin{aligned} U^{(s)}(\underline{r}) = & -\frac{k}{4}\int_S \cos\chi \; iH_1^{(1)}(k\hat{r}) \frac{\partial r'}{\partial n'} U'^{(i)} \, ds' \\ & -\frac{1}{4}\int_S iH_0^{(1)}(k\hat{r}) \, \sigma_n'^{(s)} \, ds' \quad . \end{aligned} \tag{4.17}$$

For large distances away from the scatterer,Eq.(4.17) may be approximated as

$$\begin{aligned} U^{(s)}(\underline{r}_\ell) = & -\frac{k}{4}\sum_{J=1}^{n} \cos\chi_{J\ell} \, iH_1^{(1)}(k\hat{r}_{J\ell}) \frac{\partial r_J'}{\partial n'} U^{(i)}(\underline{r}'_J) \, h_J \\ & -\frac{1}{4}\sum_{J=1}^{n} (\sigma_n'^{(s)})_J \; iH_0^{(1)}(k\hat{r}_{J\ell}) \, h_J \end{aligned} \tag{4.18}$$

where the integrals are again evaluated in a similar manner as for Eq.(4.15).

Far-field results for this case are presented in Fig.'s

5 and 9 respectively for a rigid circular and a rigid elliptical inclusion. The calculations are carried out at points such that $\underline{r}_\ell = 2000\ \underline{r}'_\ell$, where $\underline{r}'_\ell$ denotes the ℓ-th nodal point.

CHAPTER 5

CONCLUSIONS

The results for anti-plane waves scattered by a circular cavity and a rigid inclusion are presented respectively in Fig.'s 1,2,3 and in Fig.'s 4, 5 .For comparison, the exact solutions,where available,are also given at the upper right-hand side.Excellent agreement is observed for all wave numbers.

Far-field solutions,$U^{(s)}(\underline{r})$, were obtained using Eq.'s (4.15) and (4.18) for a cavity and a rigid inclusion respectively.However,in the literature[5] $U^{(s)}(\underline{r})$ is generally given as

$$U^{(s)}(r) = \frac{e^{ikr}}{\sqrt{r}} \psi^{(s)}$$

where $\psi^{(s)}$ is known as the scattering coefficient and r is the distance from the boundary to the point of interest.Furthermore the relevant graphs are plotted as $\sqrt{k}\psi^{(s)}$ vs. θ . Thus,for comparison purposes,the displacement field,$U^{(s)}$, obtained through Eq.'s (4.15) and (4.18) are multiplied by the factor $\sqrt{k}/\left(\frac{e^{ikr}}{\sqrt{r}}\right)$ and then plotted vs. θ in Fig.'s 3 and 5 .

For the elliptical case,some of the far-field solutions (Fig.'s 7 , 9) could have been compared with those that are found in reference 4.Contrary to circular geometry, the results are not equally well for all wave numbers ; for the small wave number ($k = 1$) better agreement is

observed.With increasing wave number (decreasing wavelength) within each segment of the boundary,variations of the wave function are more pronounced.Thus,the assumption that on each interval both the incident and the scattered field are constant falls short of meeting the real situation. Choosing linear or parabolic variations over each segment may improve the results obtained.However,one should be aware that when corners are encountered such choices cause problems which necessiate some modifications to avoid them. Although no comparison could have been made,near-field results (Fig.'s 6,8) are expected to be better than those of the far-field since the latter makes use of the near-field solutions through an integration which is again approximated,somewhat less precisely than the one involved in the near-field formulation.

The fact that the circular case yields better results than the elliptical one may be attributed to the geometric properties of the former.The constancy in the curvature of the circle renders the boundary to be more accurately described by straight lines than the ellipse.In addition,the values of $\partial r/\partial n'$ used for the far-field calculations are exact for the circle.

For rectangular geometry,being unable to make any comparison,results pertaining only to cavity is given.Guided by the general implication,corners may be thought to give rise to difficulties;but since the integrals are evaluated only at points within the interval,no problem occurs.

To sum up,boundary integral equation method,removing the geometrical restriction makes it possible to analyze the scattering of waves from inclusions of any shape. However,the variations of the field variables within each

interval should be taken into consideration and more precisely accounted for.The number of boundary segments may also be increased in direct proportion to the incident wave number and changes in the curvature of the configuration.

FIGURE CAPTIONS

Figure 1 displacement at the boundary of a circular cavity due to the scattered wave field

Figure 2 tangential stress, $|\partial U^{(s)}/\partial\theta|$, at the boundary of a circular cavity due to the scattered wave field

Figure 3 scattering coefficient due to the scattered wave field from a circular cavity

Figure 4 normal stress, $|\partial U^{(s)}/\partial n|$, at the boundary of a rigid circular inclusion due to the scattered wave field

Figure 5 scattering coefficient due to the scattered wave field from a rigid circular inclusion

Figure 6 displacement at the boundary of an elliptical cavity due to the scattered wave field

Figure 7 far-field displacement due to the scattered wave field from an elliptical cavity

Figure 8 normal stress, $|\partial U^{(s)}/\partial n|$, at the boundary of a rigid elliptical inclusion due to the scattered wave field

Figure 9 far-field displacement due to the scattered wave field from a rigid elliptical inclusion

Figure 10 displacement at the boundary of a rectangular cavity due to the scattered wave field

Figure 11 far-field displacement due to the scattered wave field from a rectangular cavity

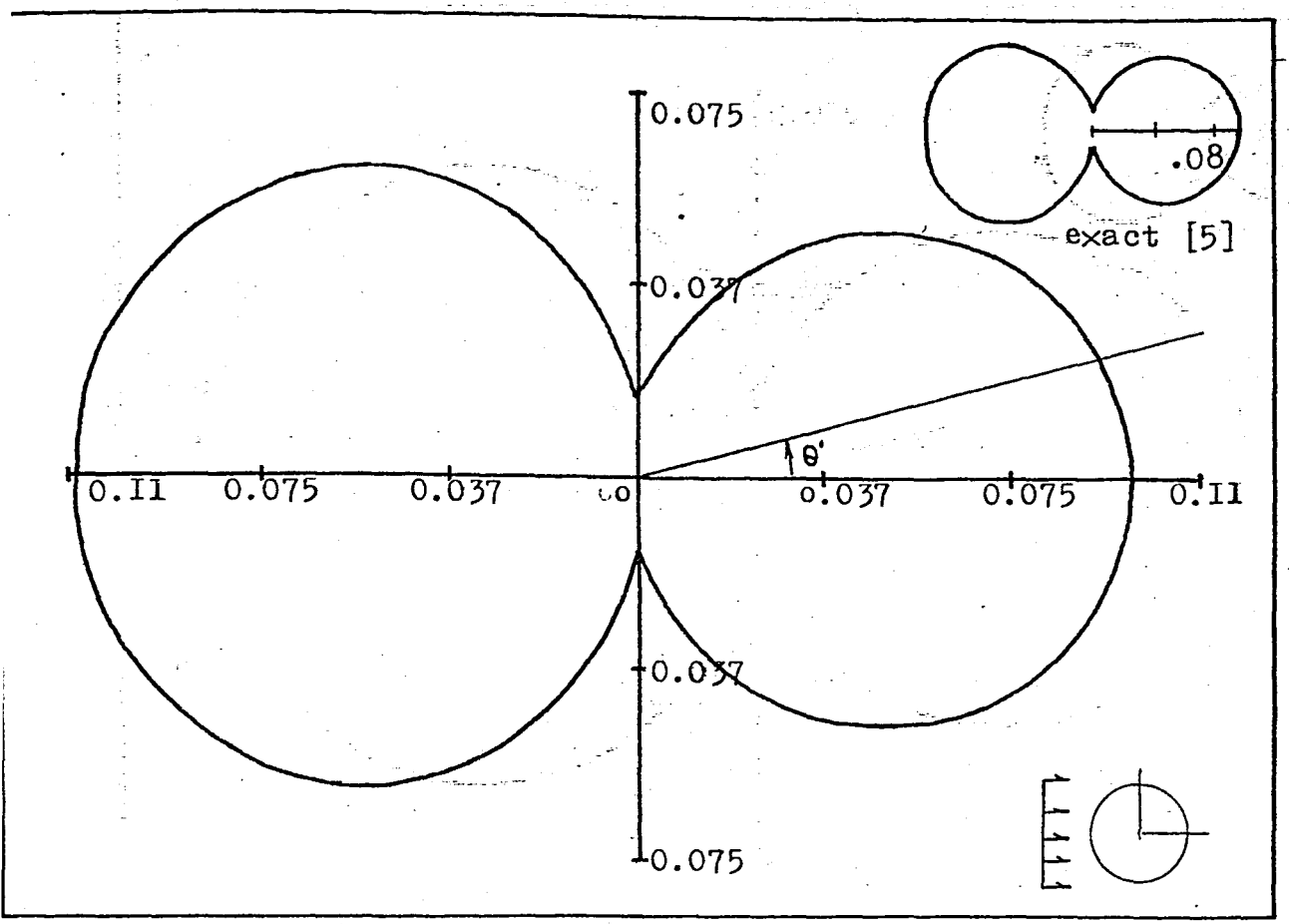

Fig. 1-a ka = 0.1

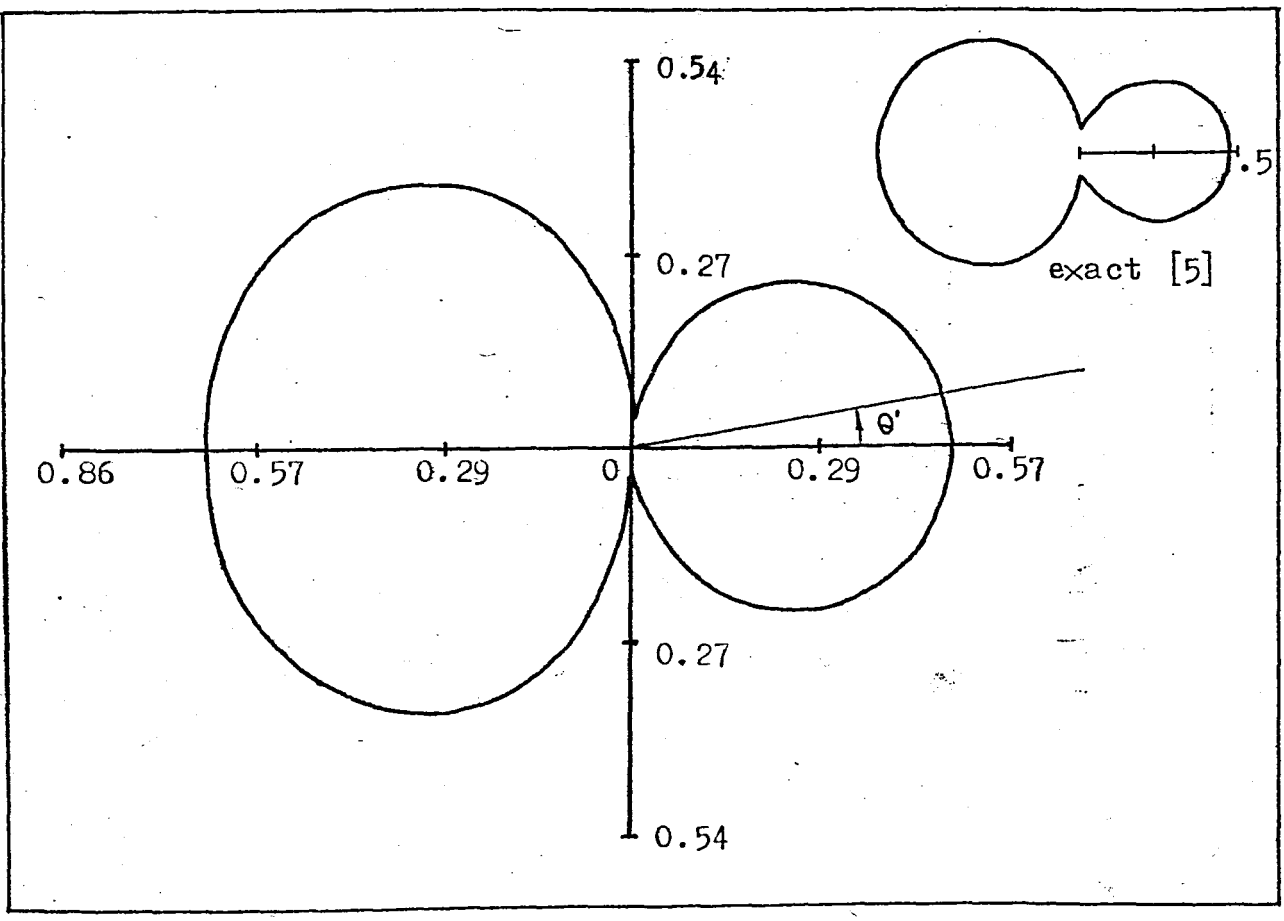

Fig. 1-b ka = 0.5

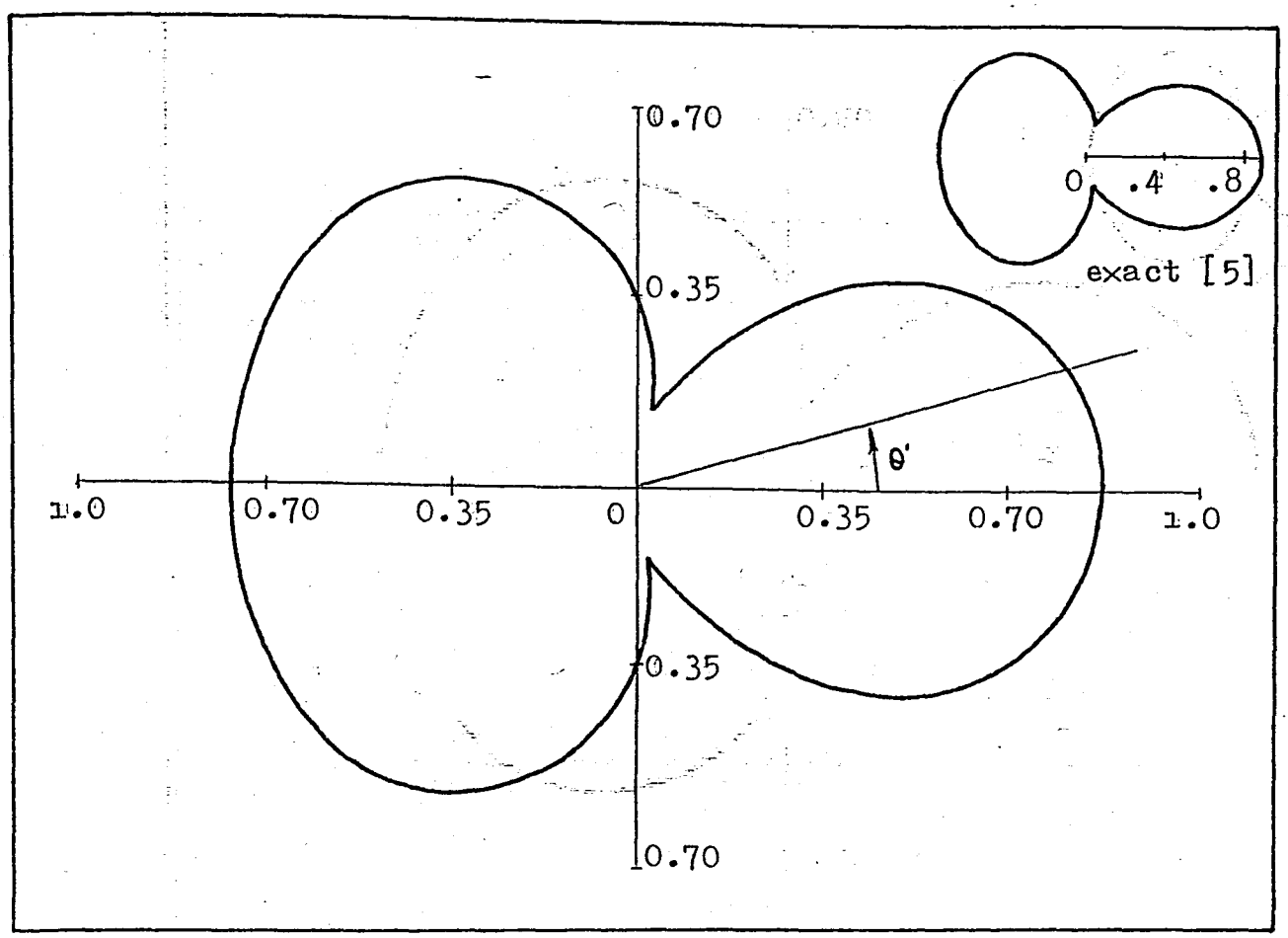

Fig. 1-c ka = 1.0

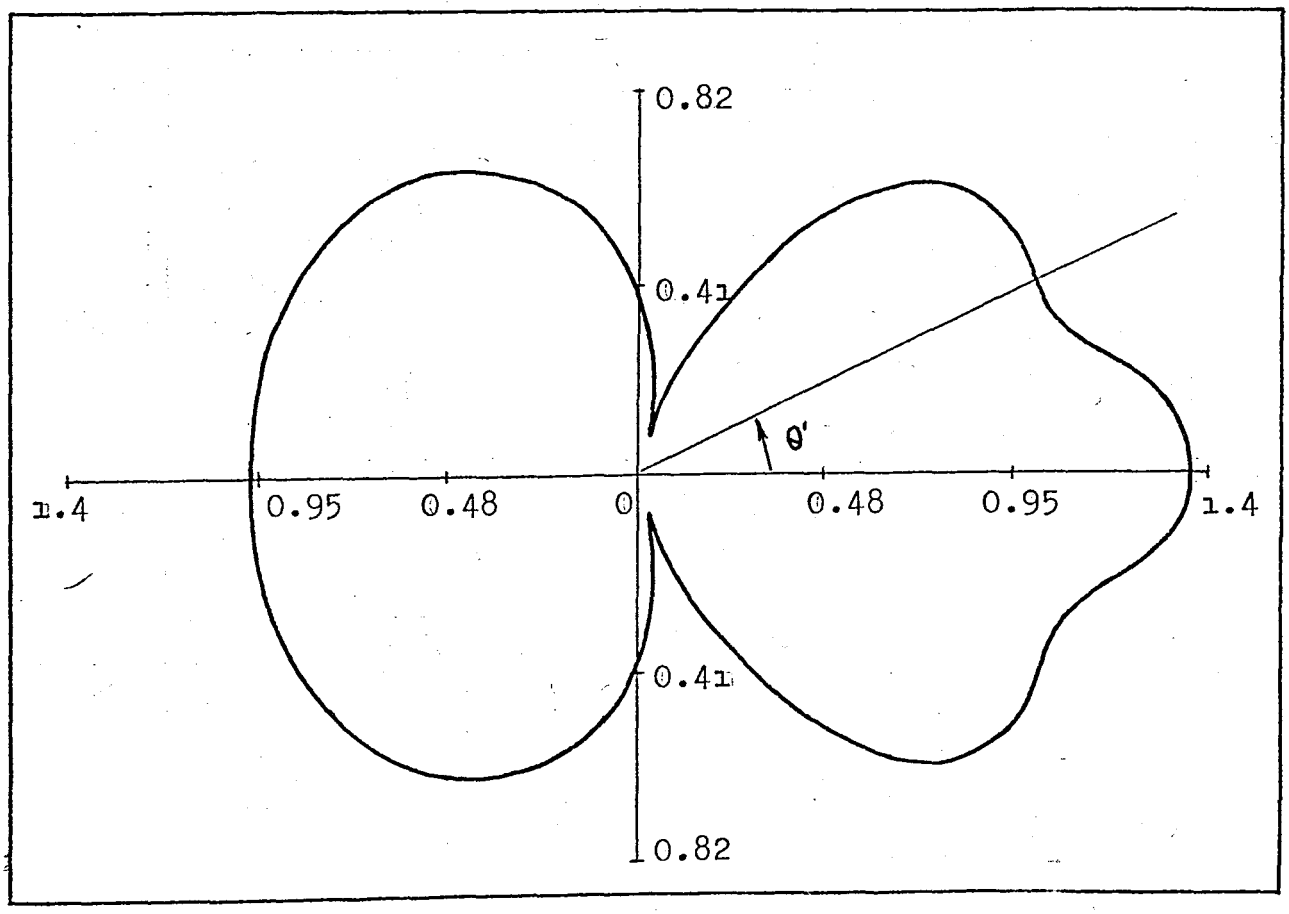

Fig. 1-d ka = 5.0

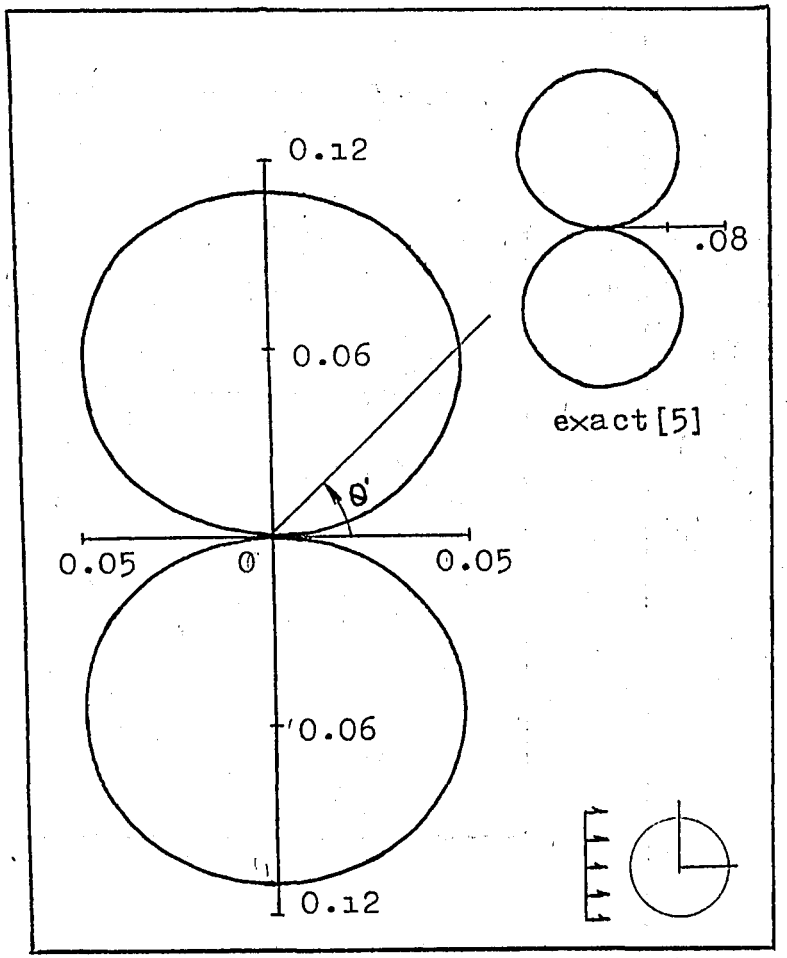

Fig. 2-a ka = 0.1

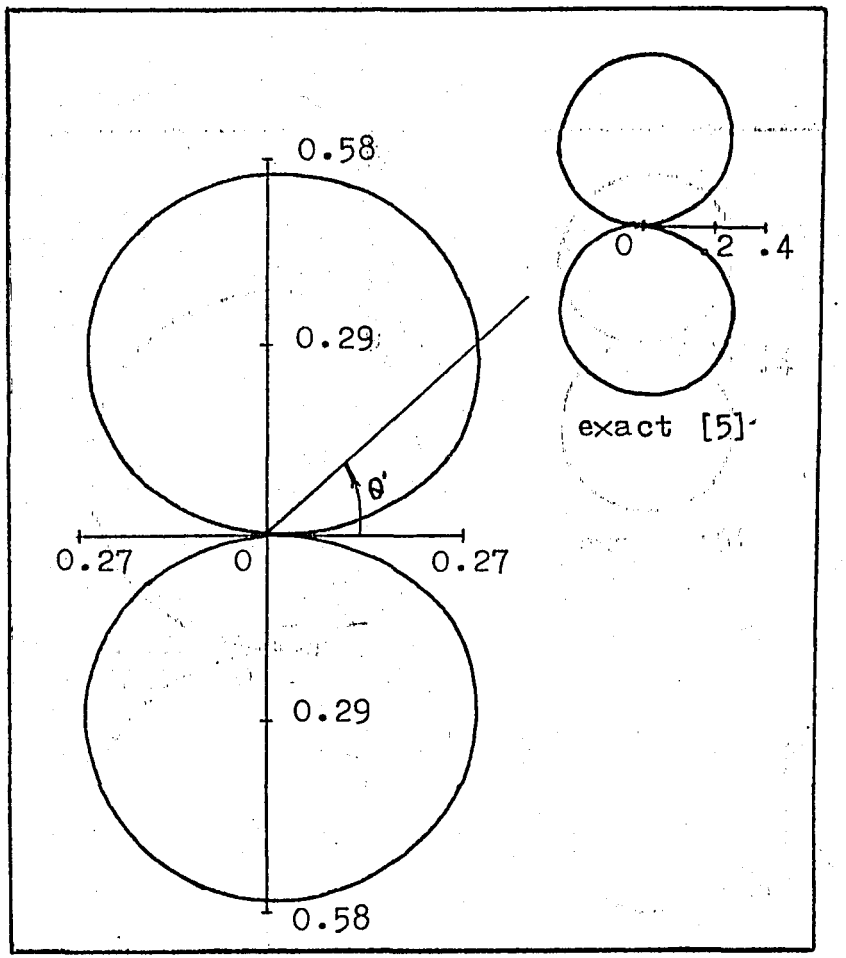

Fig. 2-b ka = 0.5

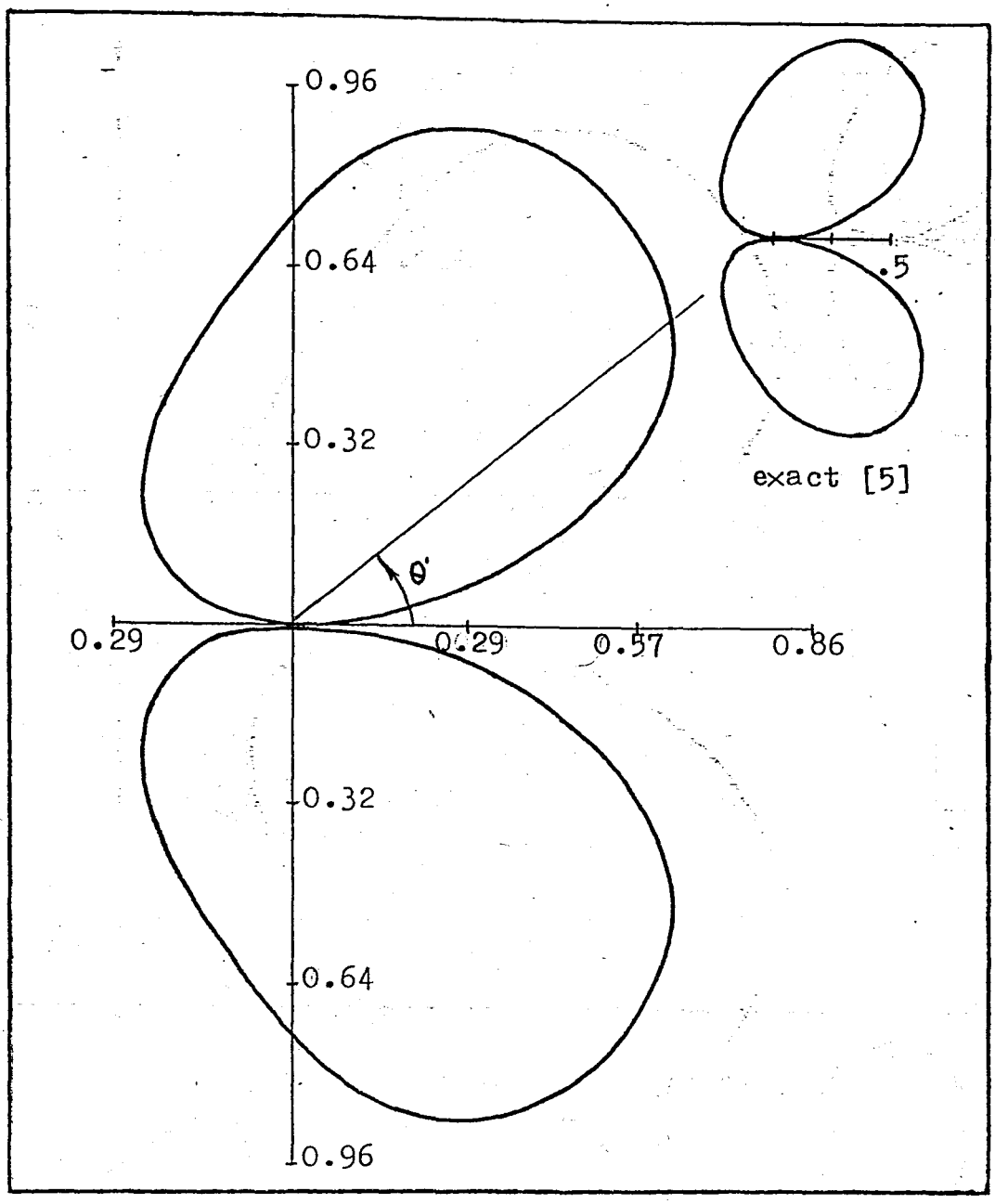

Fig. 2-c ka = 1.0

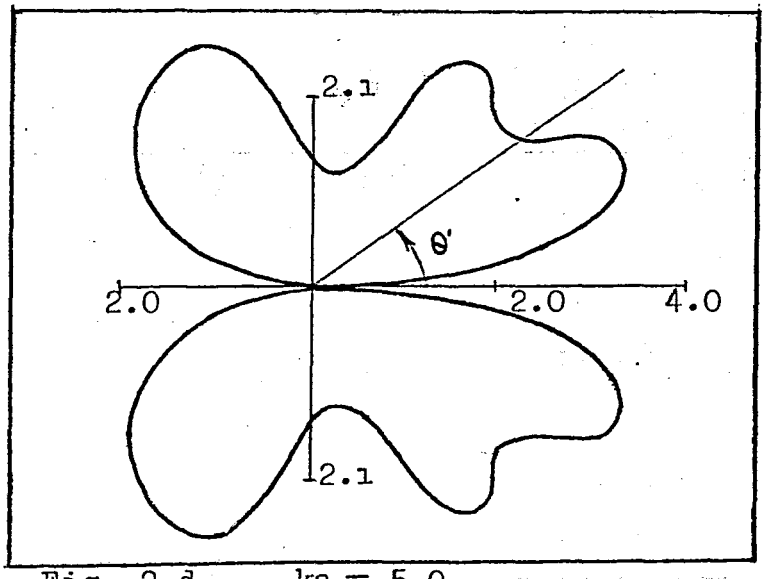

Fig. 2-d ka = 5.0

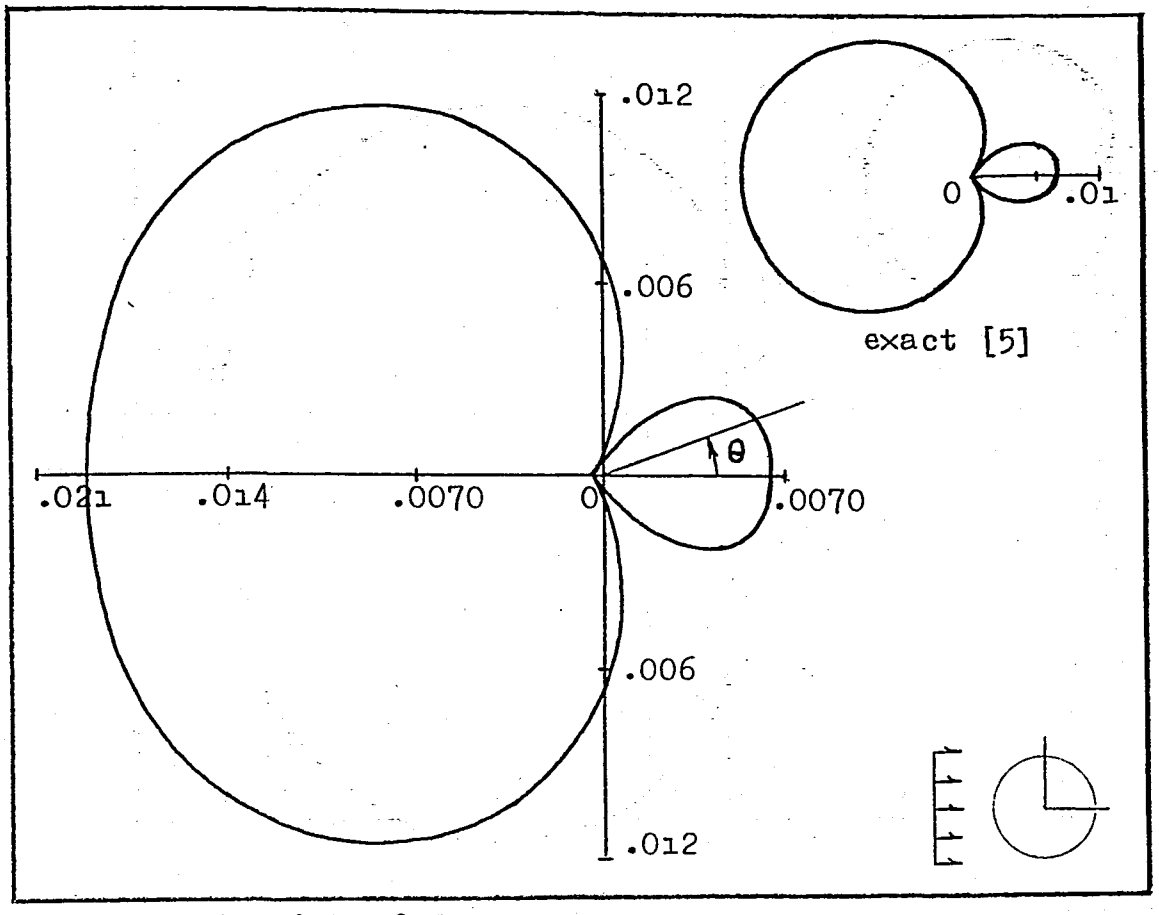

Fig. 3-a ka = 0.1

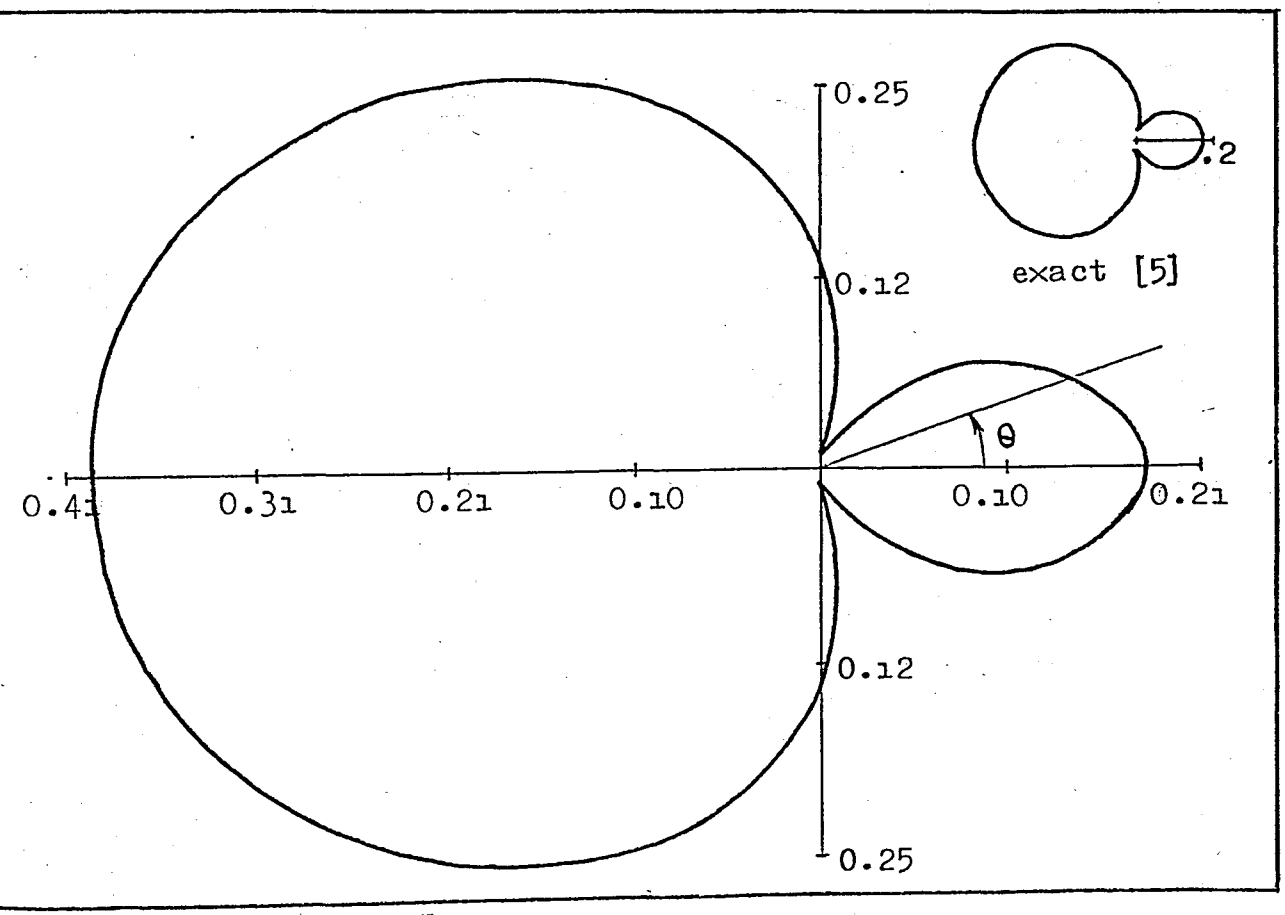

Fig. 3-b ka = 0.5

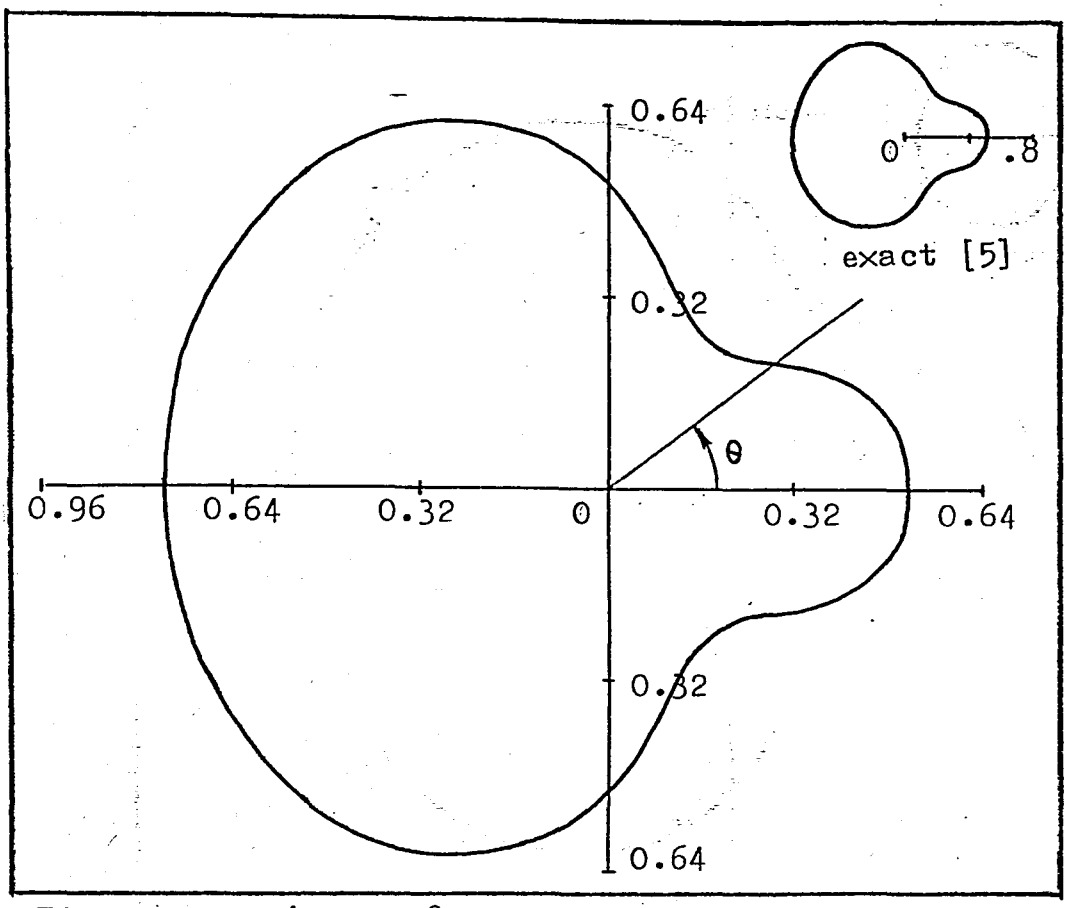

Fig. 3-c ka = 1.0

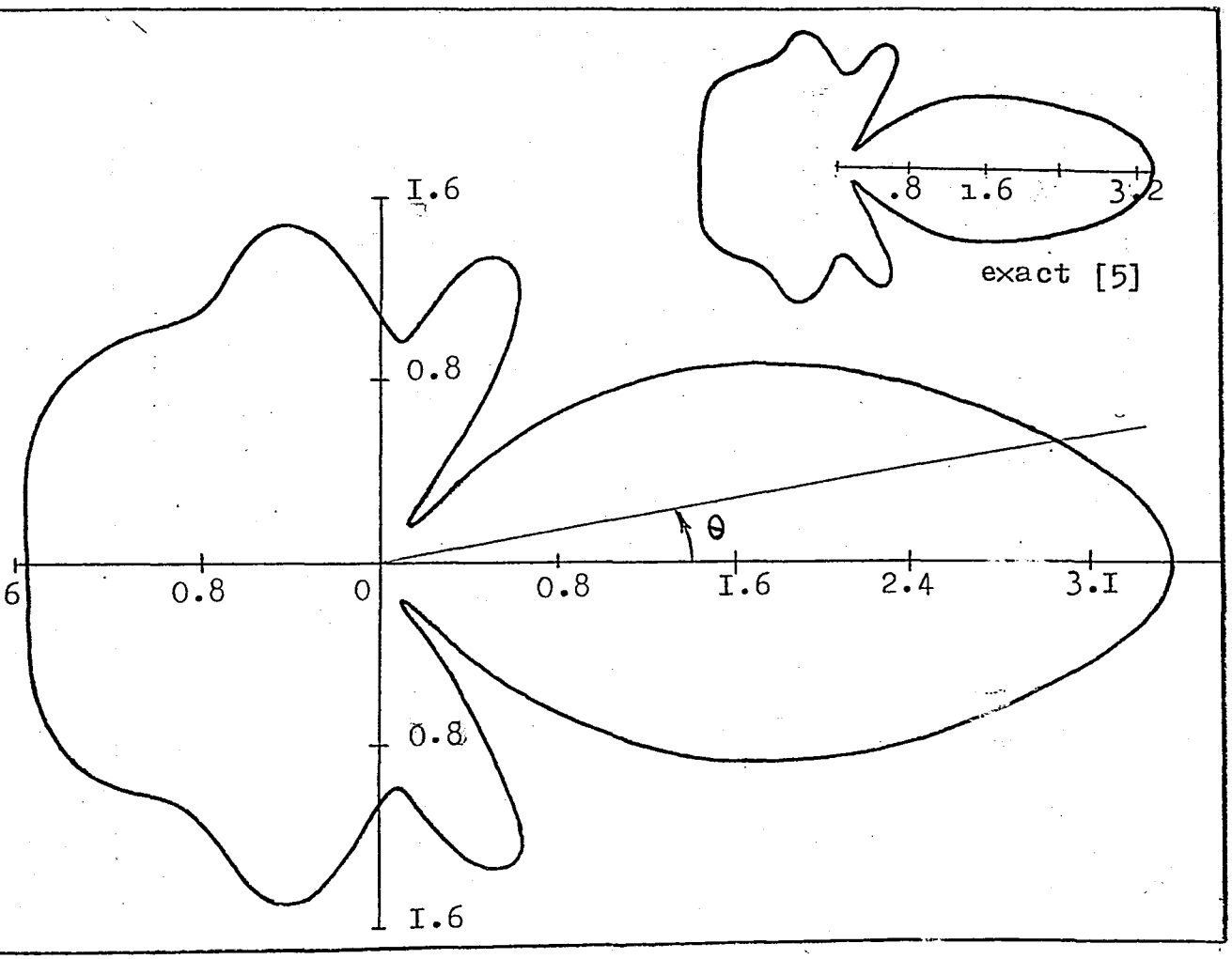

. 3-d ka = 5.0

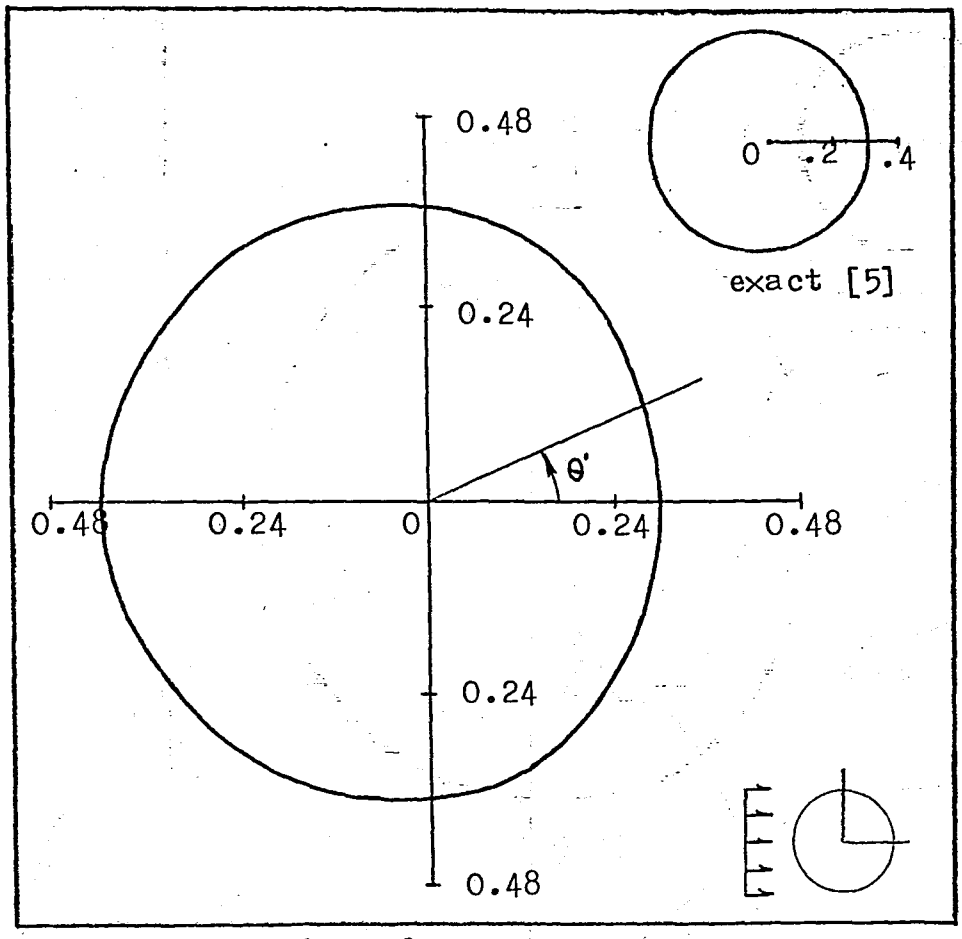

Fig. 4-a ka = 0.1

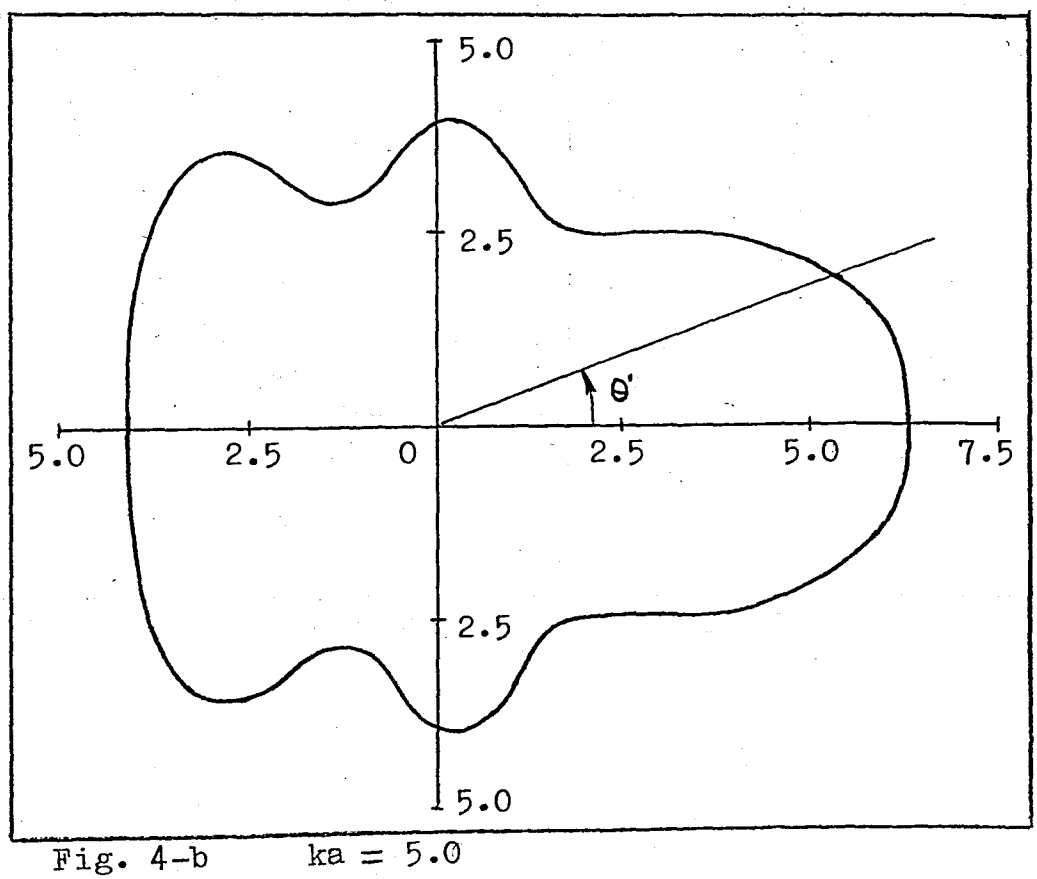

Fig. 4-b ka = 5.0

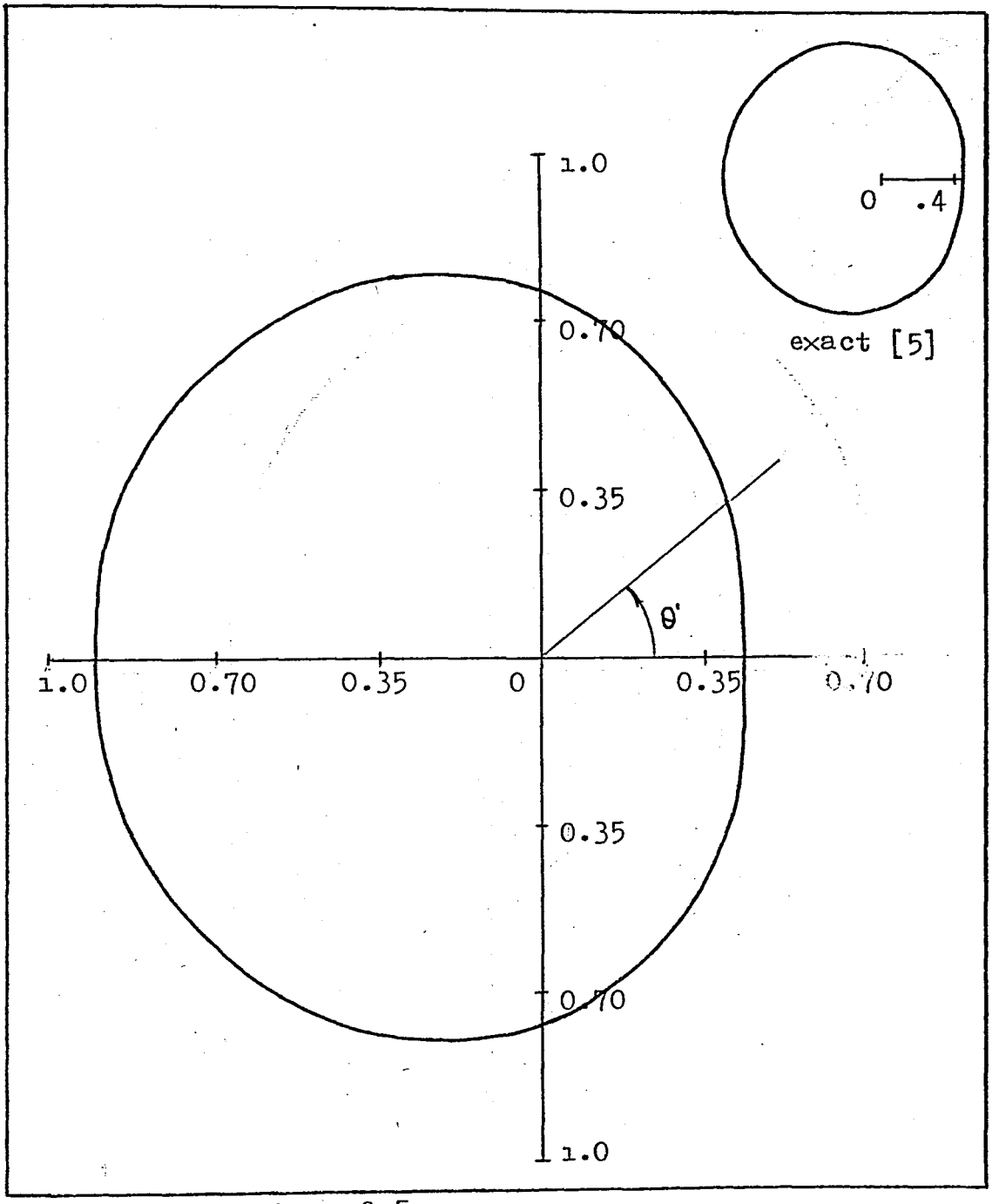

Fig. 4-c ka = 0.5

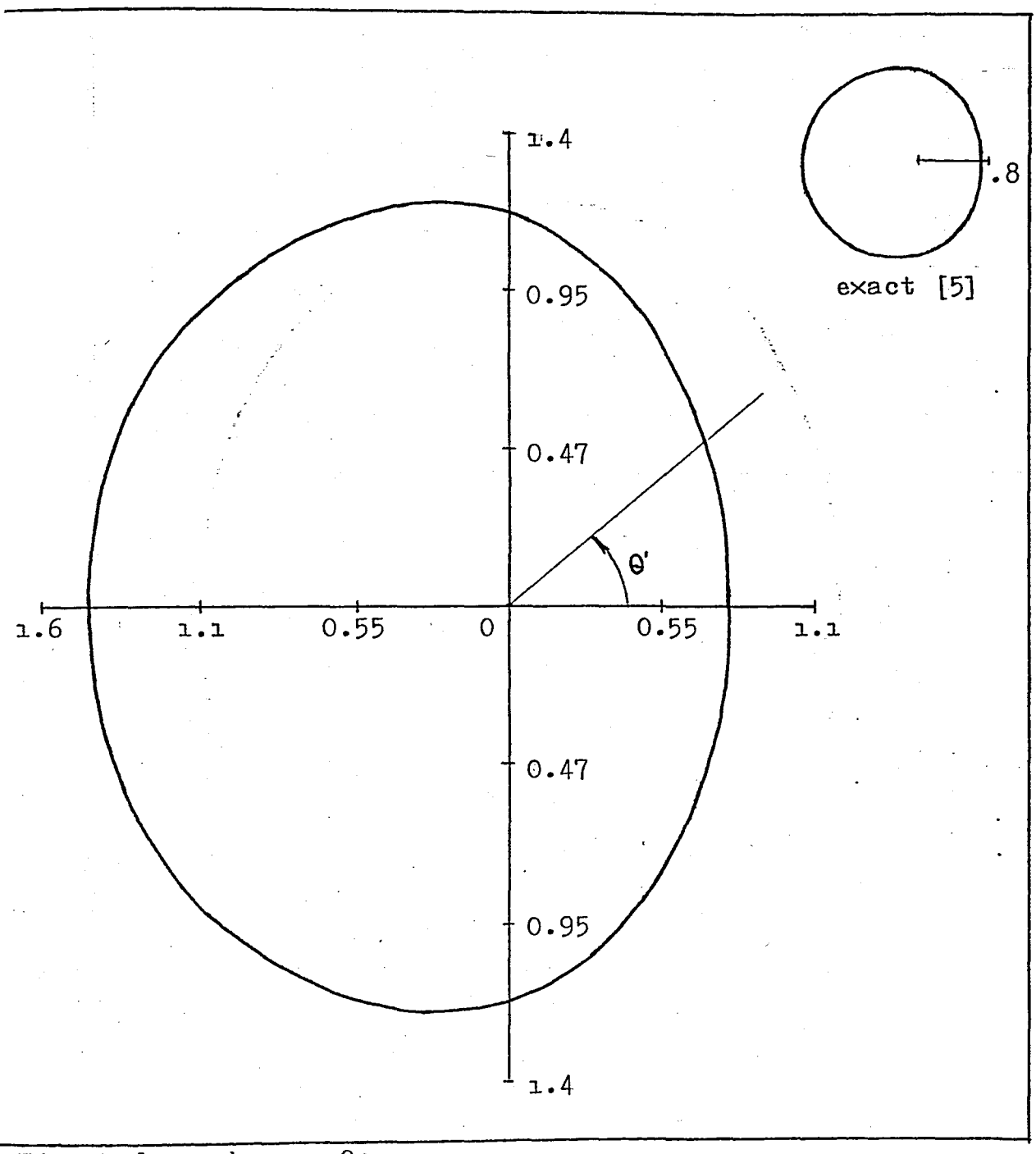

Fig. 4-d ka = 1.0

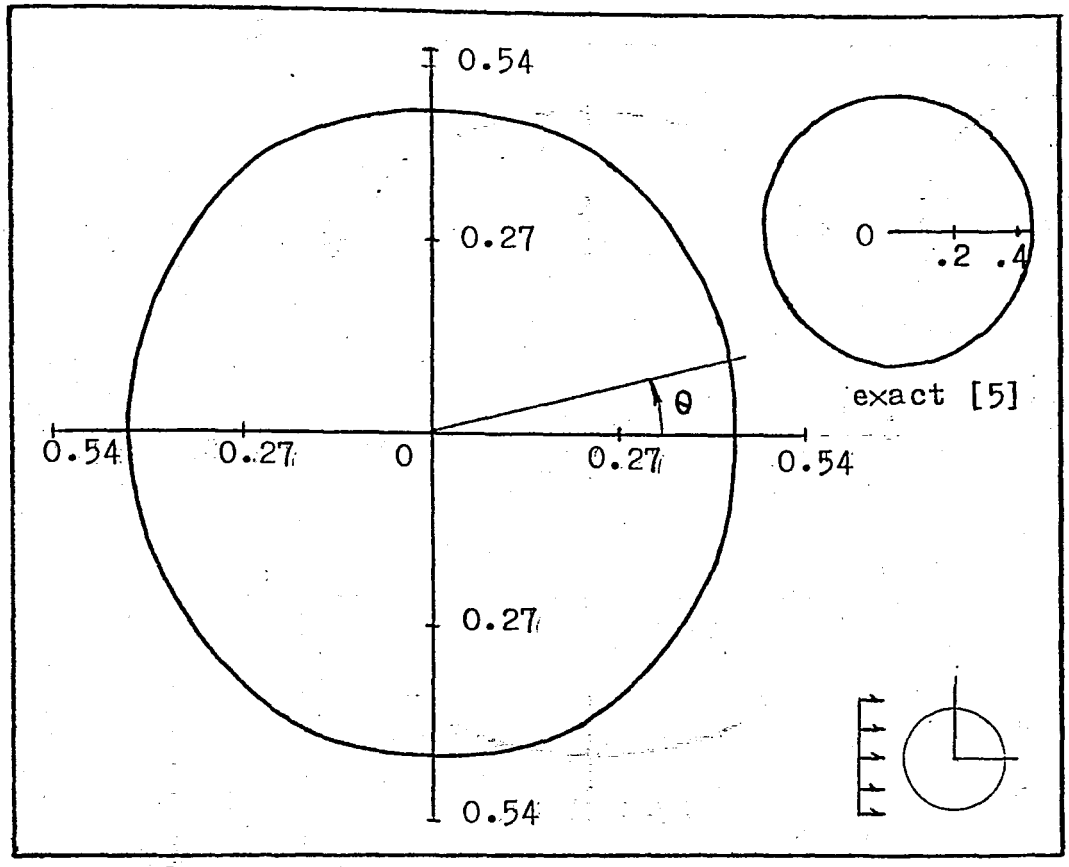

Fig. 5-a ka = 0.1

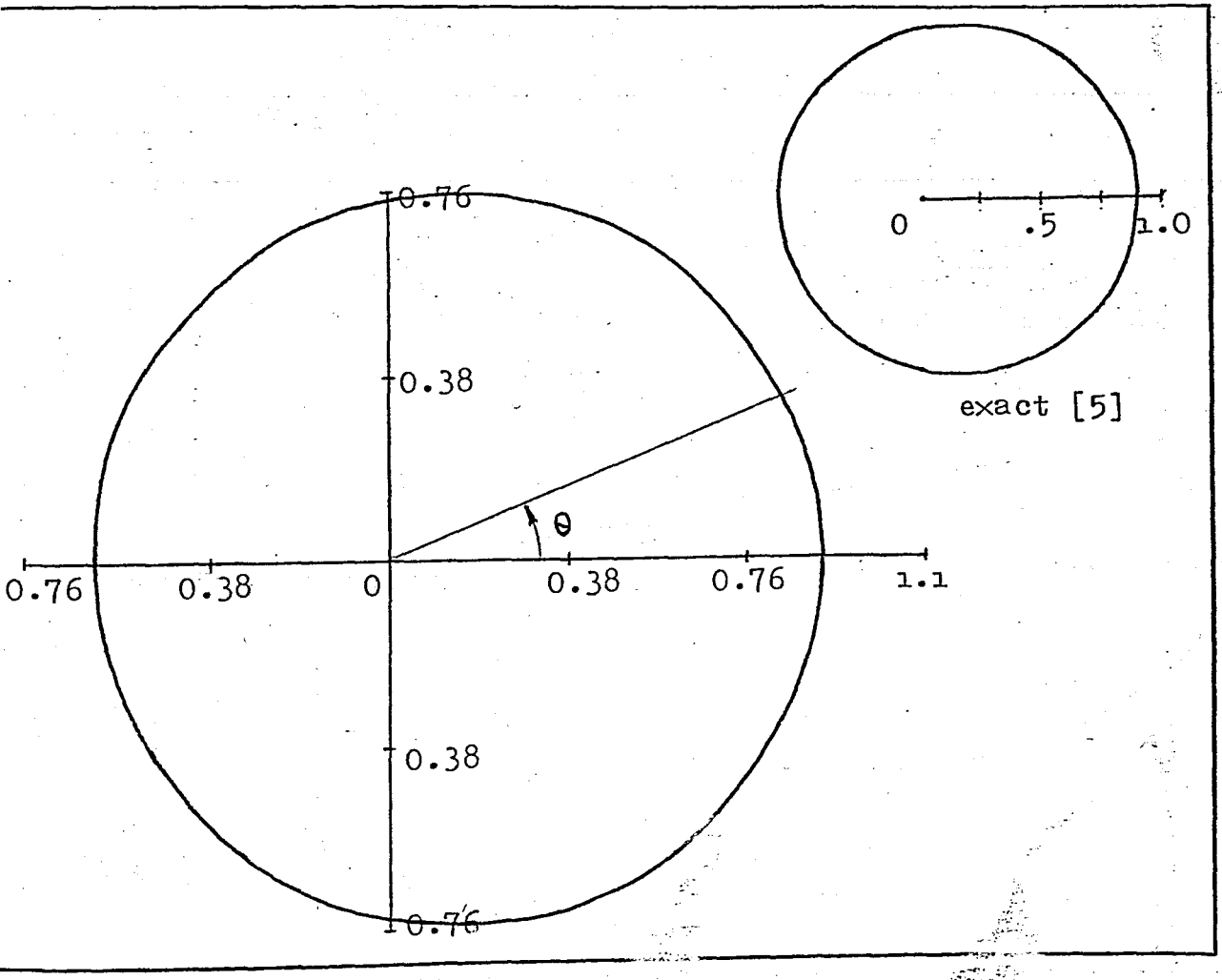

Fig. 5-b ka = 0.5

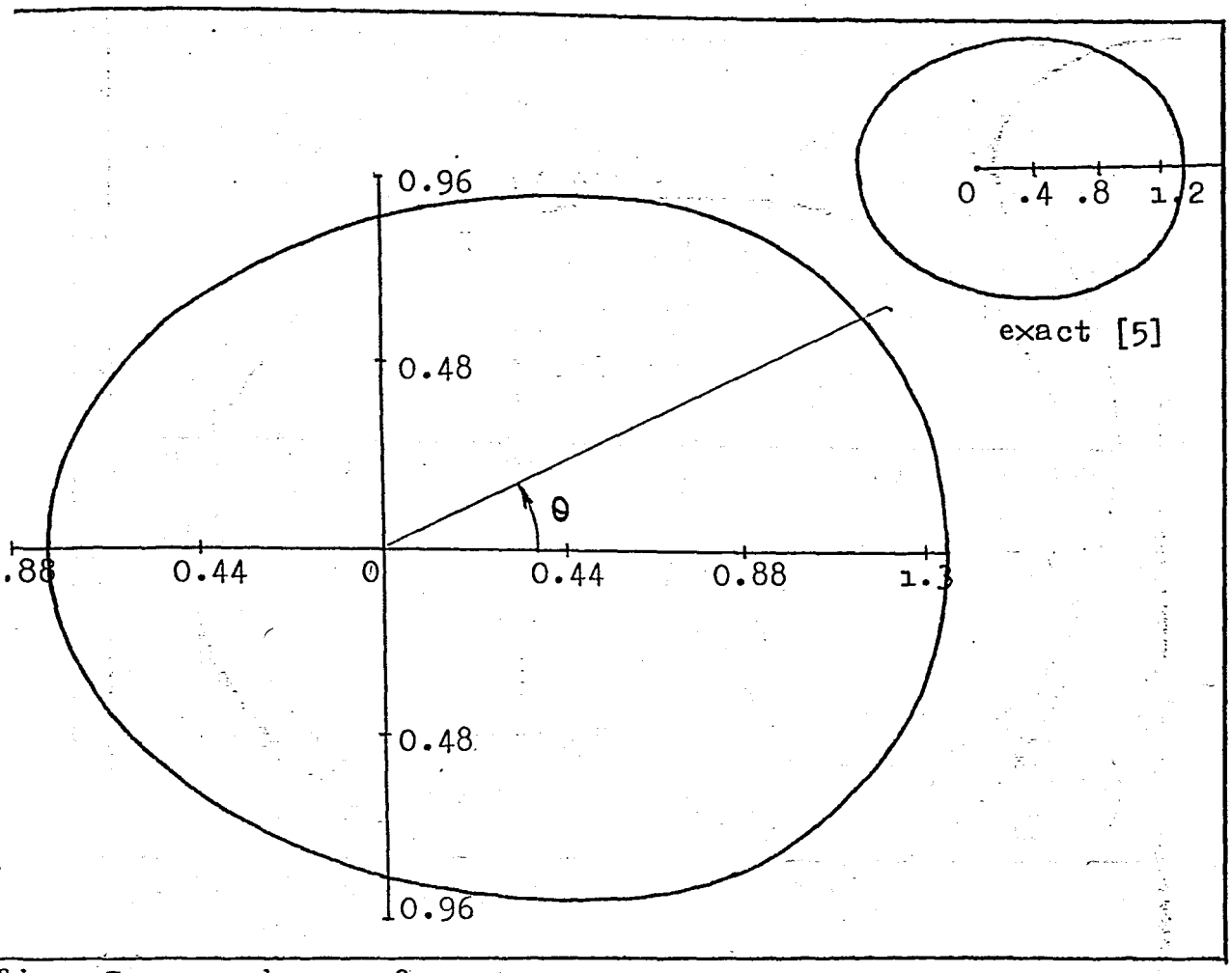

fig. 5-c ka = 1.0

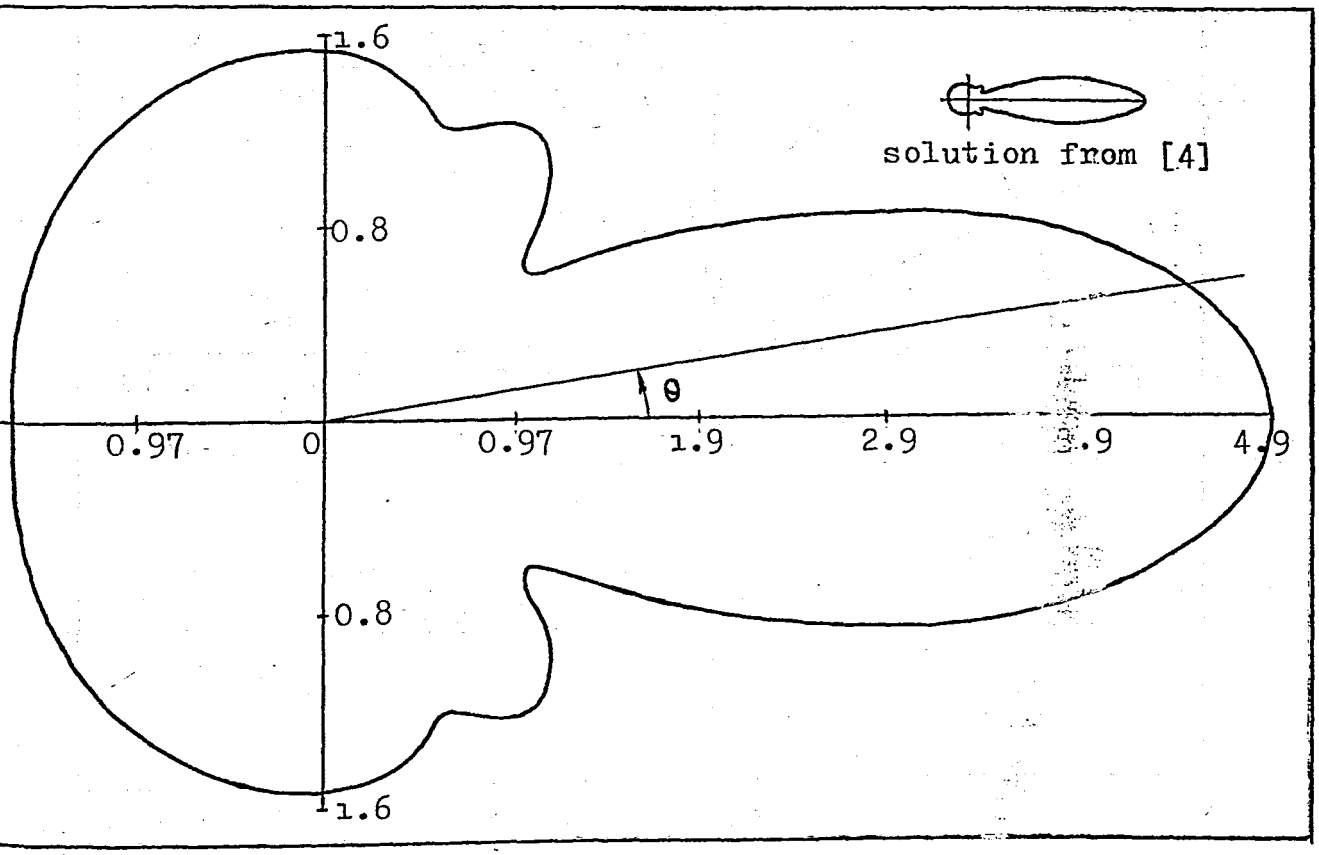

g. 5-d ka = 5.0

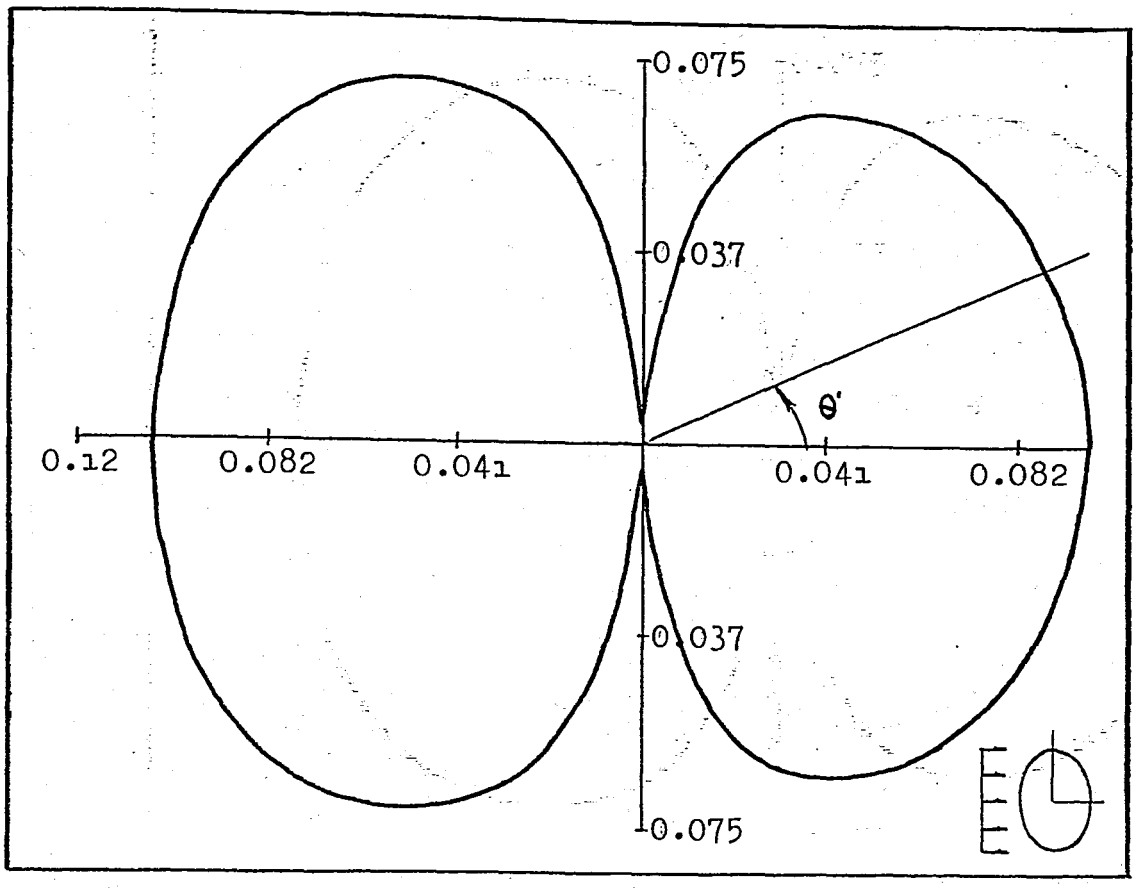

Fig. 6-a a = 0.5, b = 1.0, k = 0.1

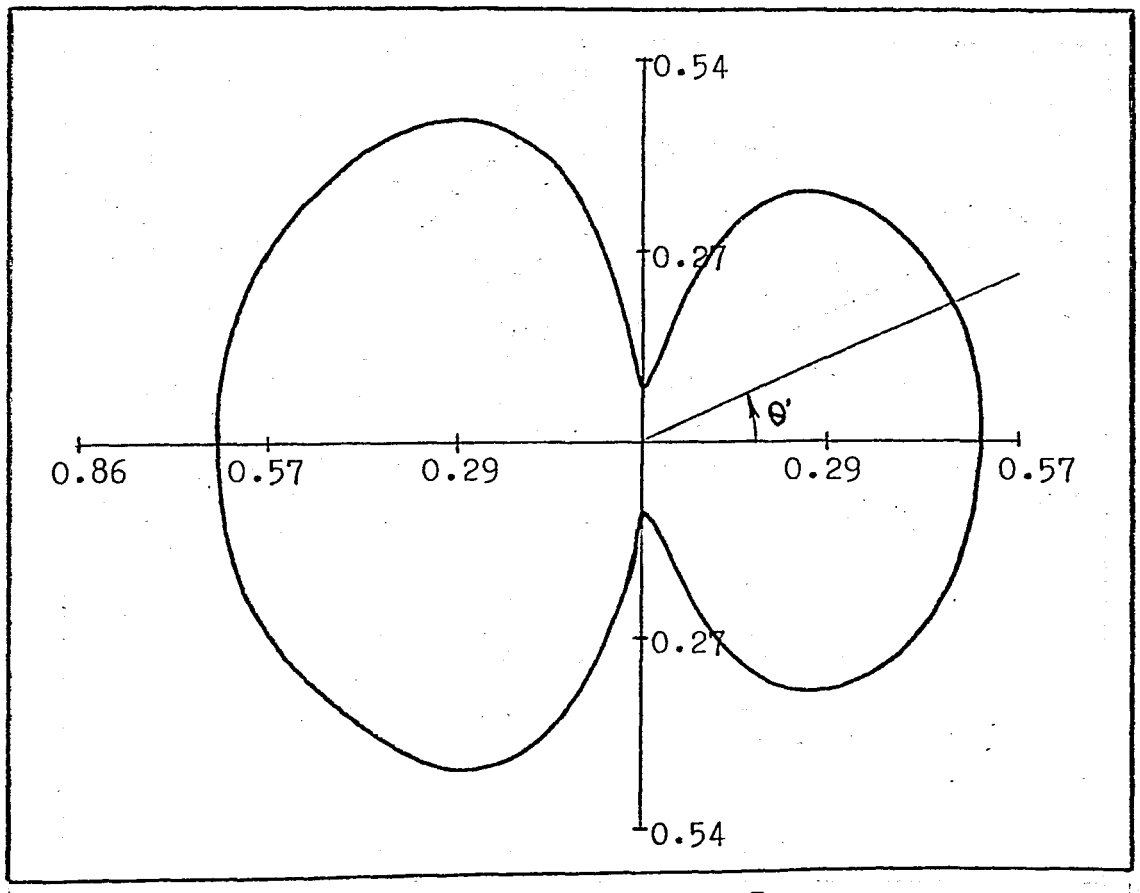

Fig. 6-b a = 0.5, b=1.0, k=0.5

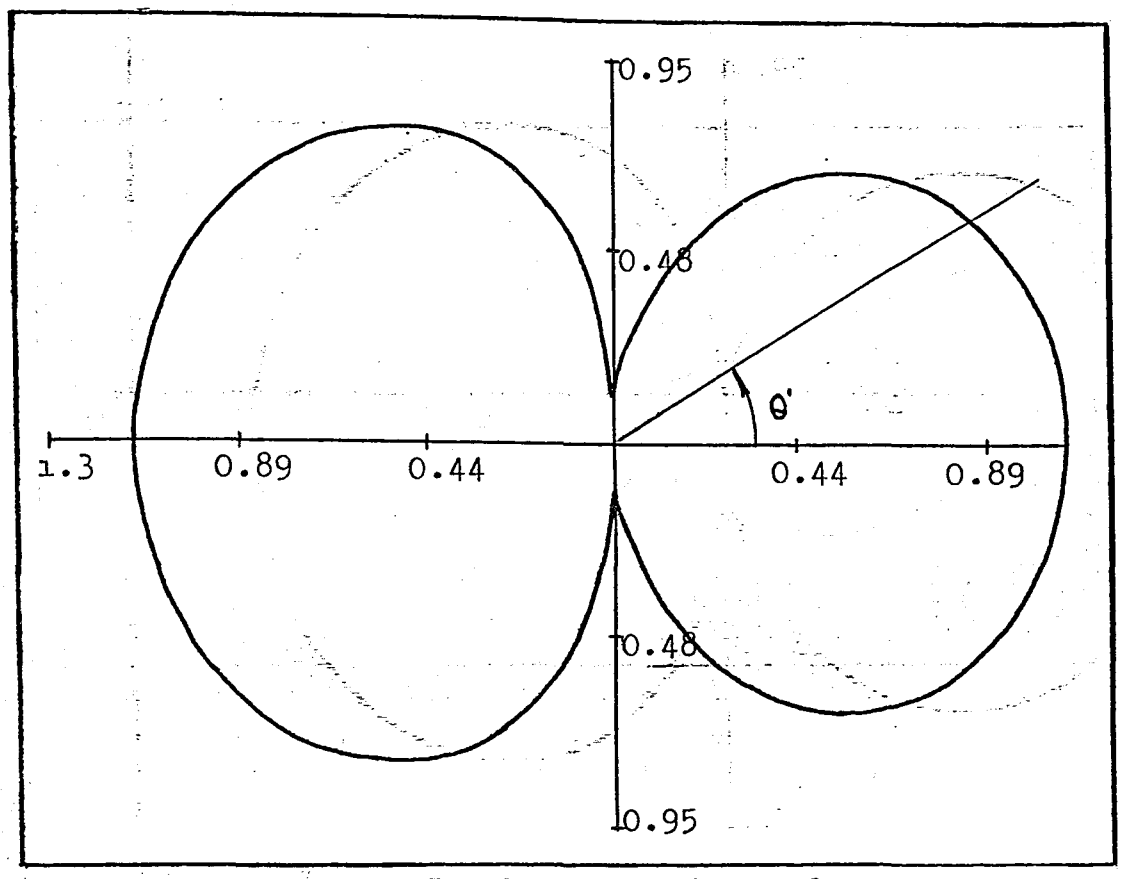

Fig. 6-c a = 0.5, b = 1.0, k = 1.0

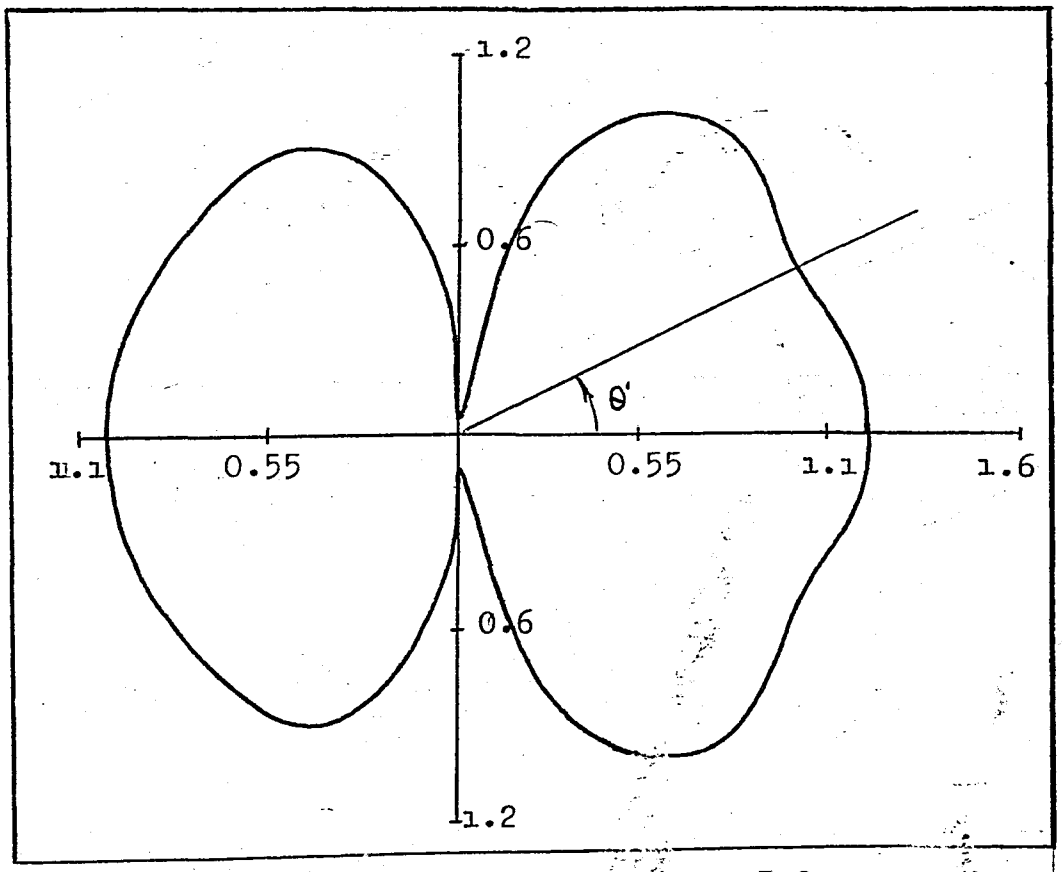

Fig. 6-d a = 0.5, b = 1.0, k = 5.0

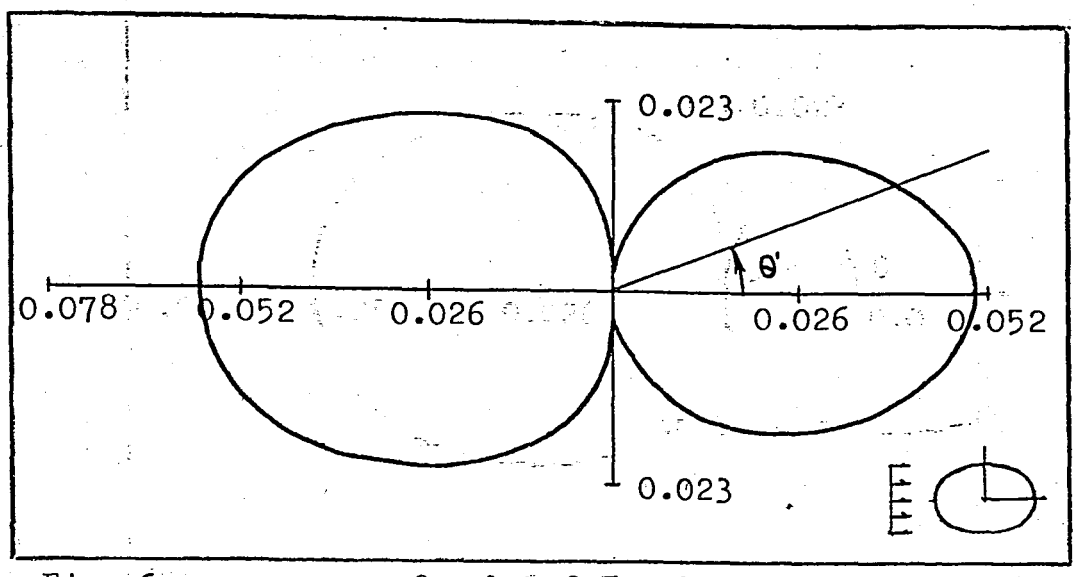

Fig. 6-e a = 1.0, b = 0.5, k = 0.1

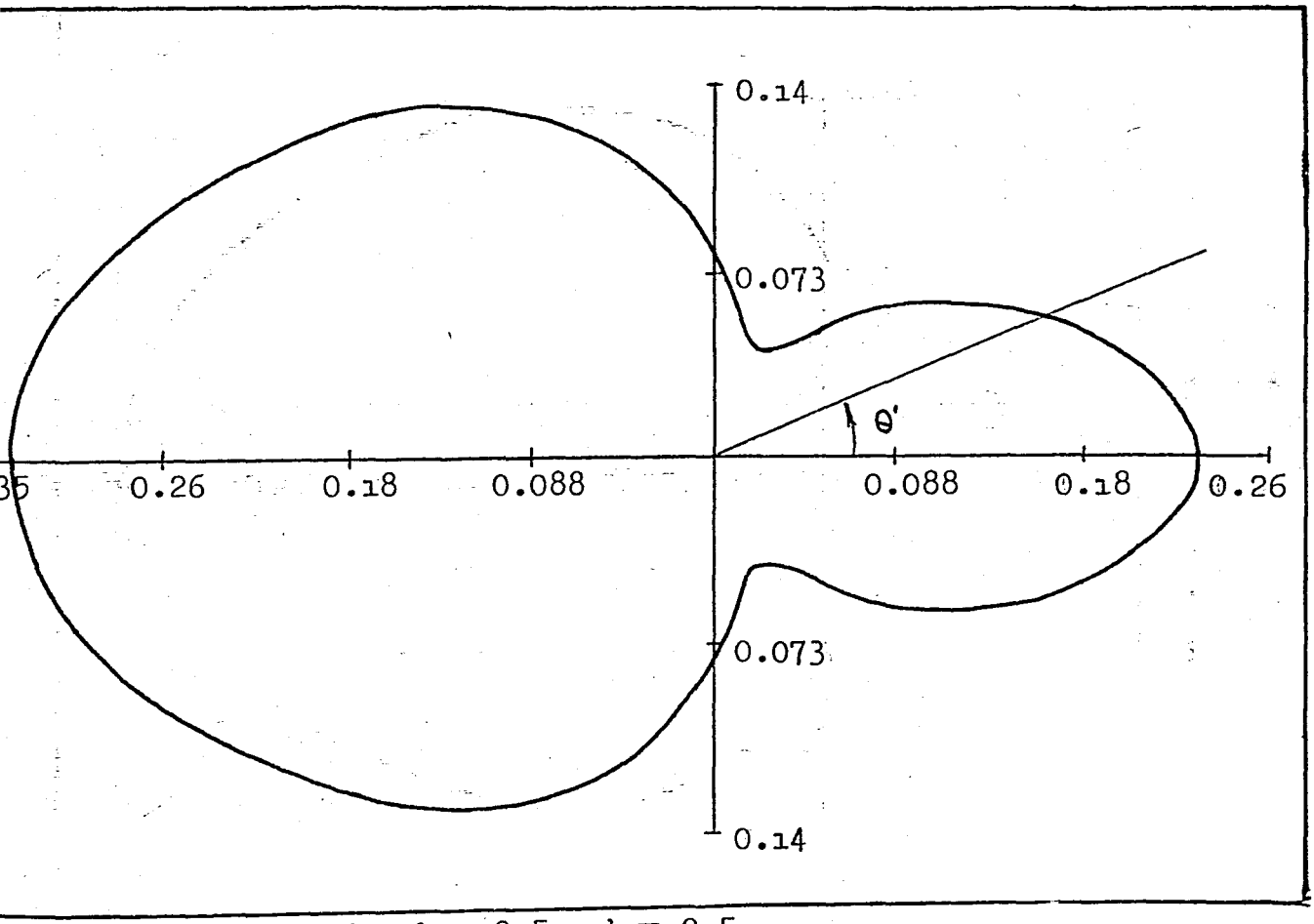

ig. 6-f a = 1.0, b = 0.5, k = 0.5

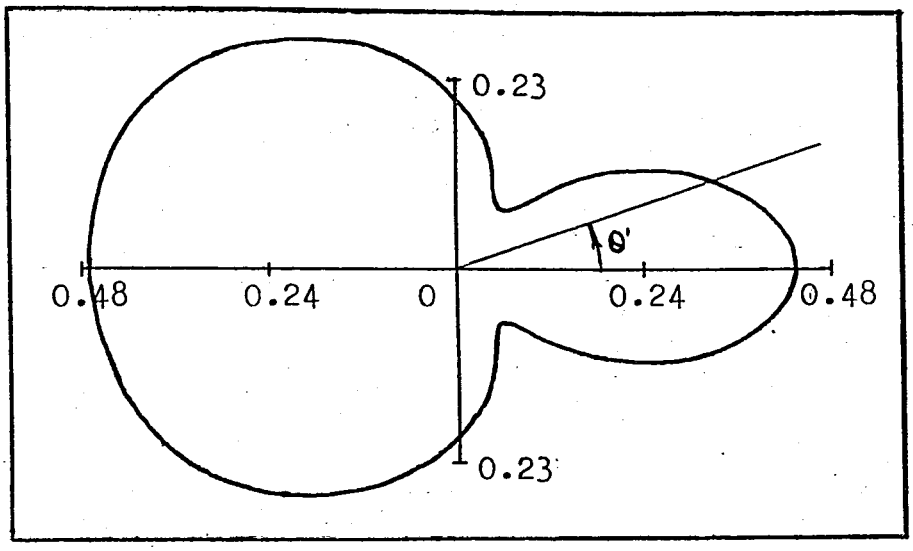

Fig. 6-g a = 1.0, b = 0.5, k = 1.0

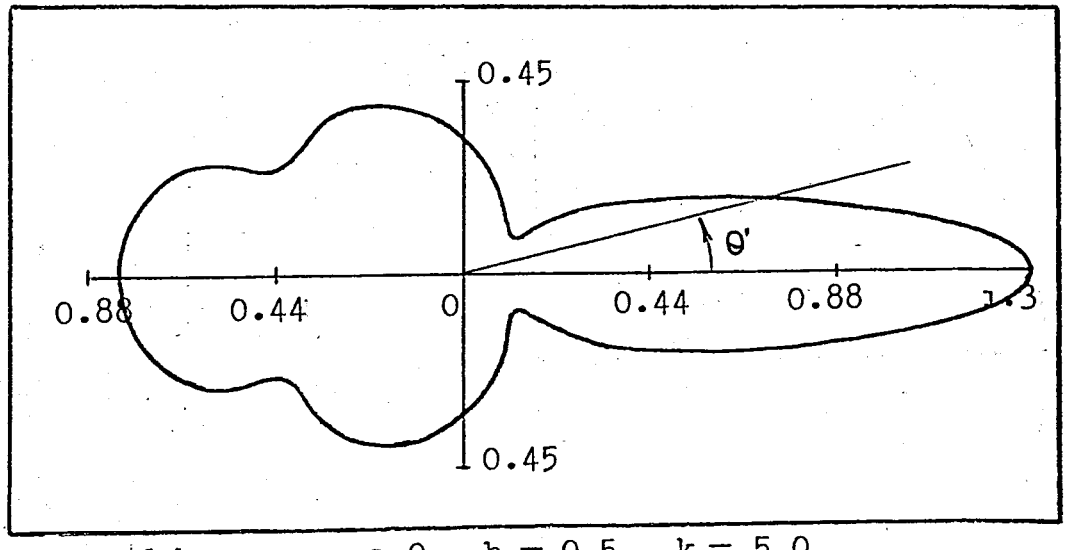

Fig. 6-h a = 1.0, b = 0.5, k = 5.0

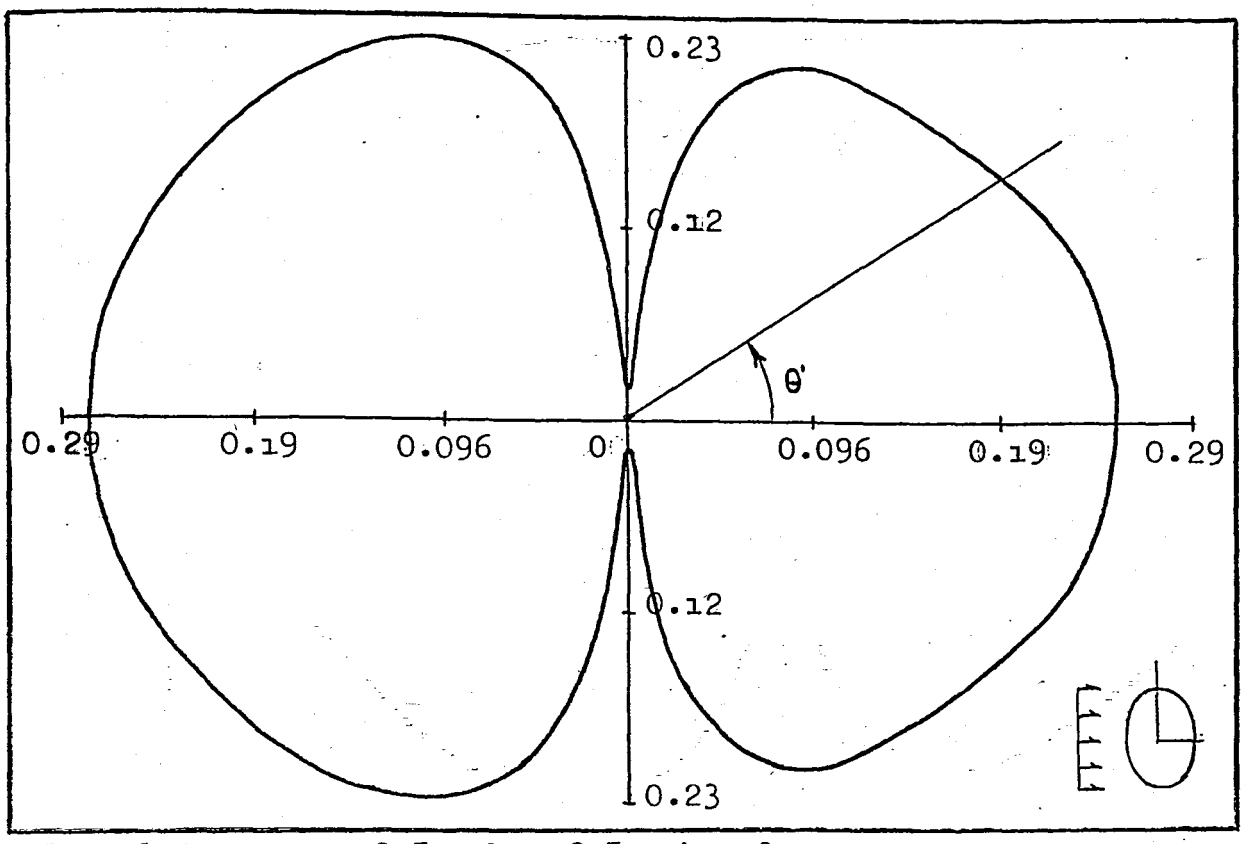

Fig. 6-i a = 0.5, b = 2.5, k = 0.1

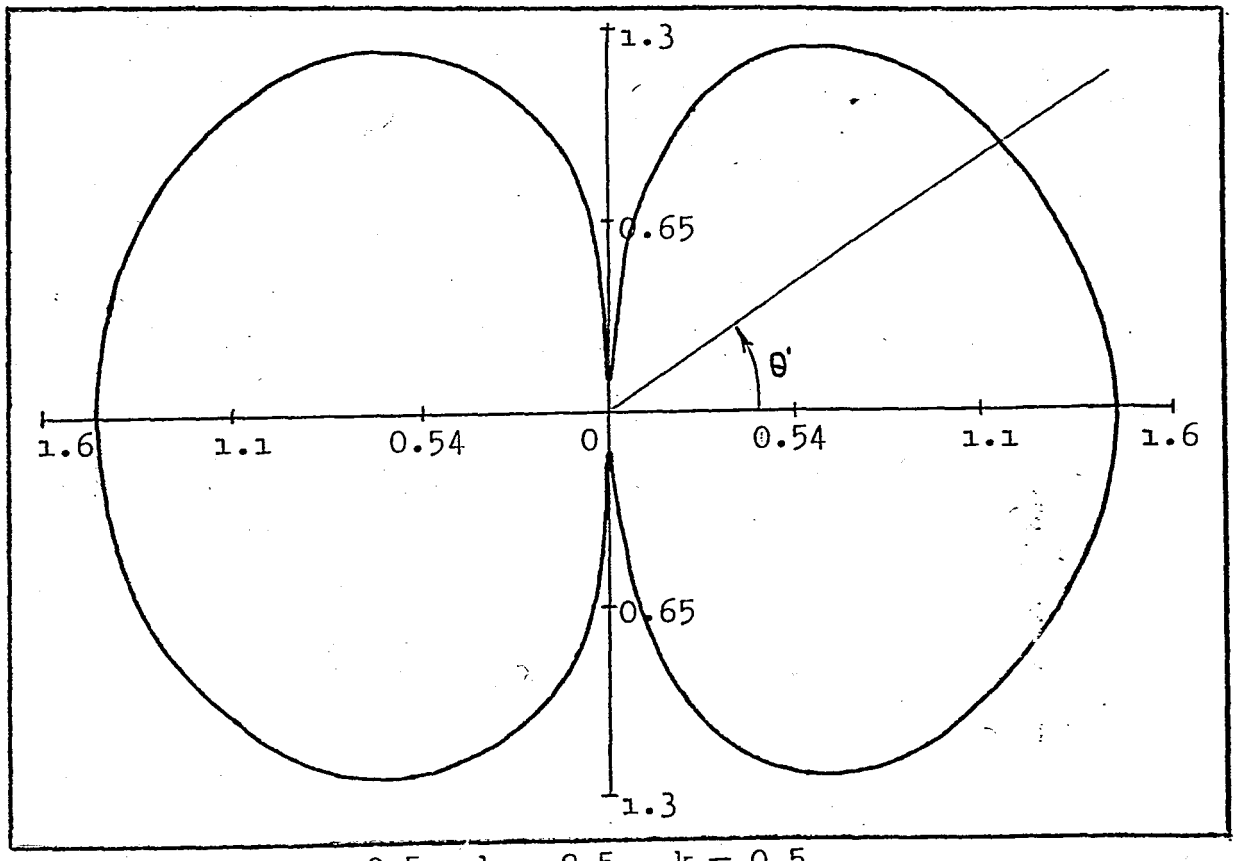

Fig. 6-j a = 0.5, b = 2.5, k = 0.5

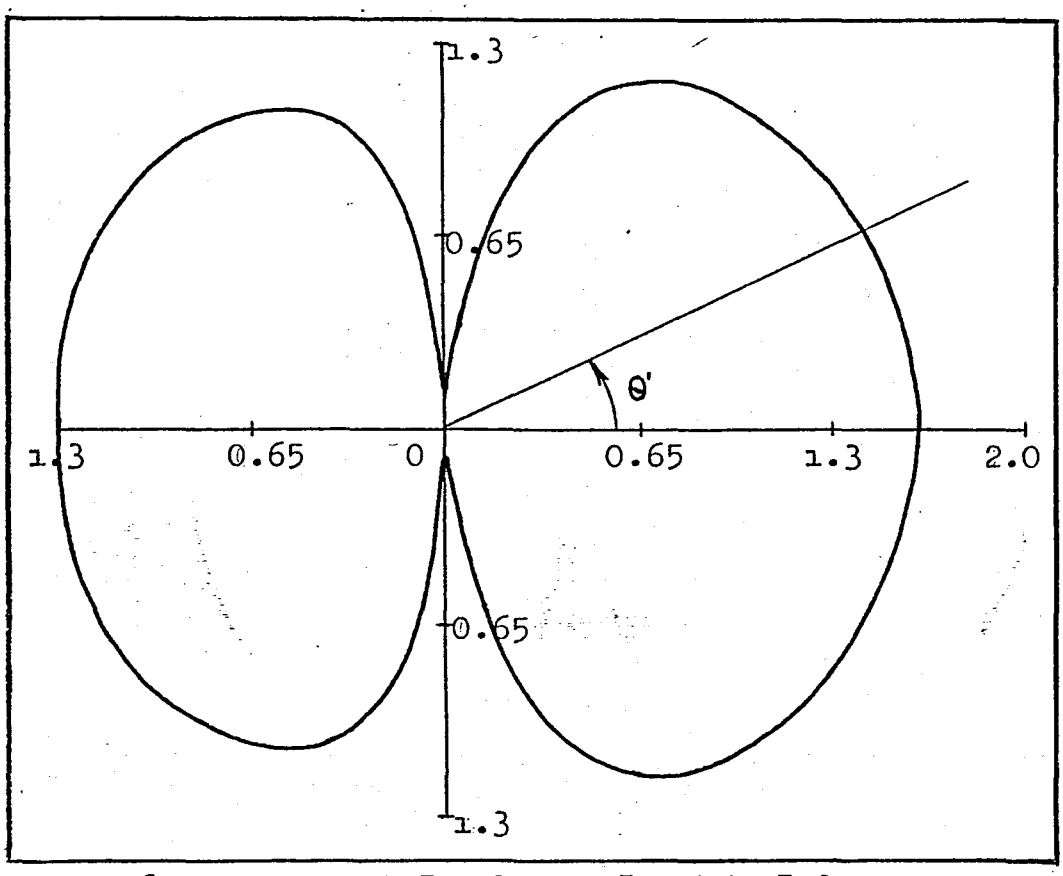

Fig. 6-k a = 0.5, b = 2.5, k = 5.0

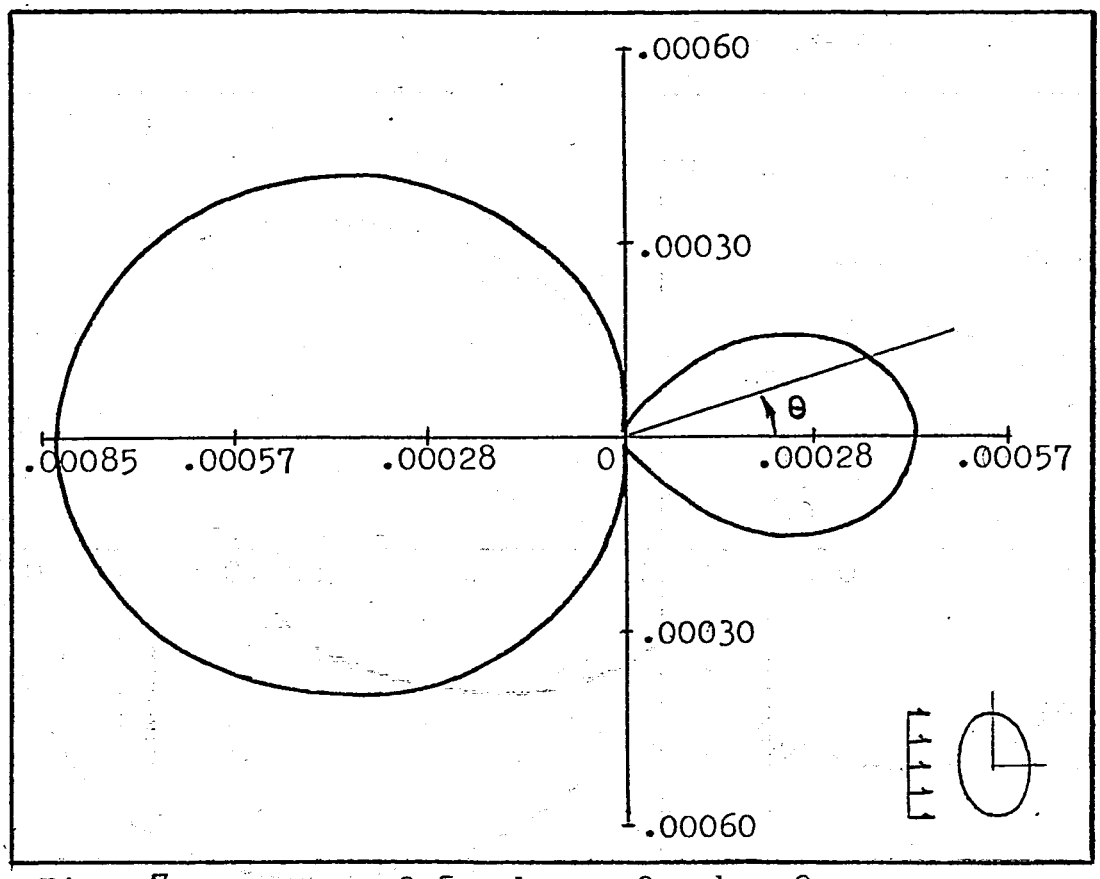

Fig. 7-a a = 0.5, b = 1.0, k = 0.1

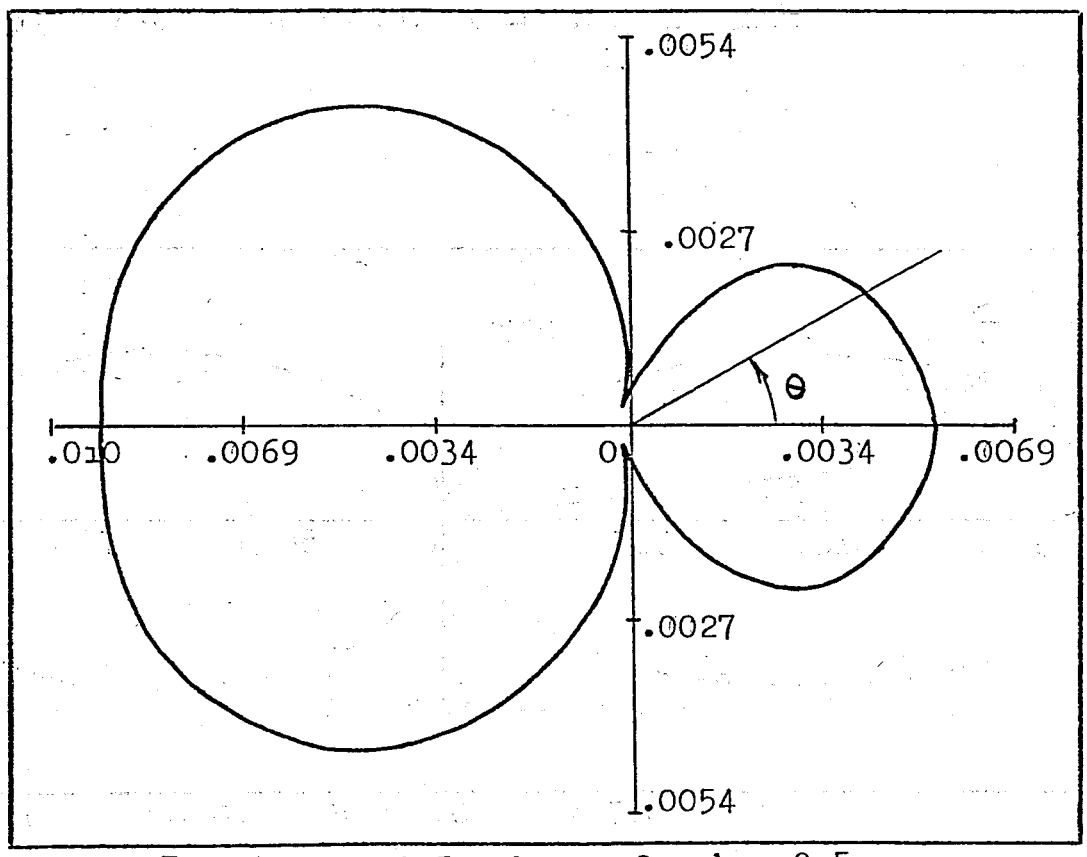

Fig. 7-b a = 0.5, b = 1.0, k = 0.5

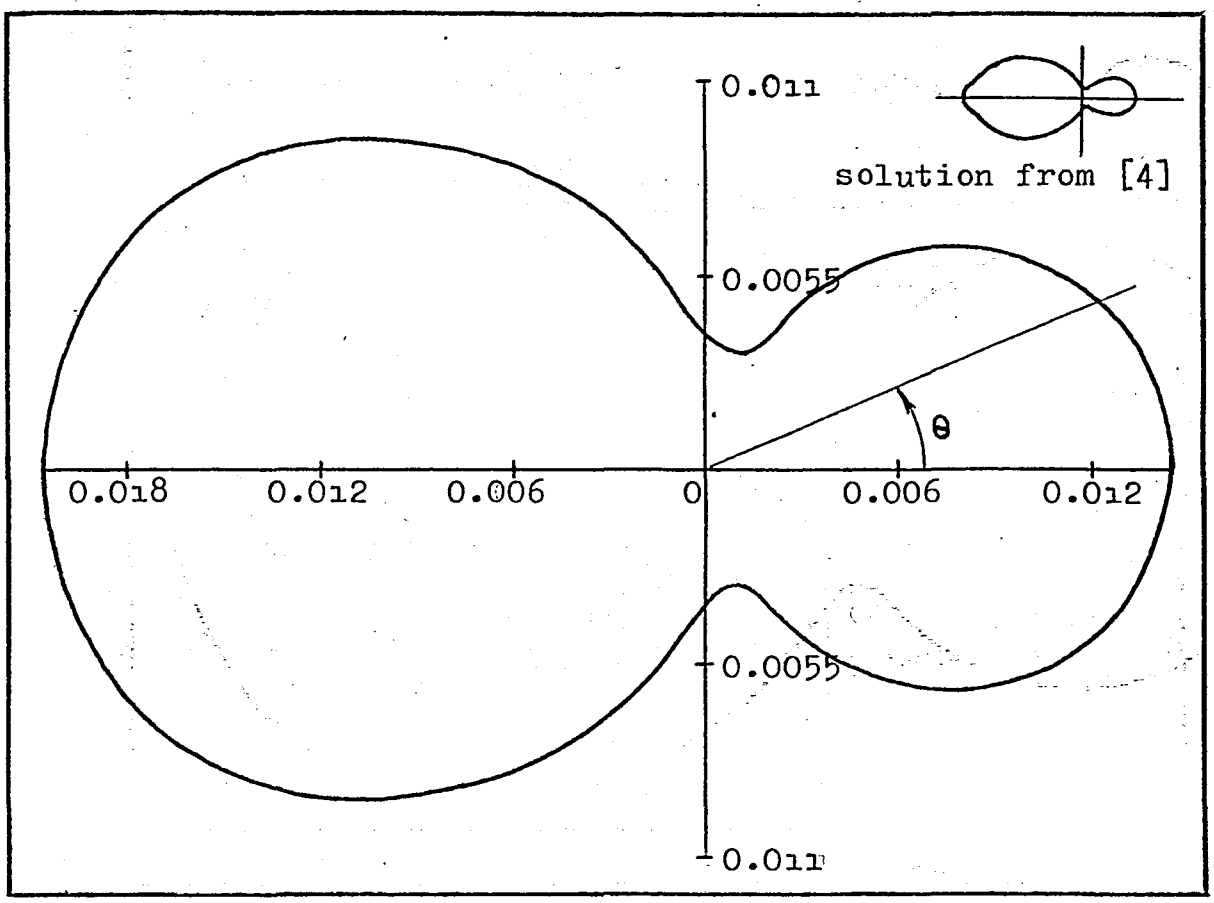

Fig. 7-c a = 0.5, b = 1.0, k = 1.0

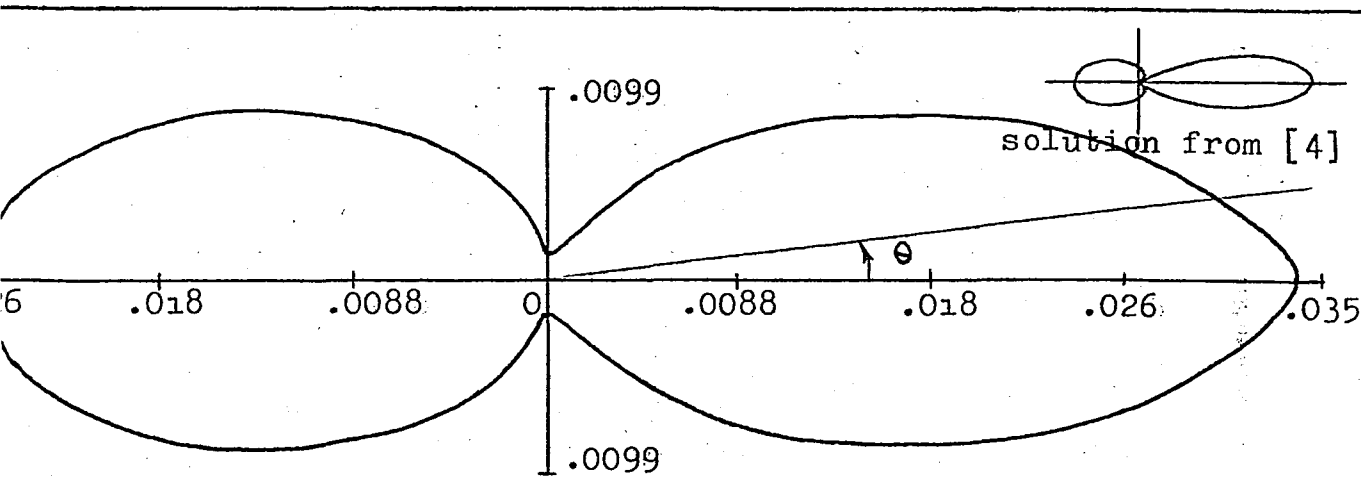

g. 7-d a = 0.5, b = 1.0, k = 5.0

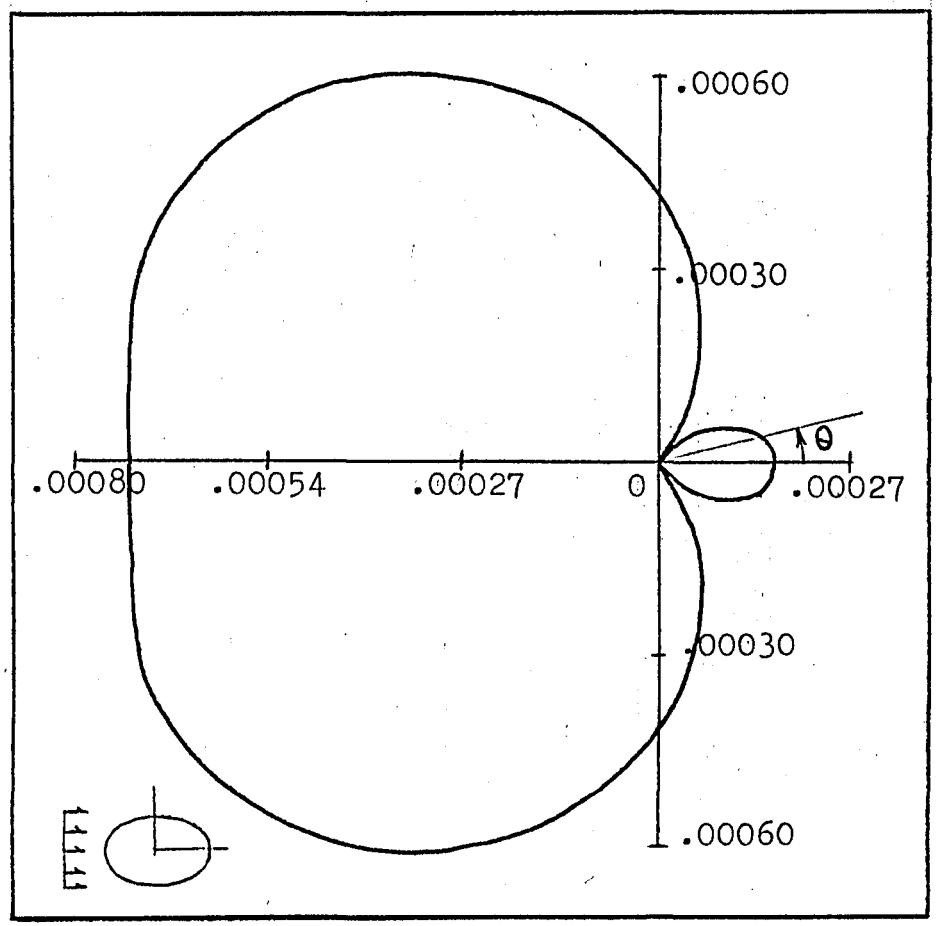

Fig. 7-e a = 1.0, b = 0.5, k = 0.1

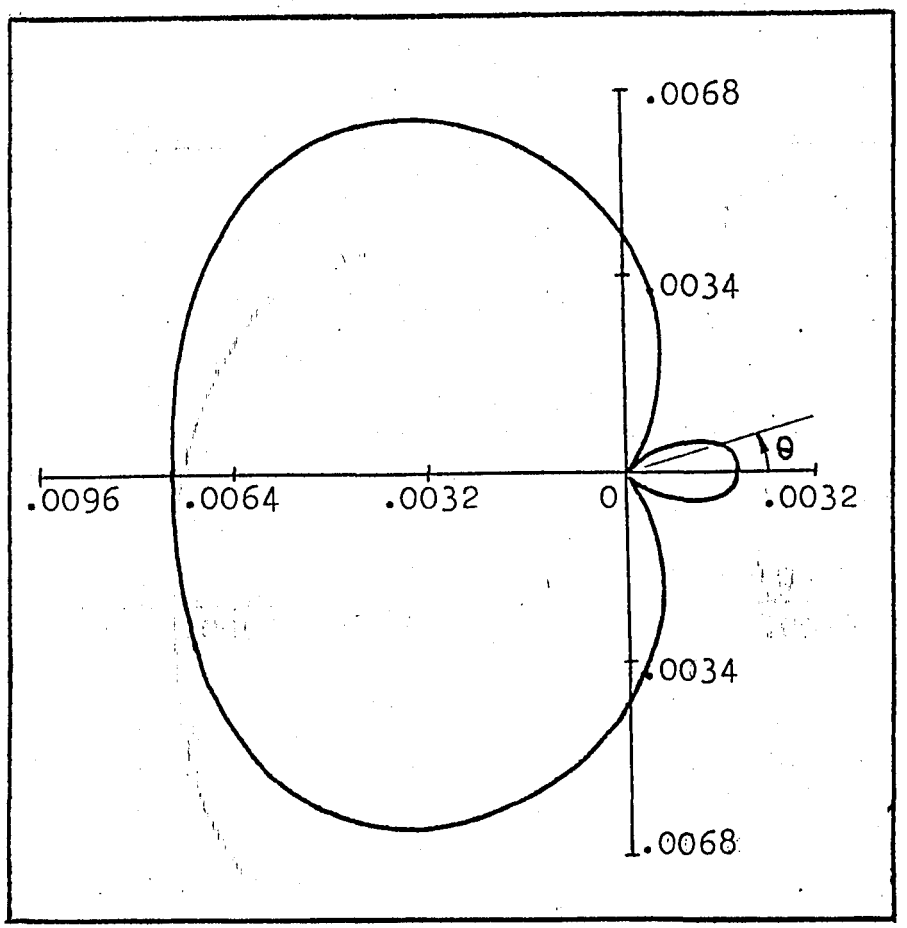

Fig. 7-f a = 1.0, b = 0.5, k = 0.5

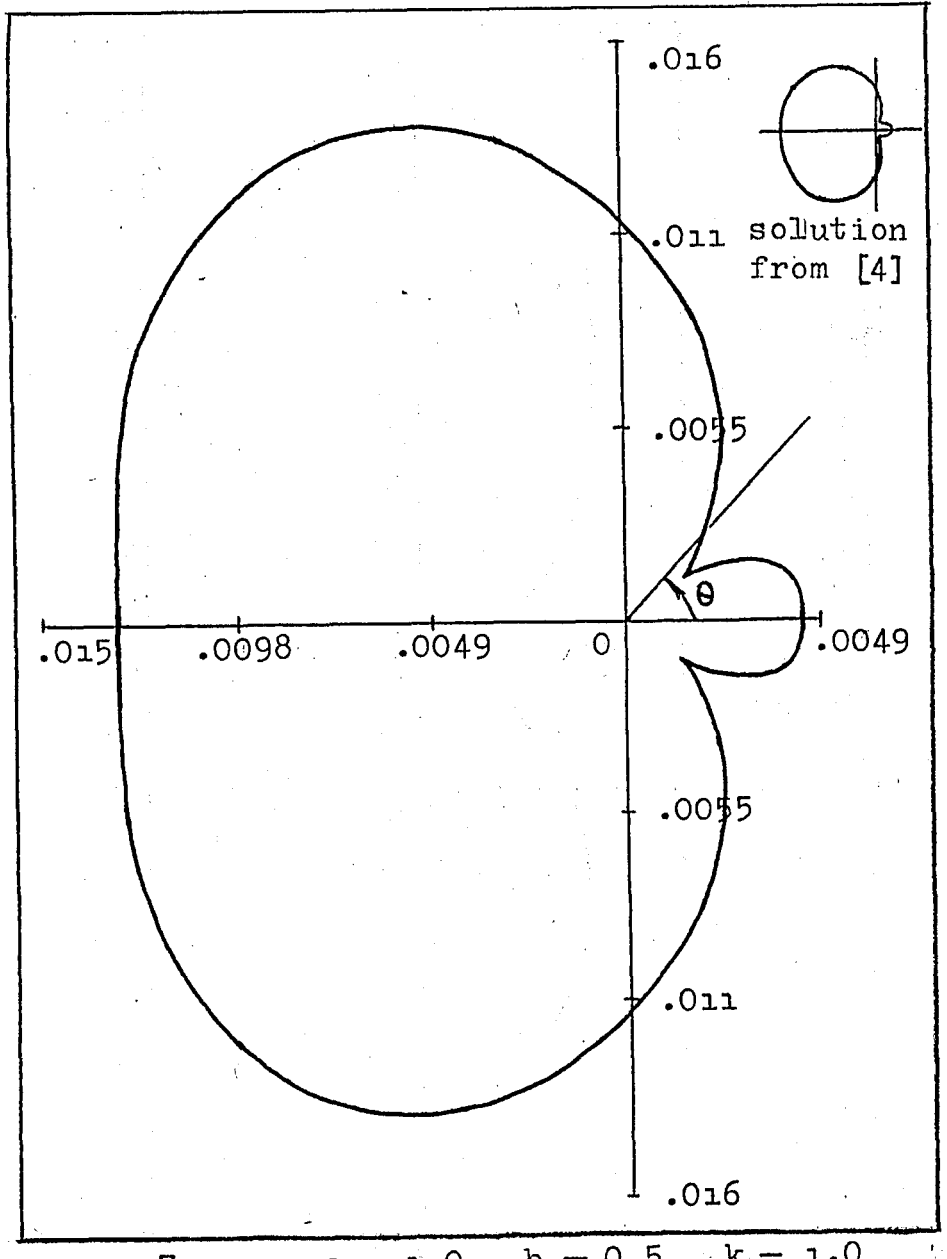

Fig. 7-g a = 1.0, b = 0.5, k = 1.0

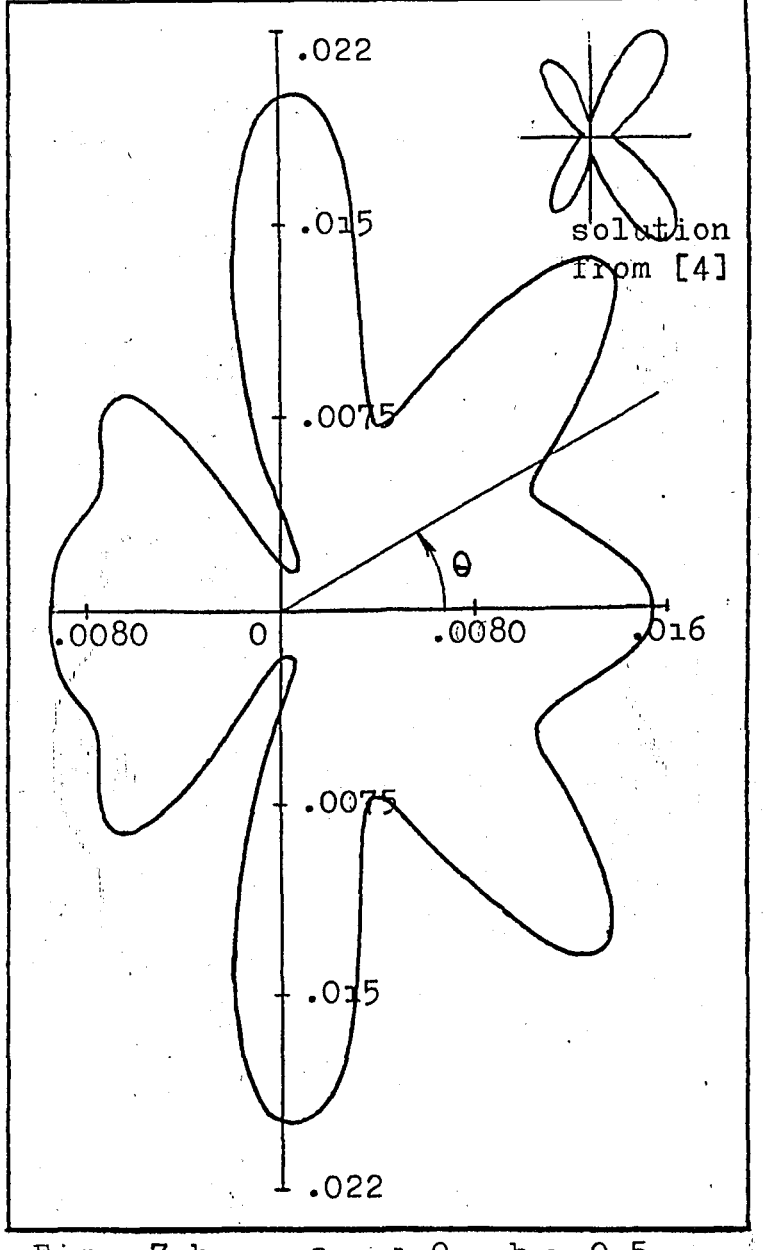

Fig. 7-h a = 1.0, b = 0.5, k = 5.0

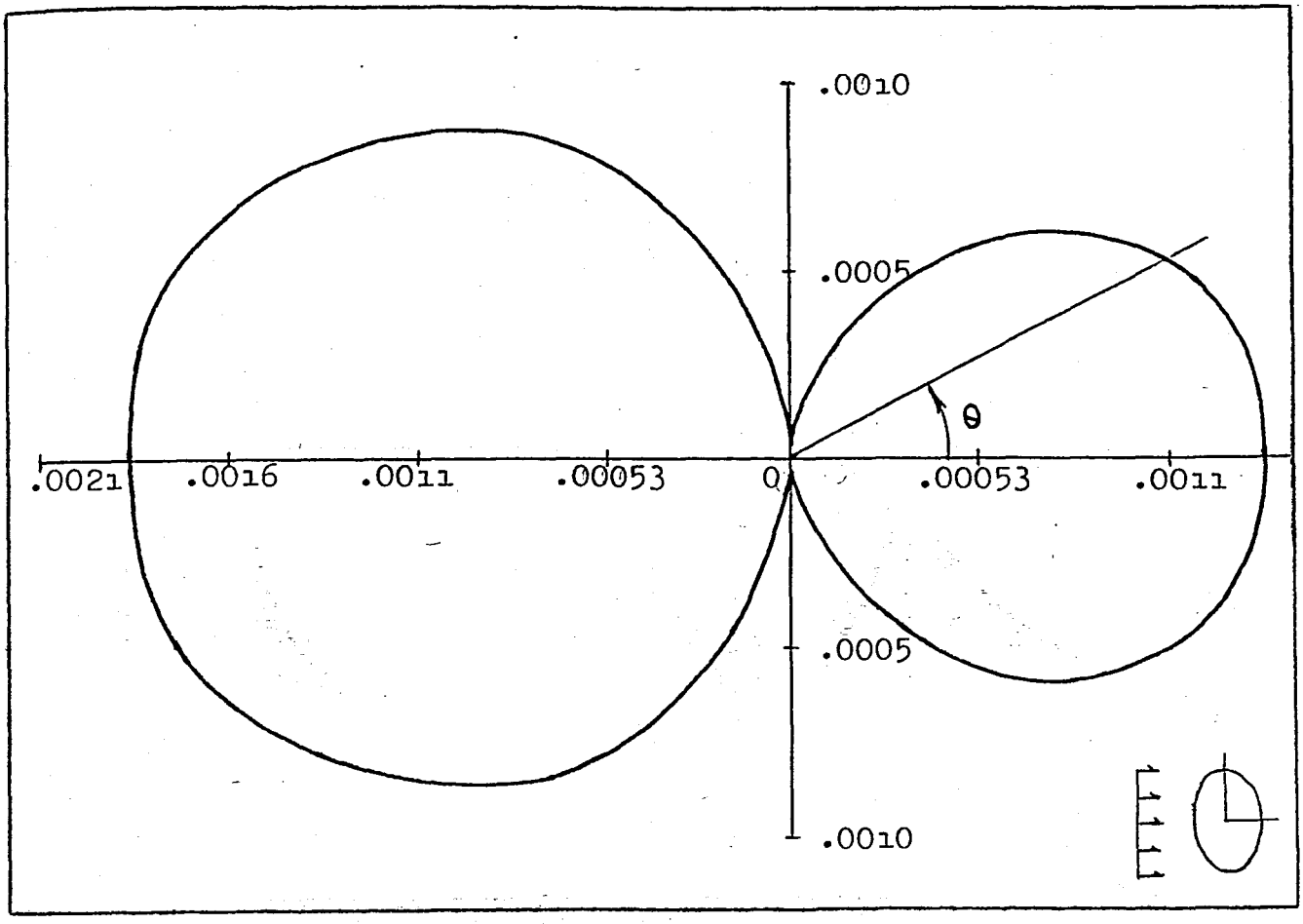

Fig. 7-i a = 0.5, b = 2.5, k = 0.1

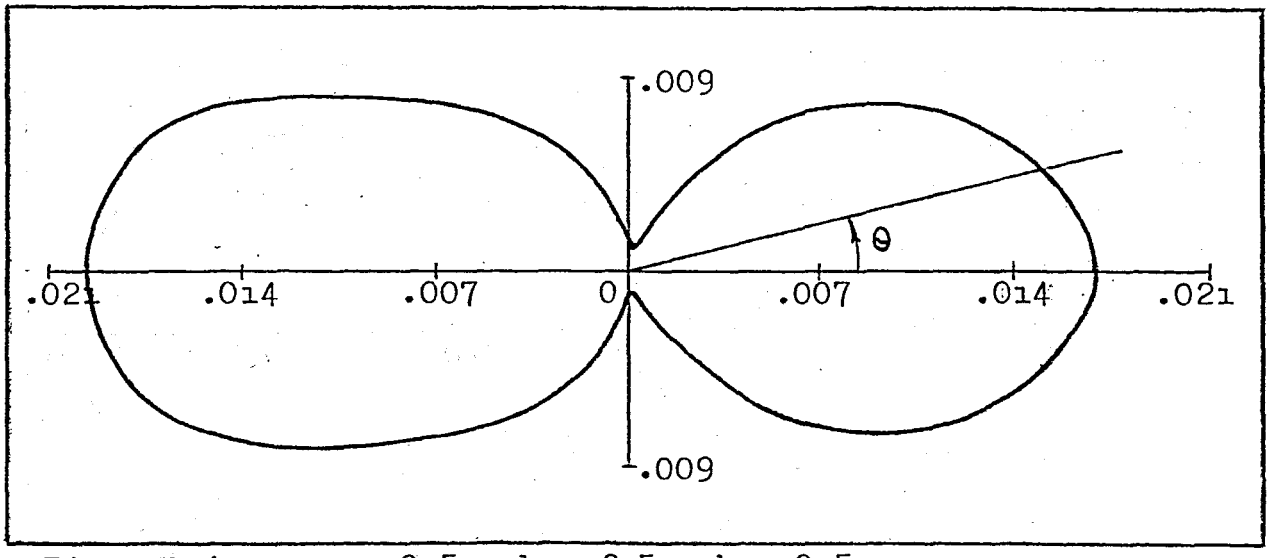

Fig. 7-j a = 0.5, b = 2.5, k = 0.5

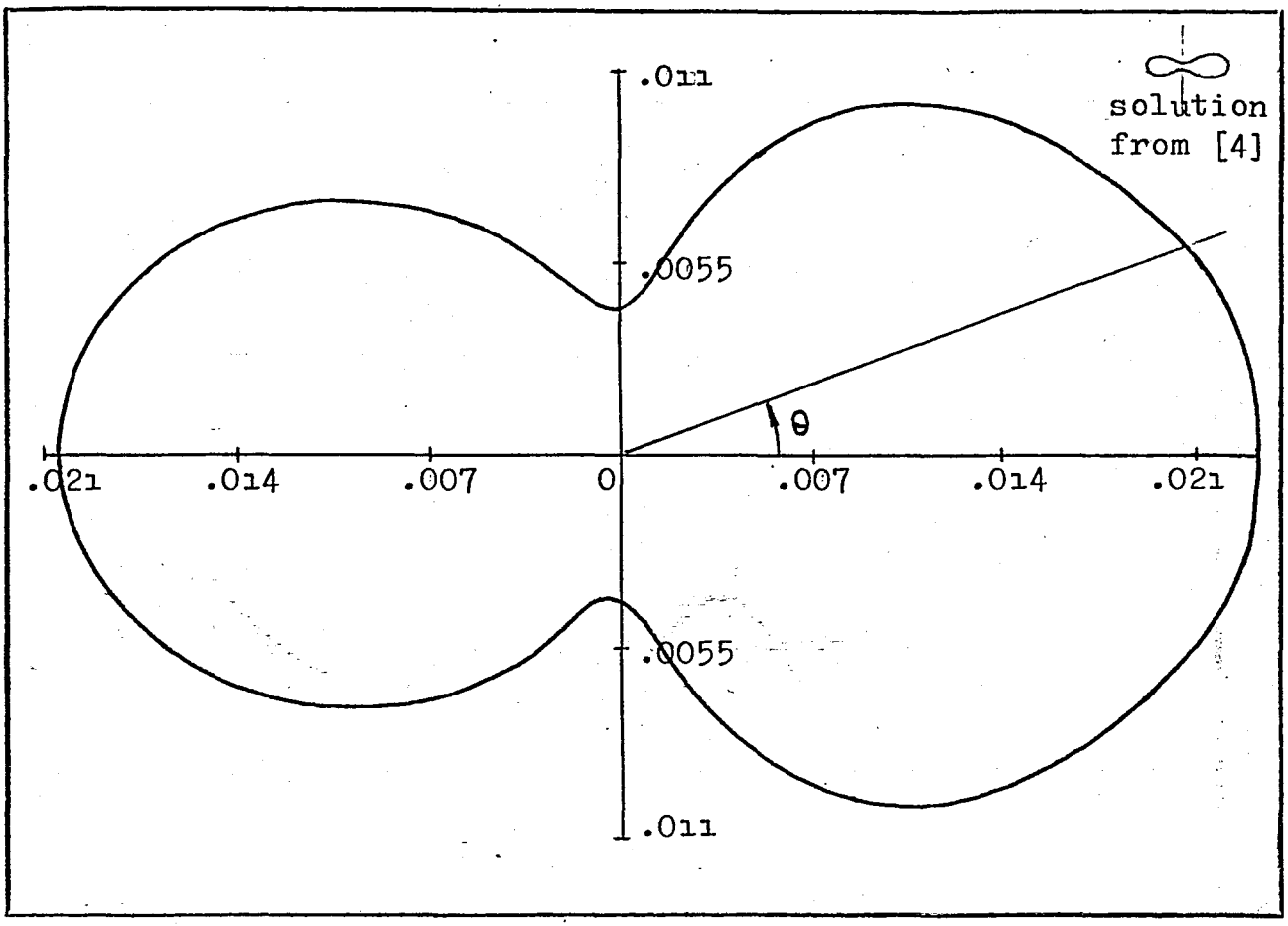

Fig. 7-k a = 0.5, b = 2.5, k = 1.0

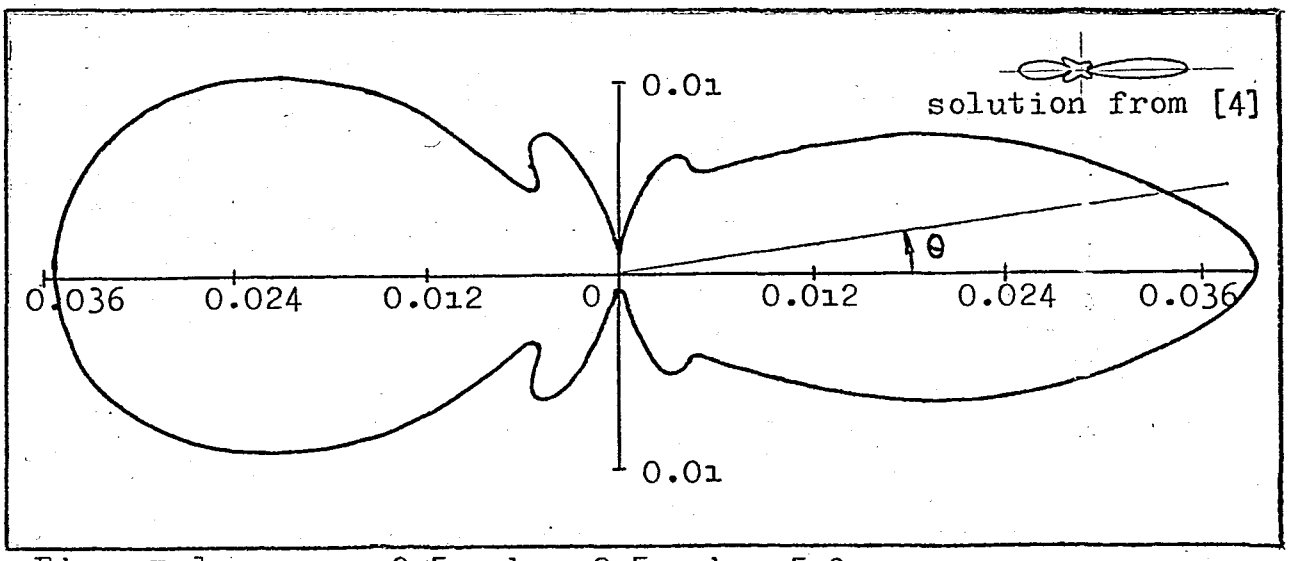

Fig. 7-l a = 0.5, b = 2.5, k = 5.0

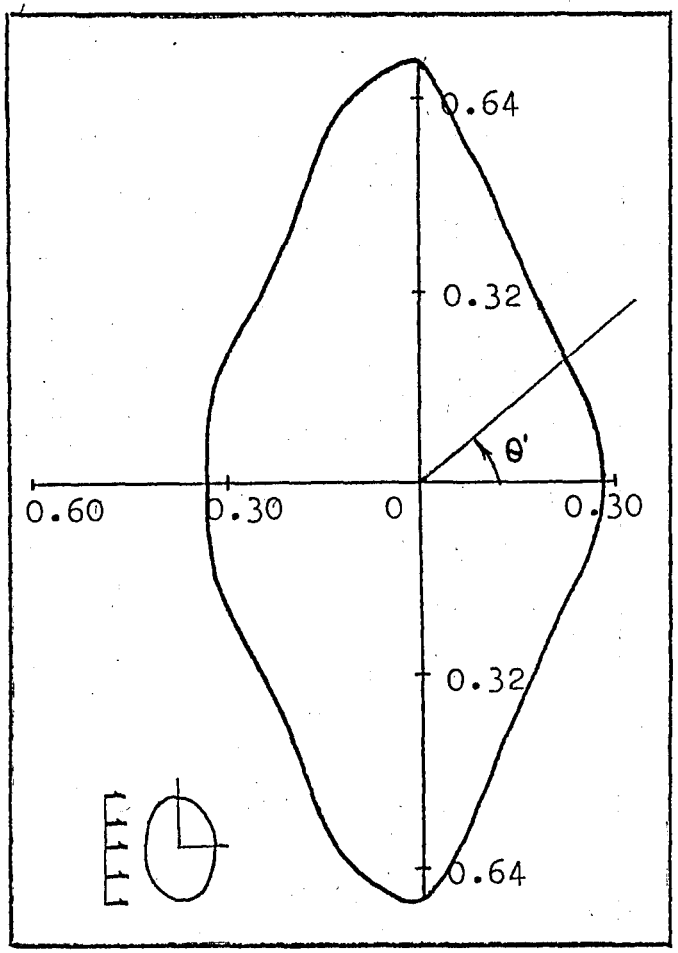

Fig. 8-a a = 0.5, b = 1.0, k = 0.1

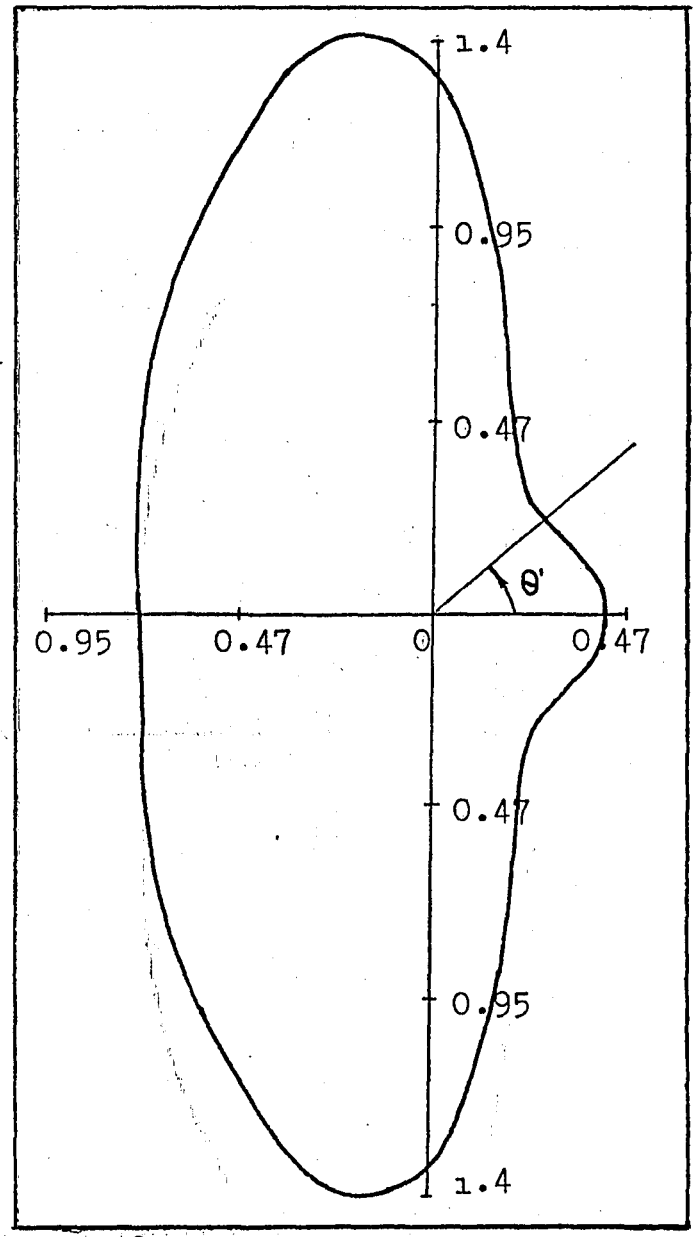

Fig. 8-b a = 0.5, b = 1.0, k = 0.5

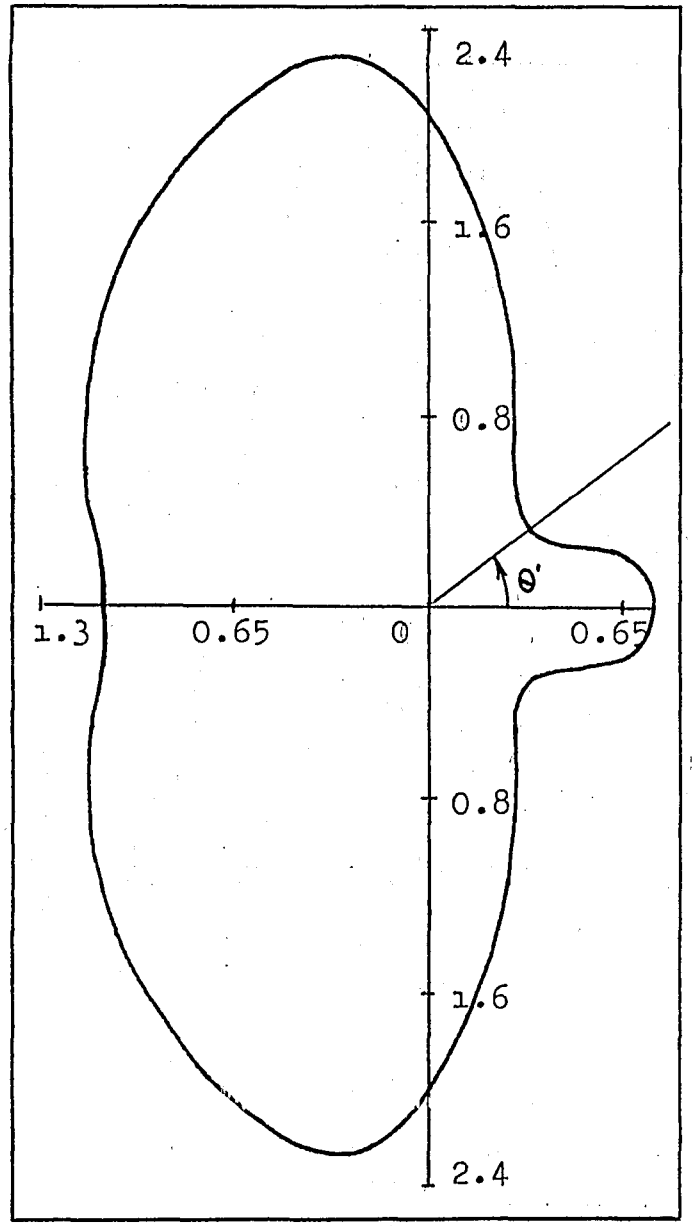

Fig. 8-c a = 0.5, b = 1.0, k = 1.0

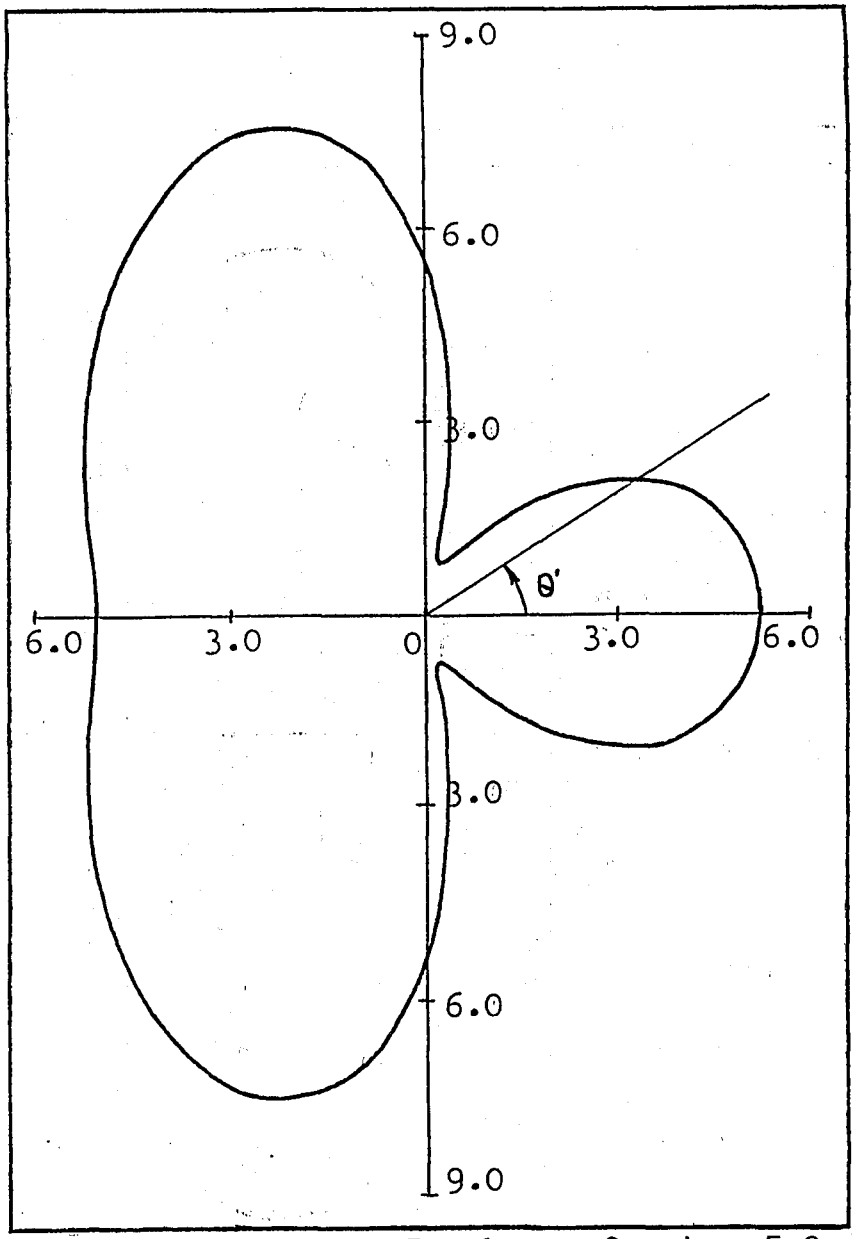

Fig. 8-d a = 0.5, b = 1.0, k = 5.0

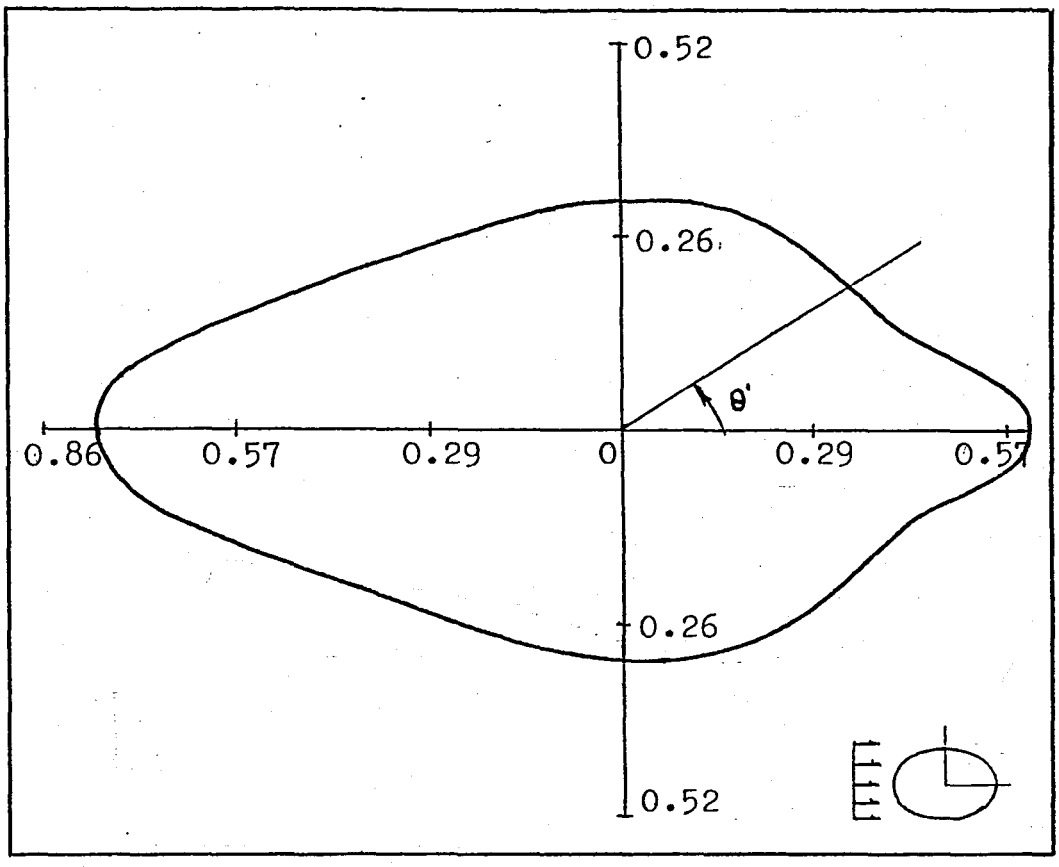

Fig. 8-e a = 1.0, b = 0.5, k = 0.1

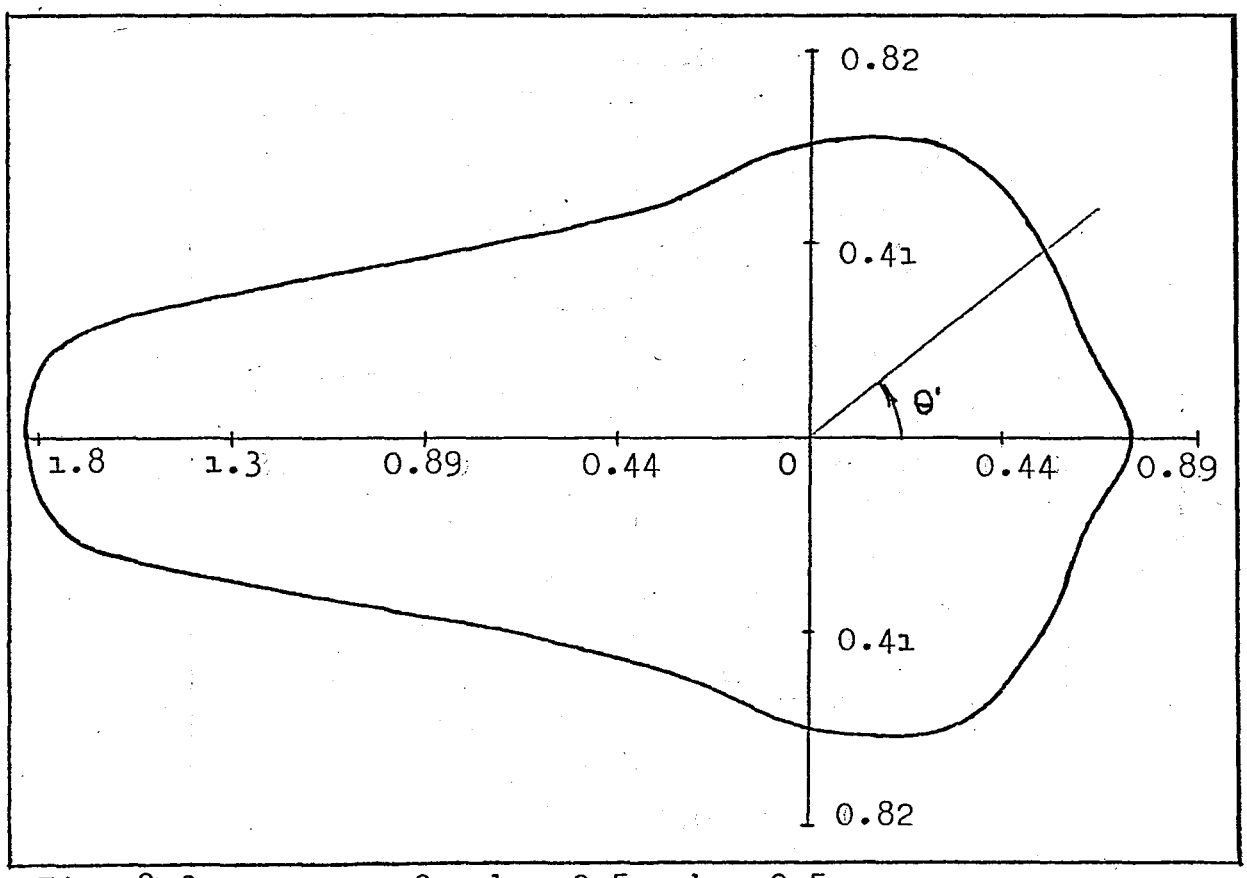

Fig. 8-f a = 1.0, b = 0.5, k = 0.5

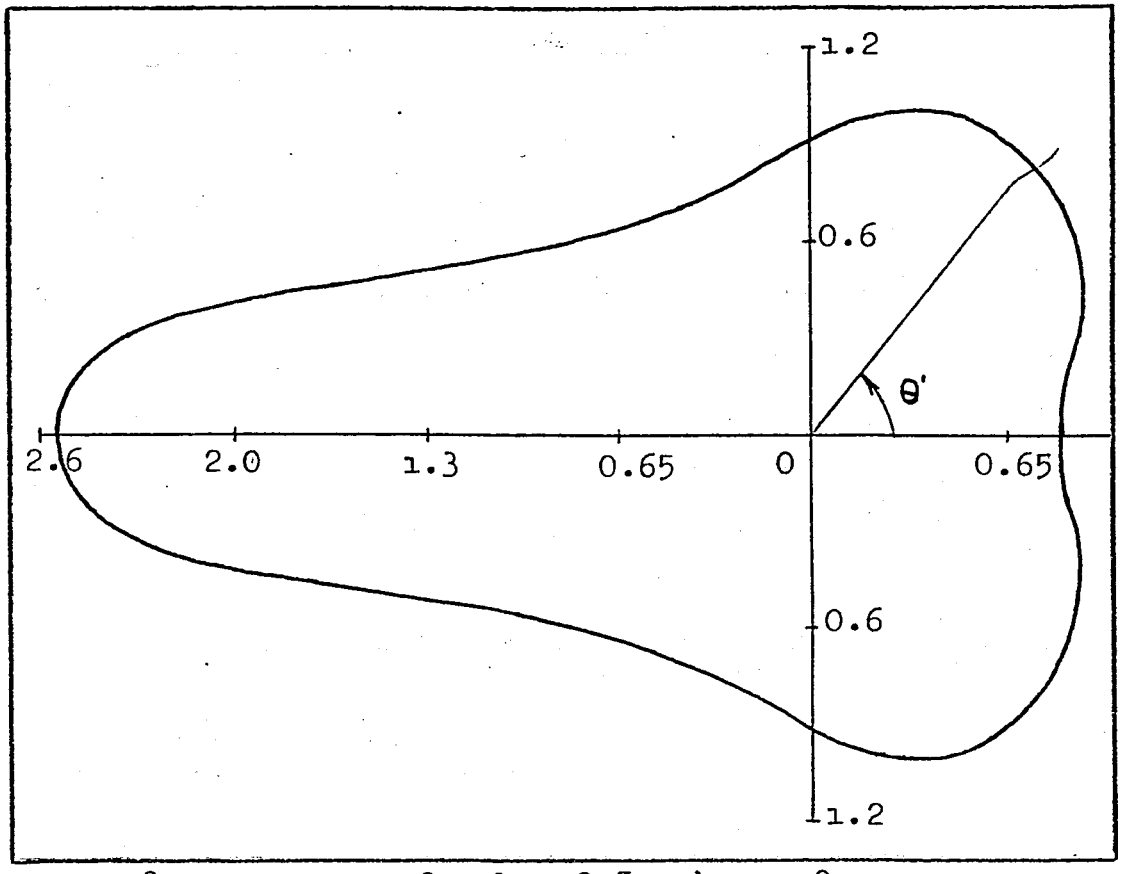

Fig. 8-g a = 1.0, b = 0.5, k = 1.0

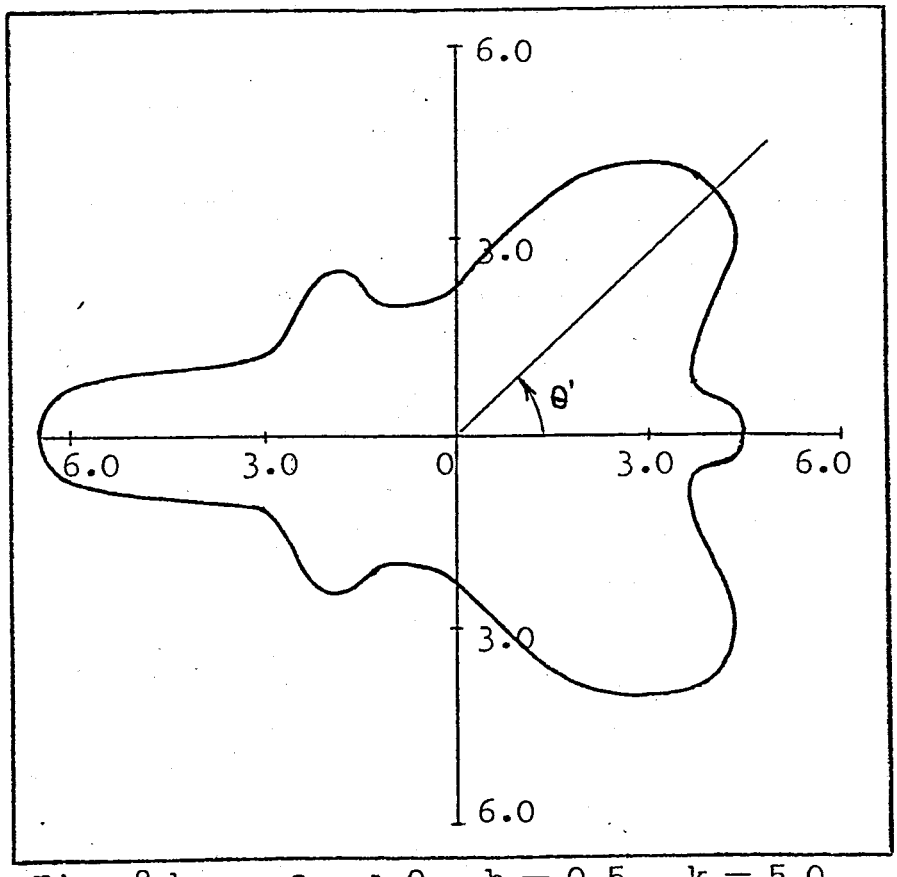

Fig. 8-h a = 1.0, b = 0.5, k = 5.0

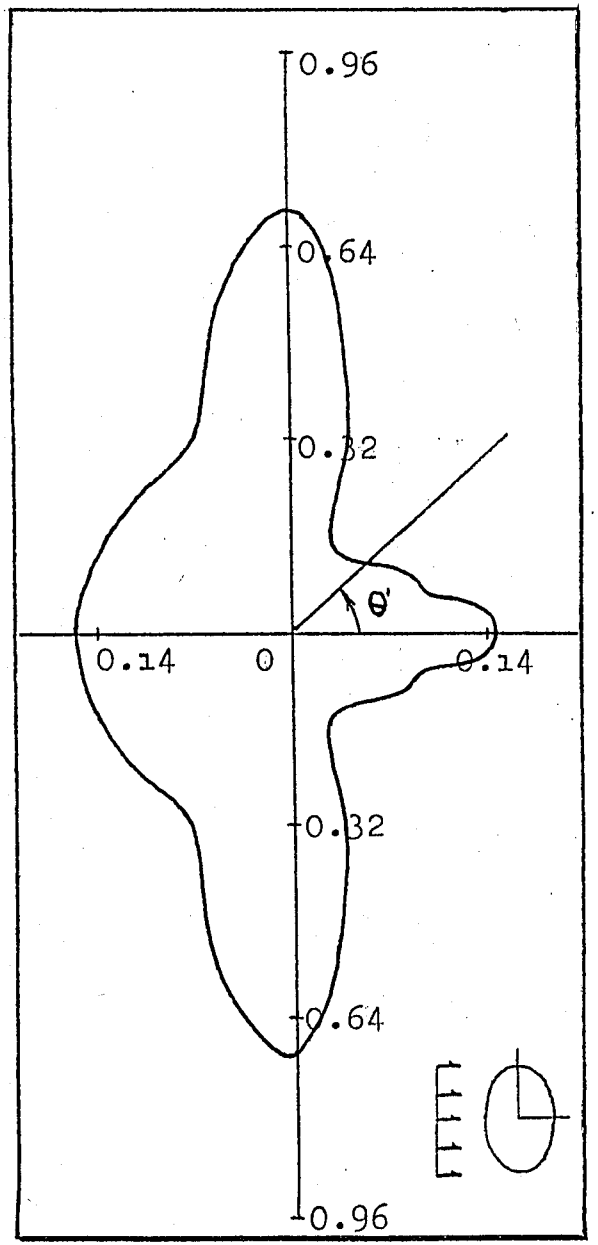

Fig. 8-i a = 0.5, b = 2.5,

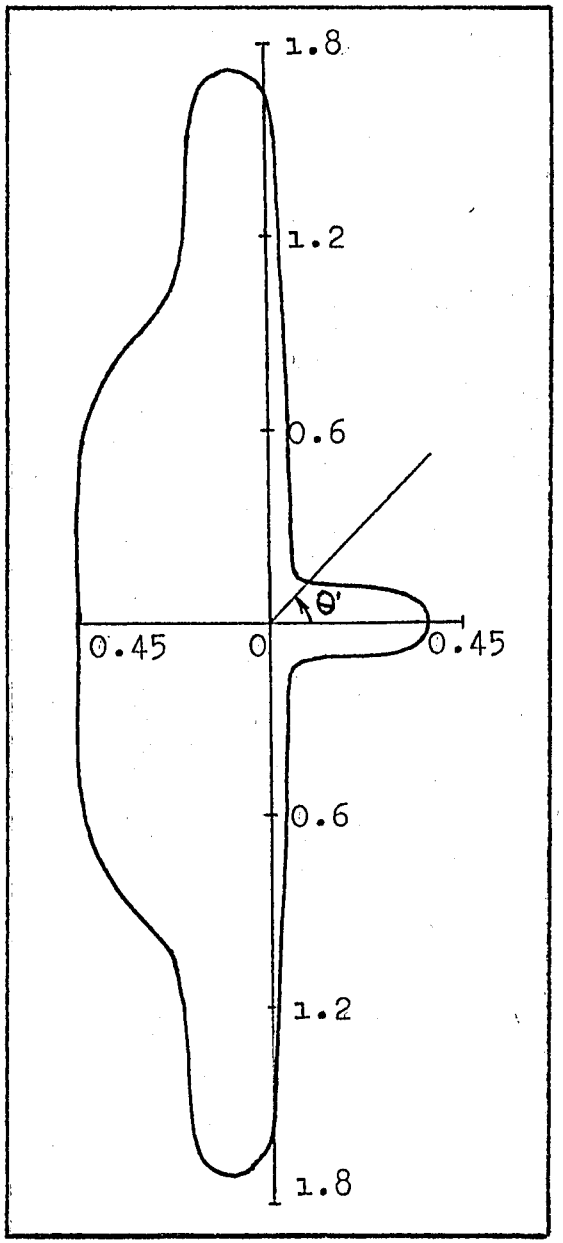

Fig. 8-j a = 0.5, b = 2.5,

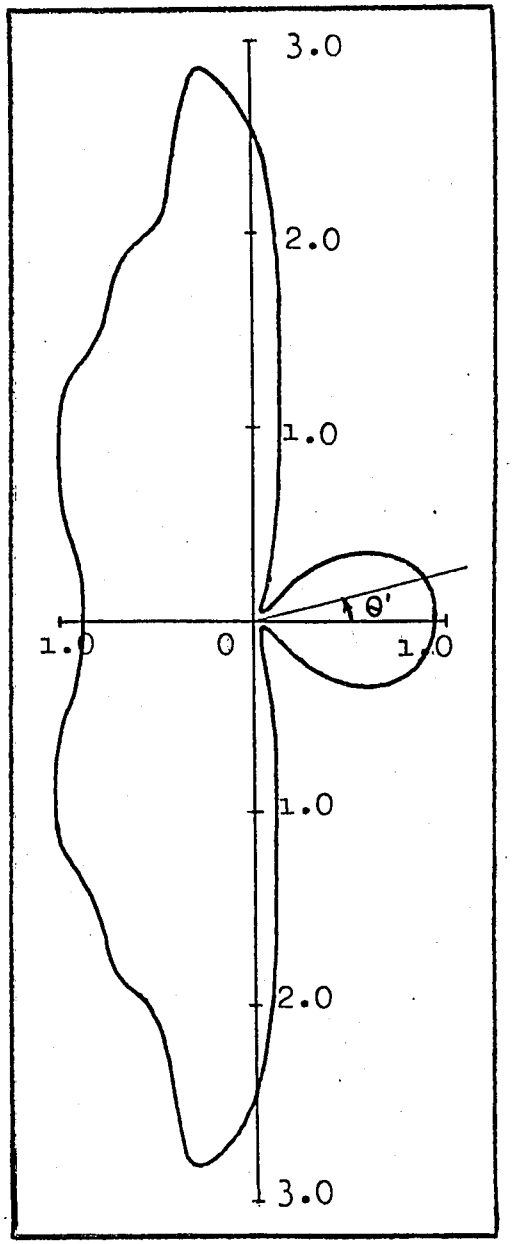

Fig. 8-k a = 0.5, b = 2.5,

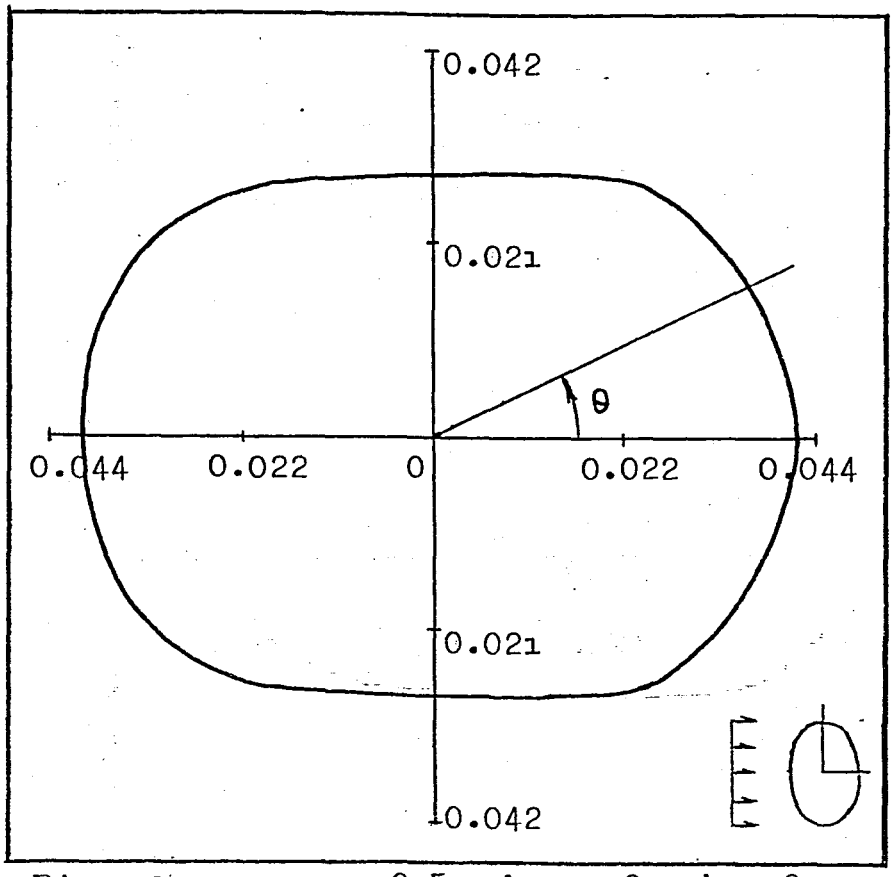

Fig. 9-a a = 0.5, b = 1.0, k = 0.1

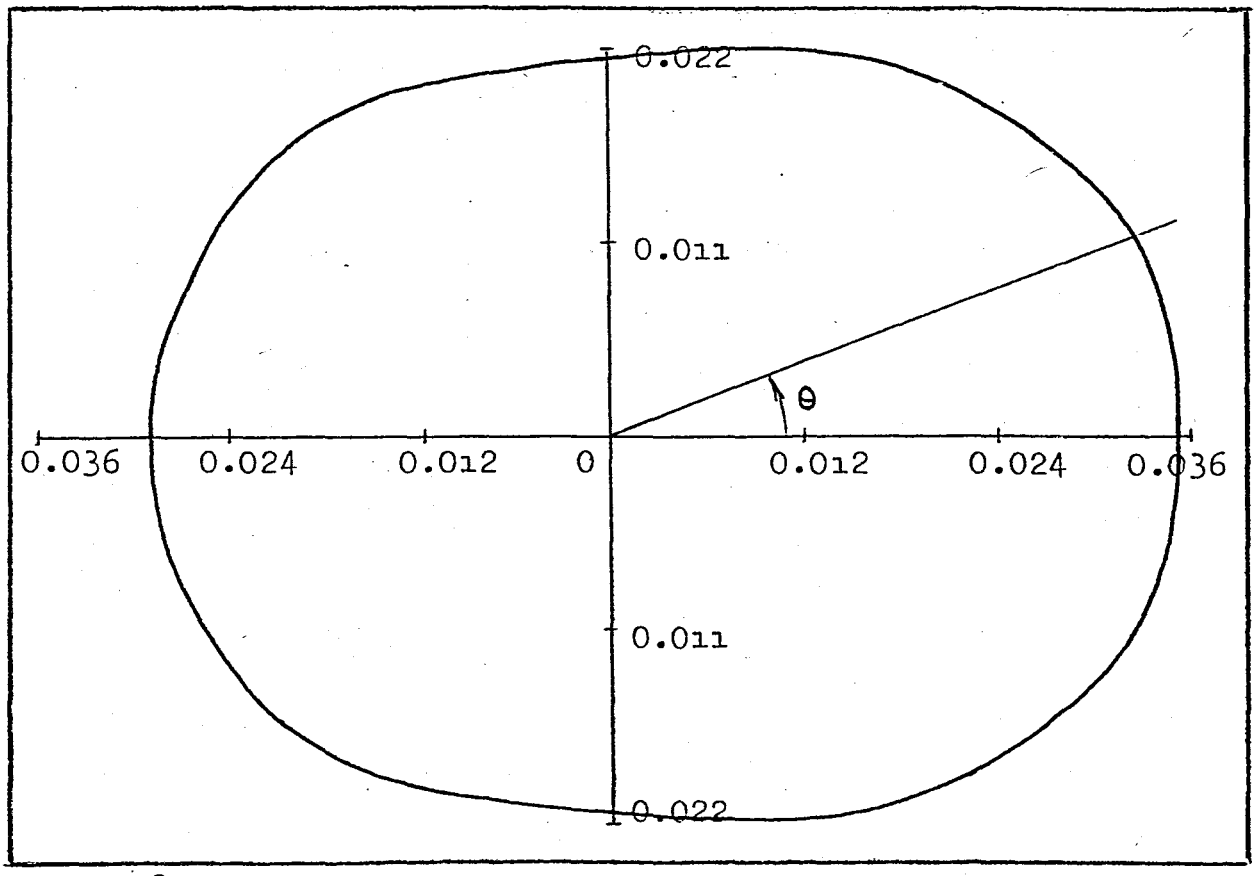

Fig. 9-b a = 0.5, b = 1.0, k = 0.5

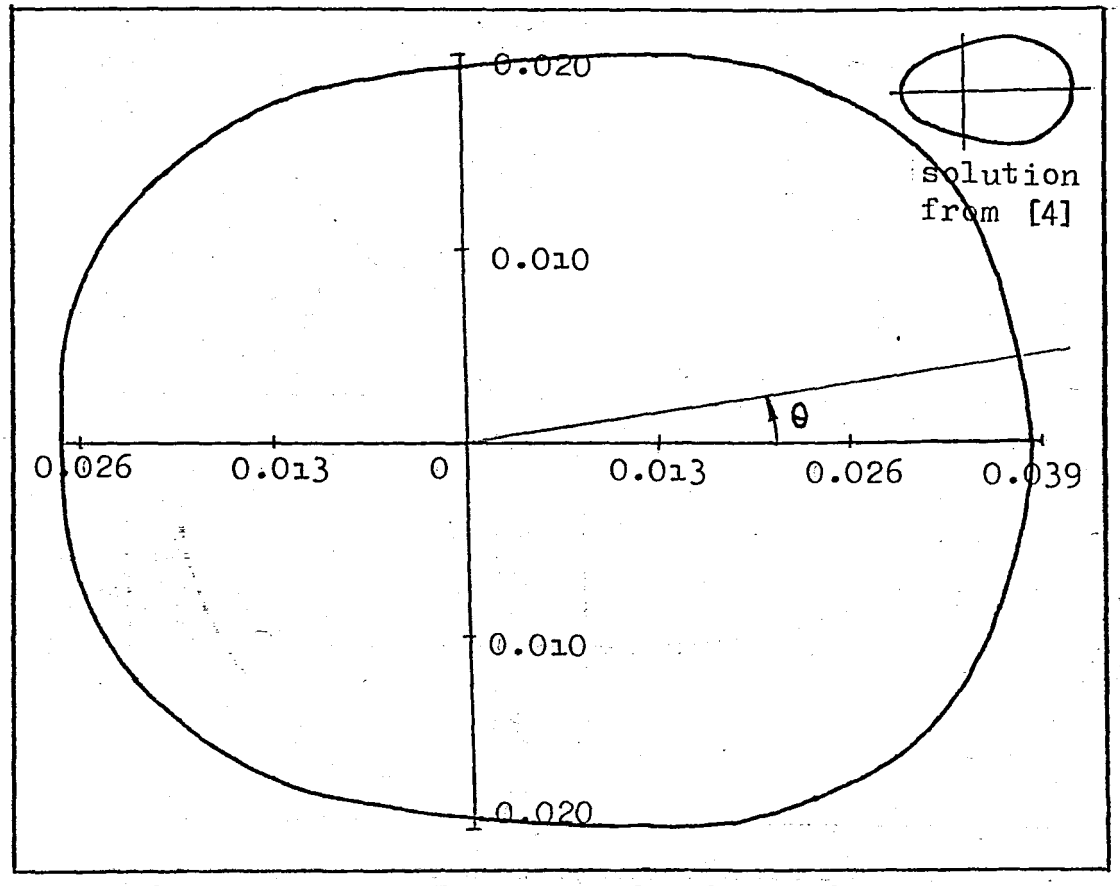

Fig. 9-c a = 0.5, b = 1.0, k = 1.0

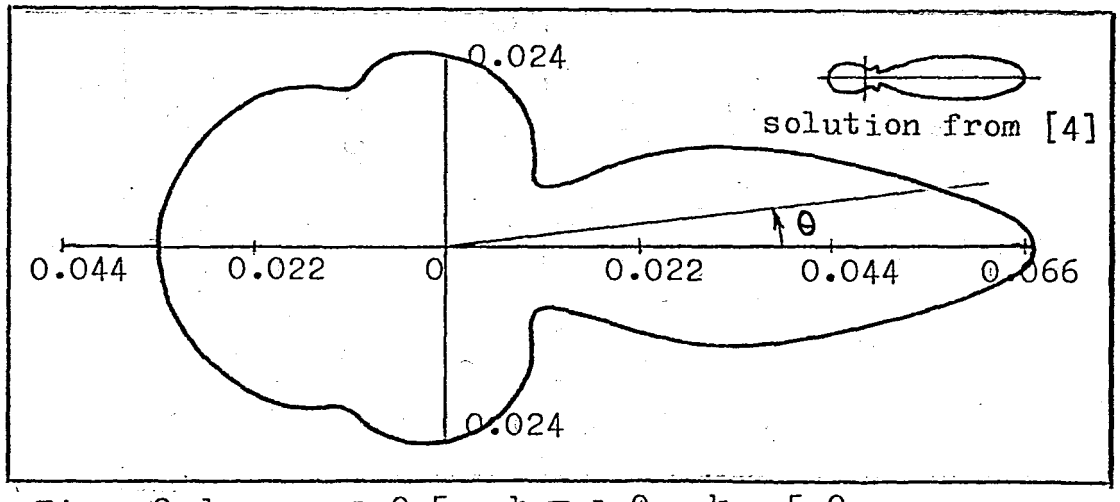

Fig. 9-d a = 0.5, b = 1.0, k = 5.0

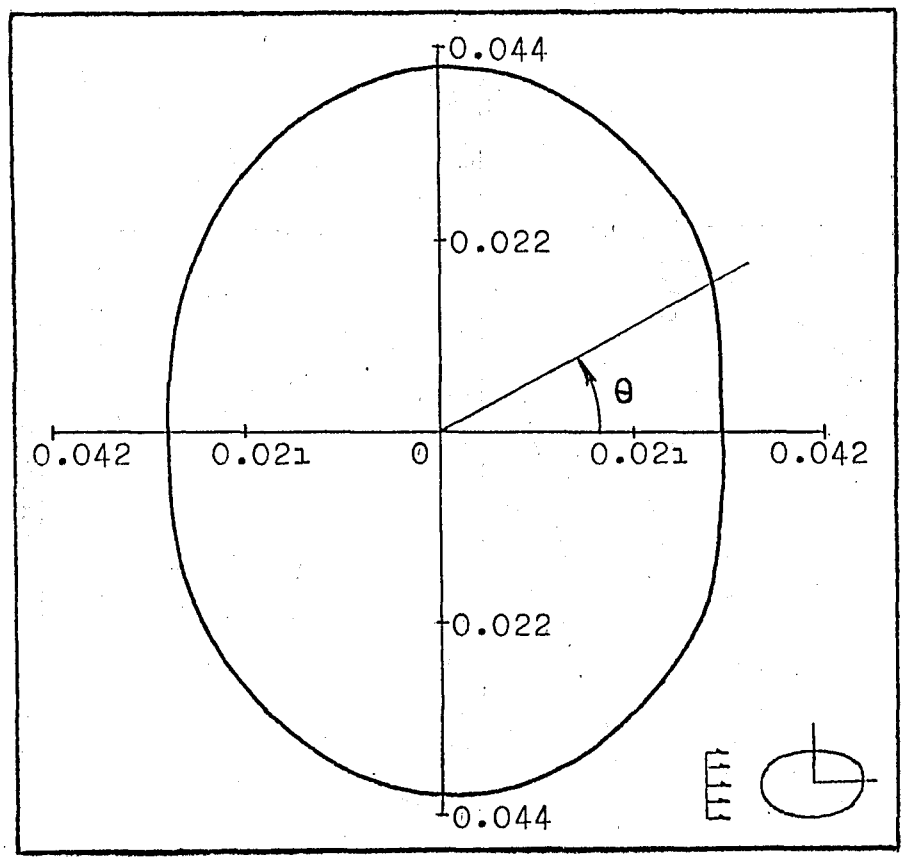

Fig. 9-e a = 1.0, b = 0.5, k = 0.1

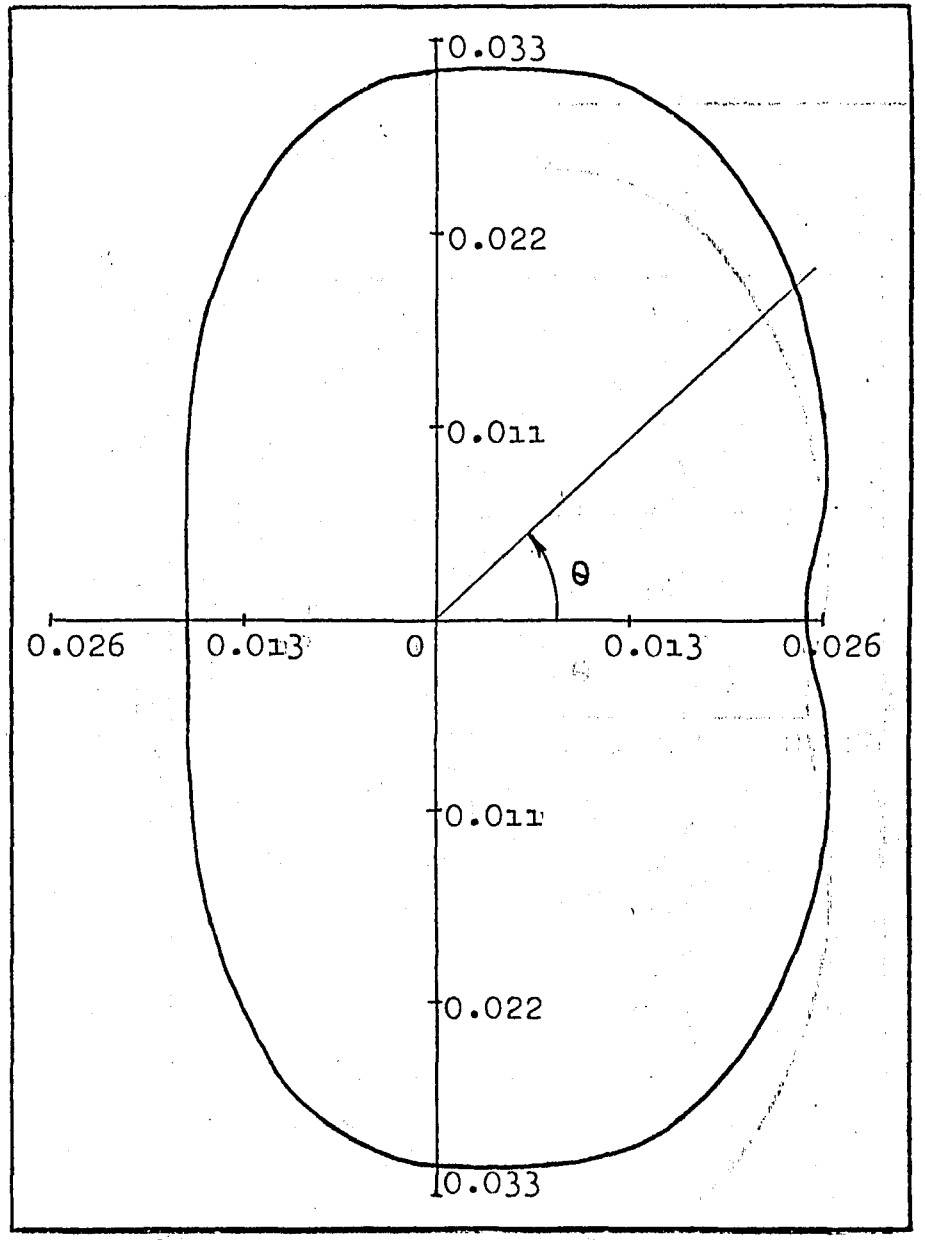

Fig. 9-f a = 1.0, b = 0.5, k = 0.5

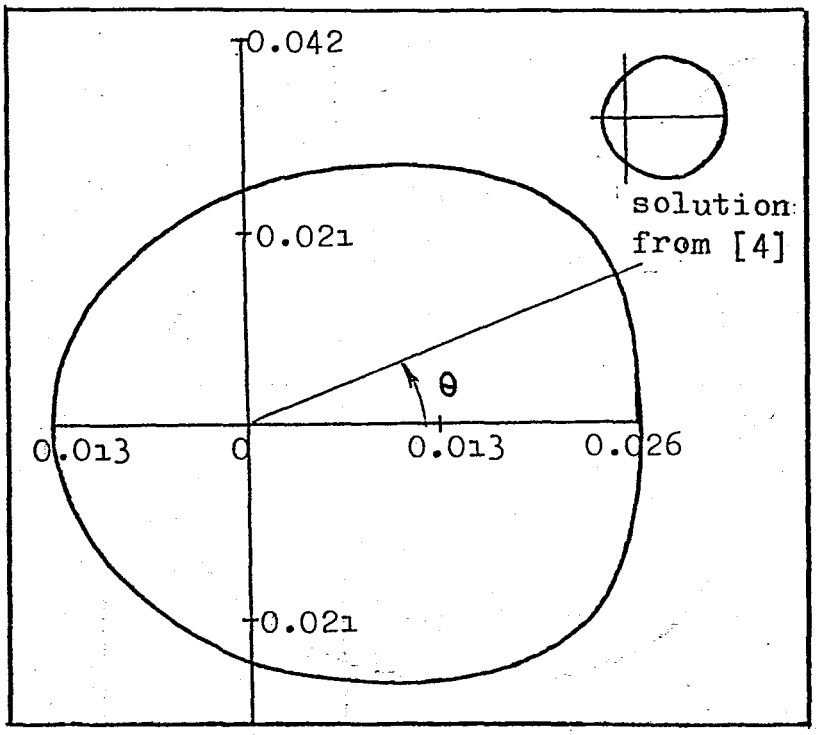

Fig. 9-g a = 1.0, b = 0.5, k = 1.0

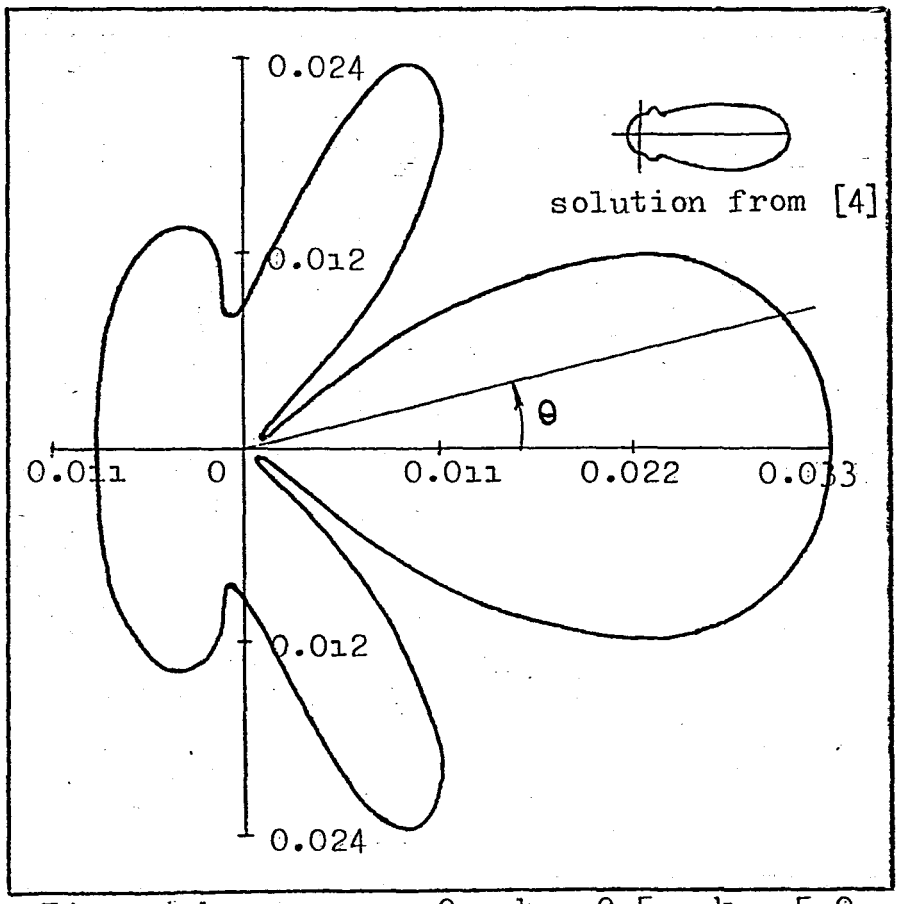

Fig. 9-h a = 1.0, b = 0.5, k = 5.0

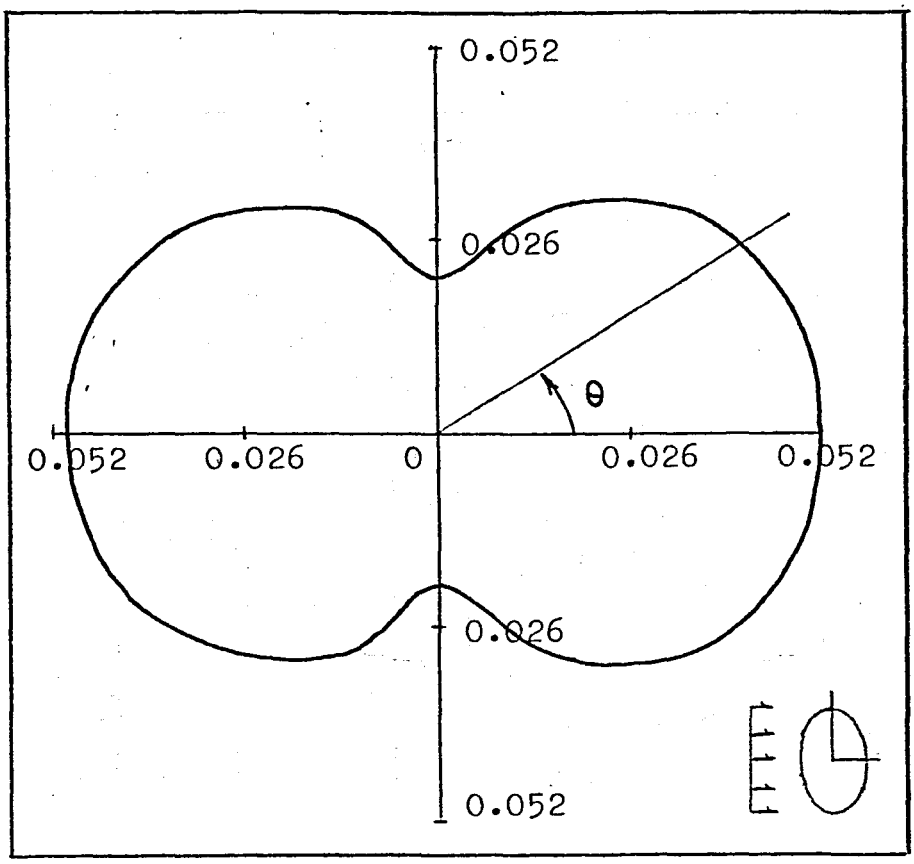

Fig. 9-i a = 0.5, b = 2.5, k = 0.1

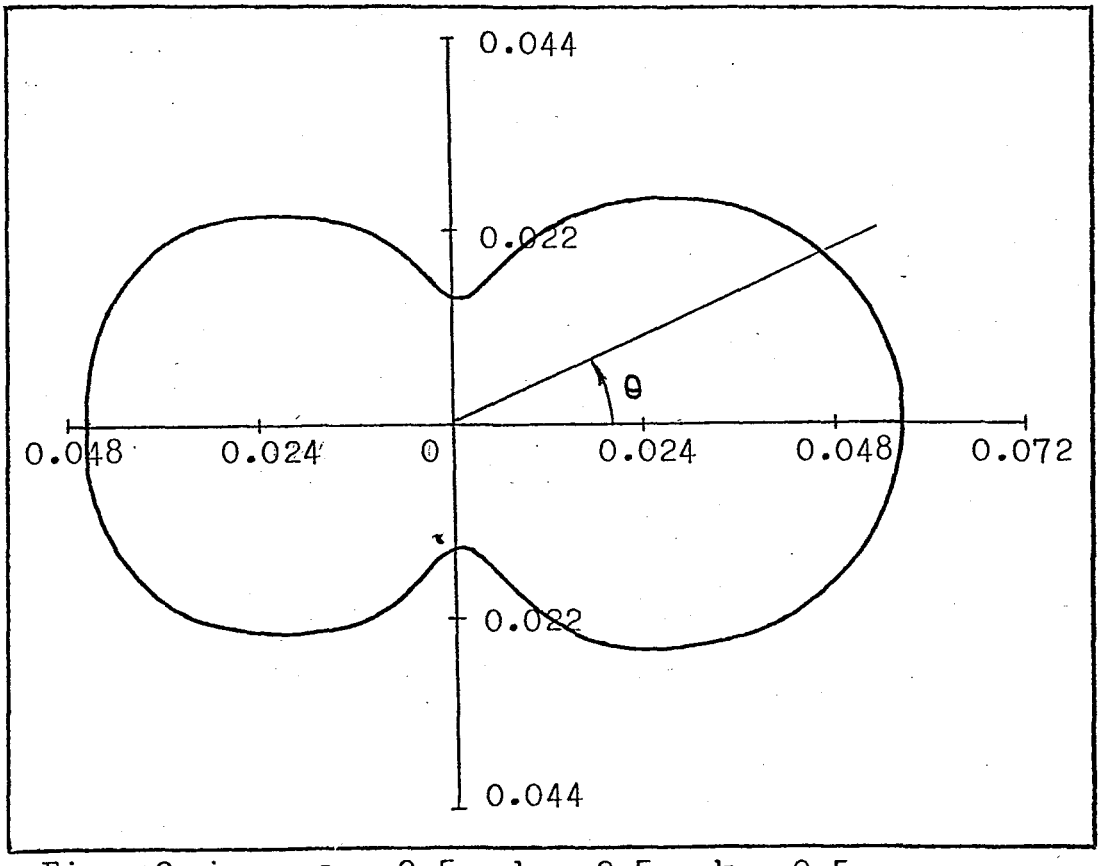

Fig. 9-j a = 0.5, b = 2.5, k = 0.5

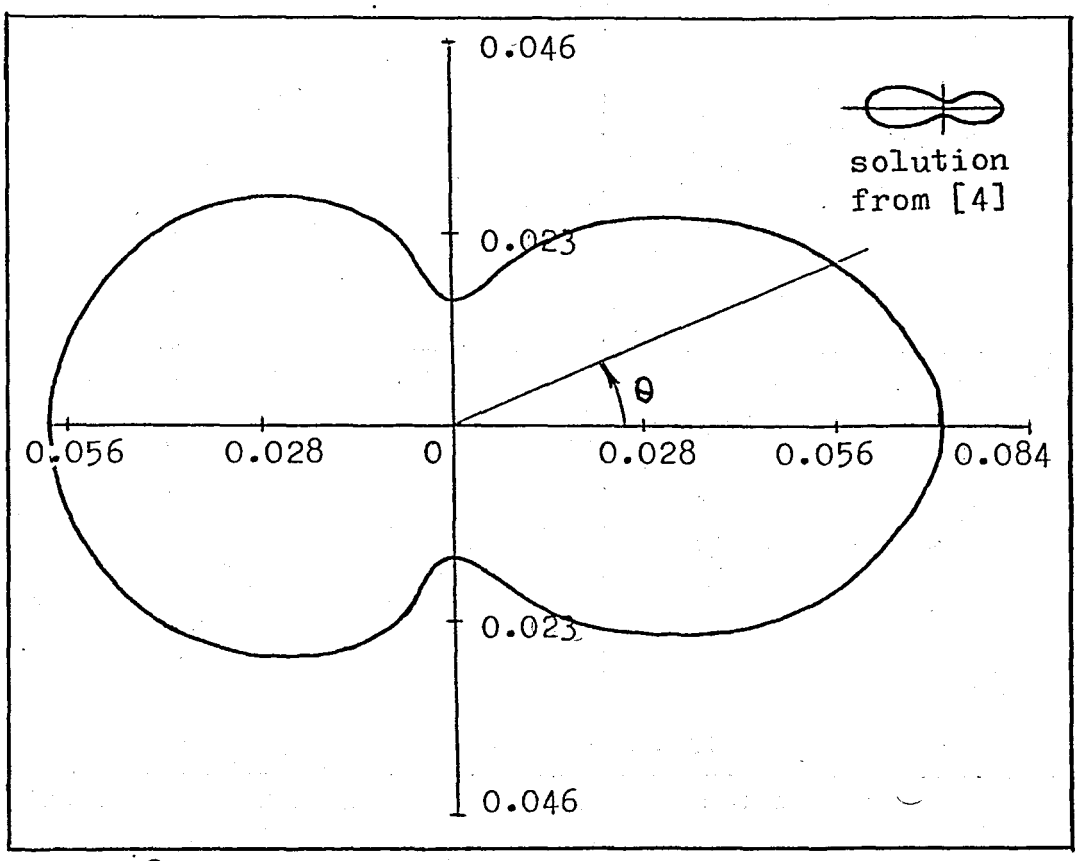

Fig. 9-k a = 0.5, b = 2.5, k = 1.0

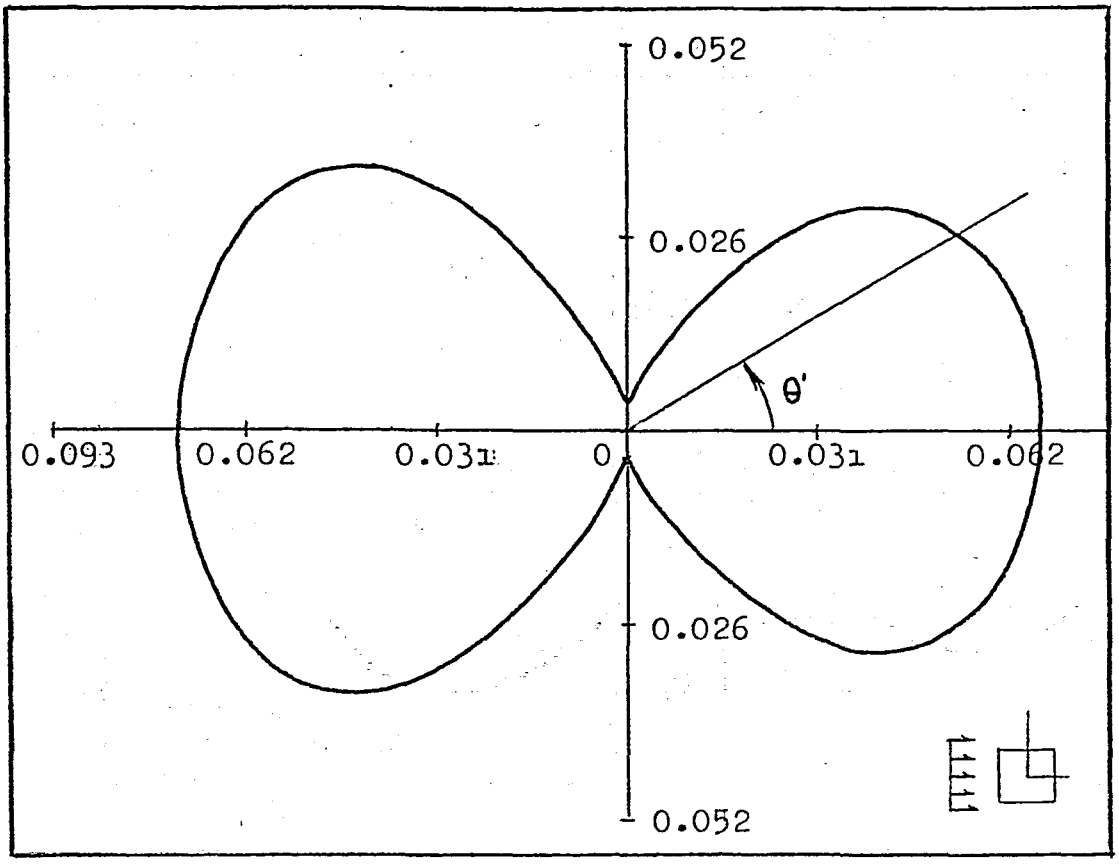

Fig. 10-a a = 1.0, b = 1.0, k = 0.1

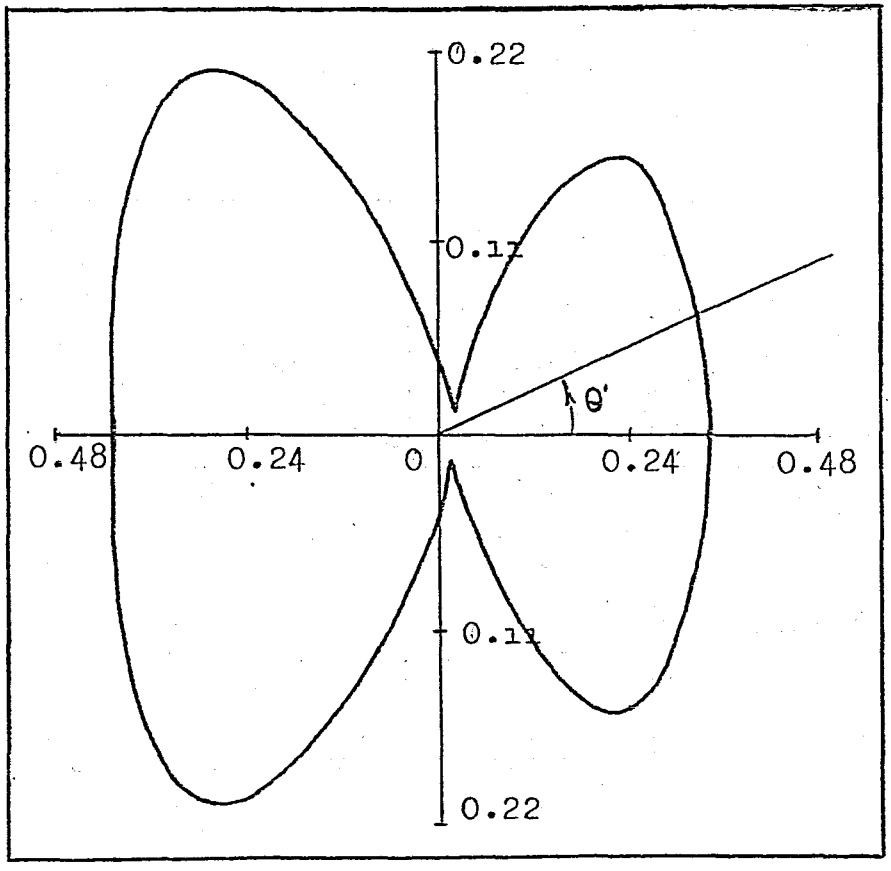

Fig. 10-b a = 1.0, b = 1.0, k = 0.5

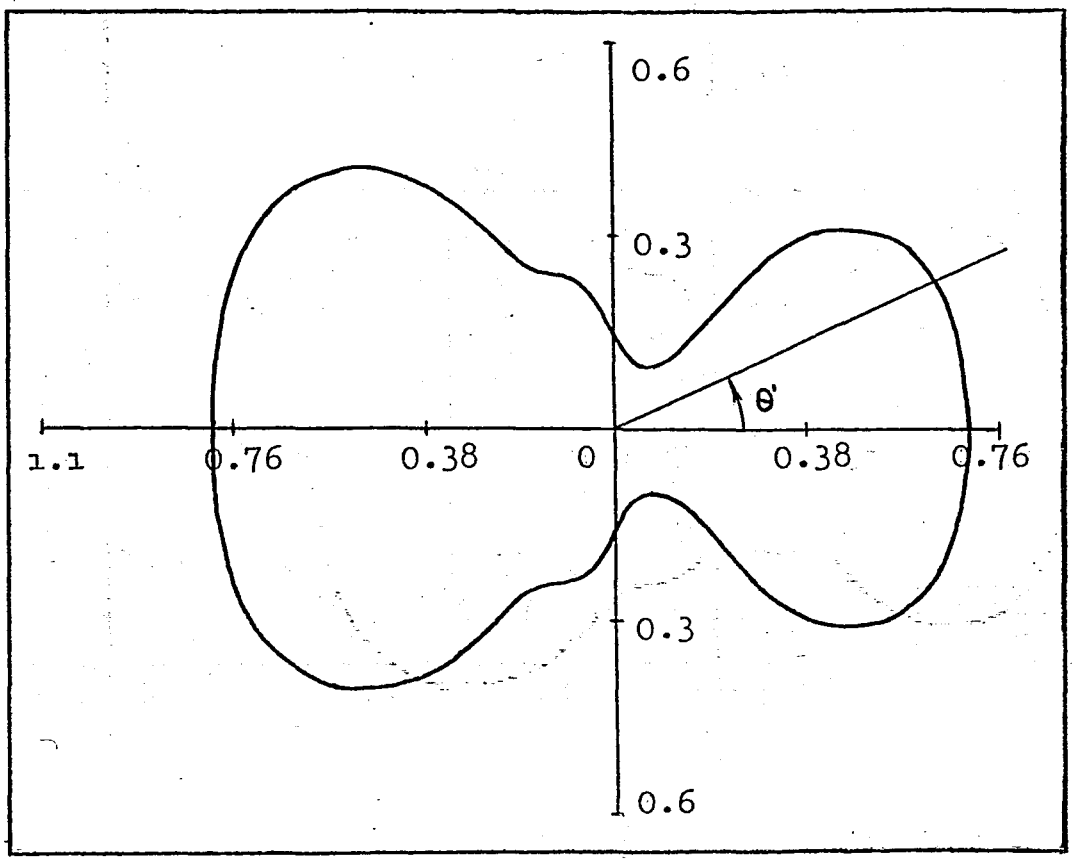

Fig. 10-c a = 1.0, b = 1.0, k = 1.0

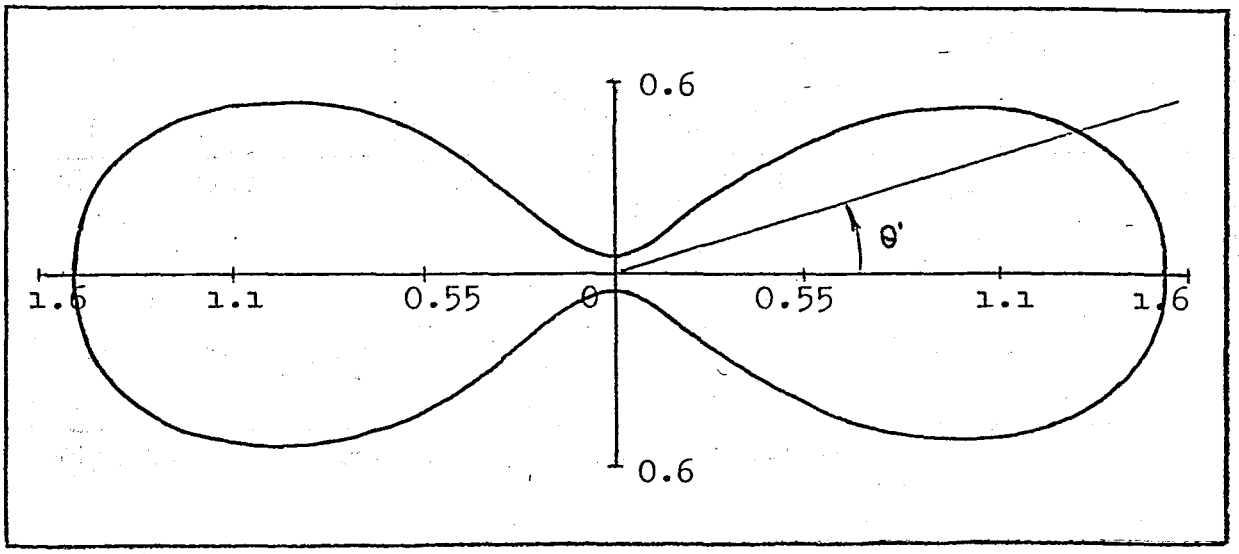

Fig. 10-d a = 1.0, b = 1.0, k = 5.0

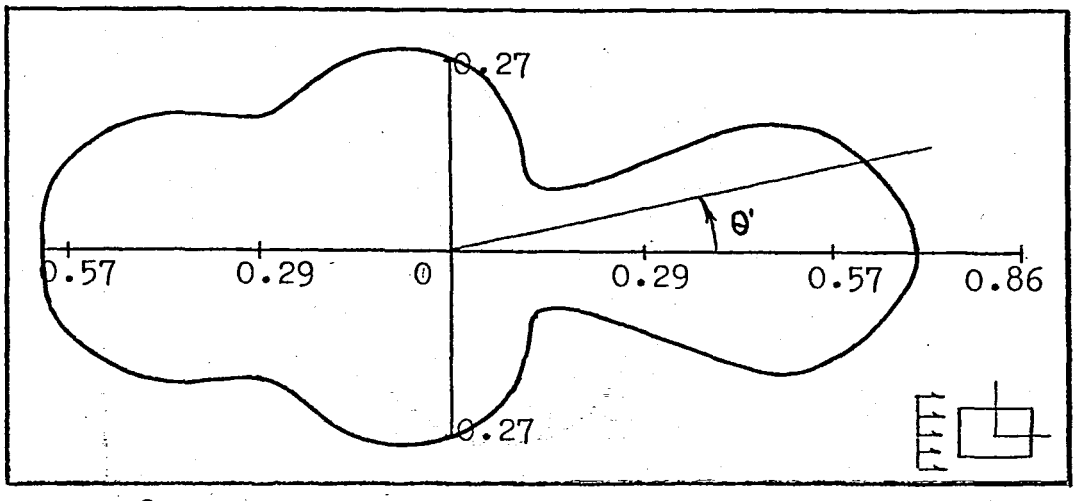

Fig. 10-e a = 1.0, b = 2.0, k = 1.0

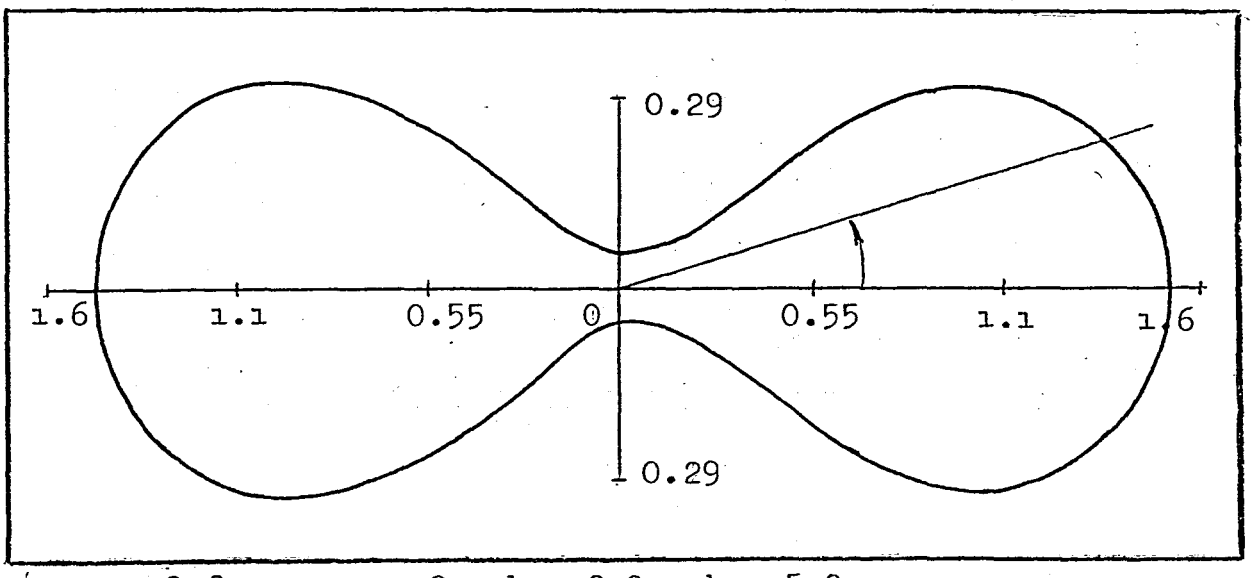

Fig. 10-f a = 1.0, b = 2.0, k = 5.0

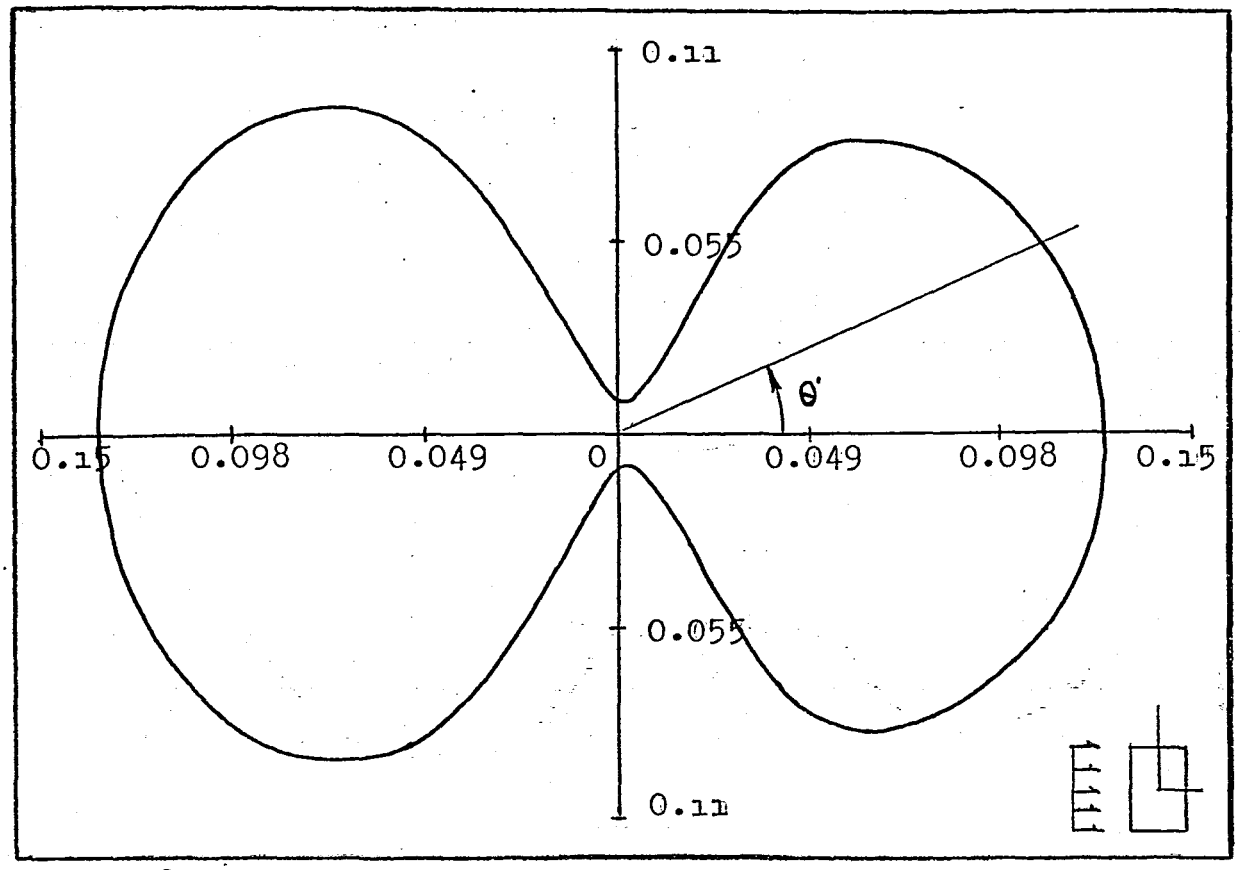

Fig. 10-g a = 2.0, b = 1.0, k = 0.1

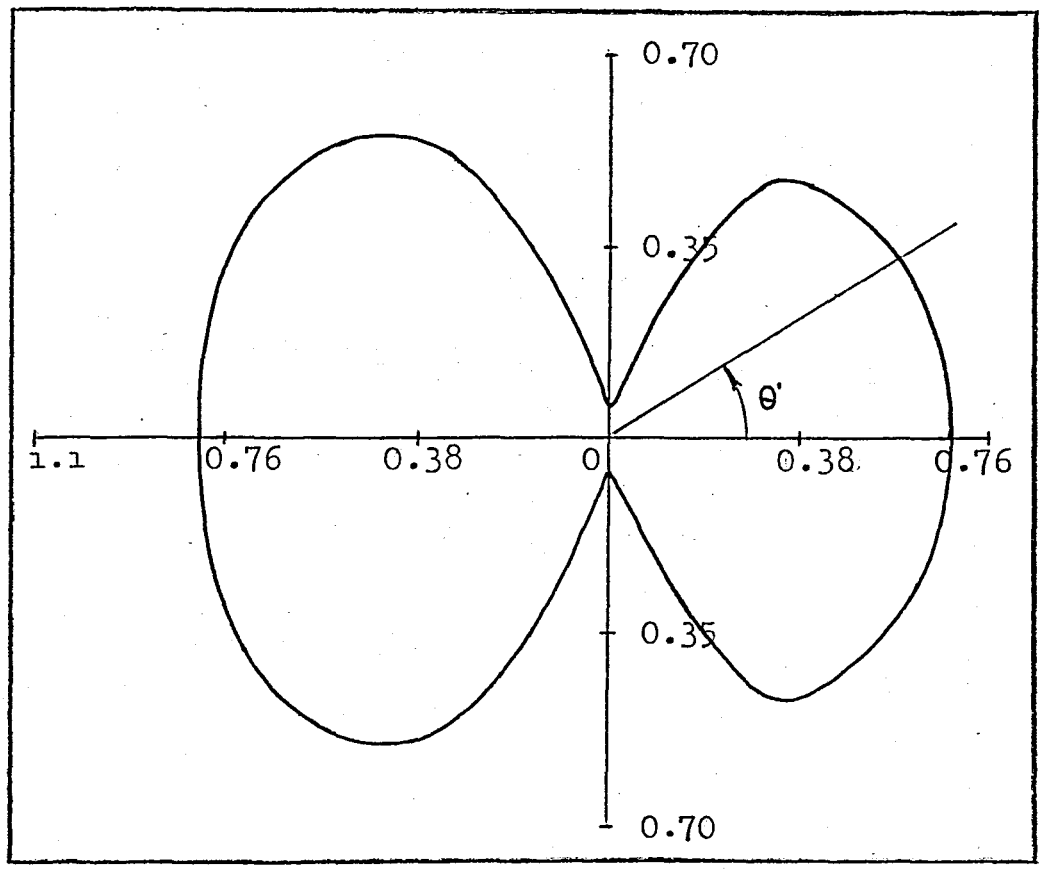

Fig. 10-h a = 2.0, b = 1.0, k = 0.5

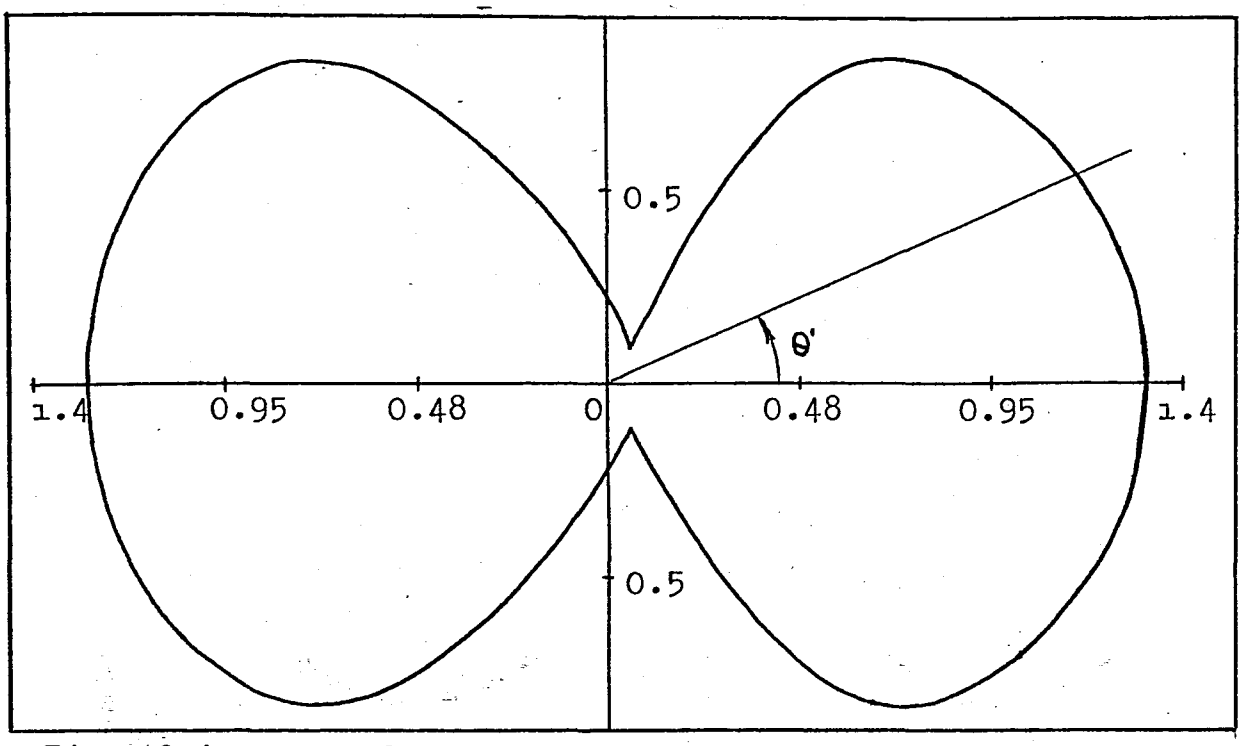

Fig. 10-i a = 2.0, b = 1.0, k = 1.0

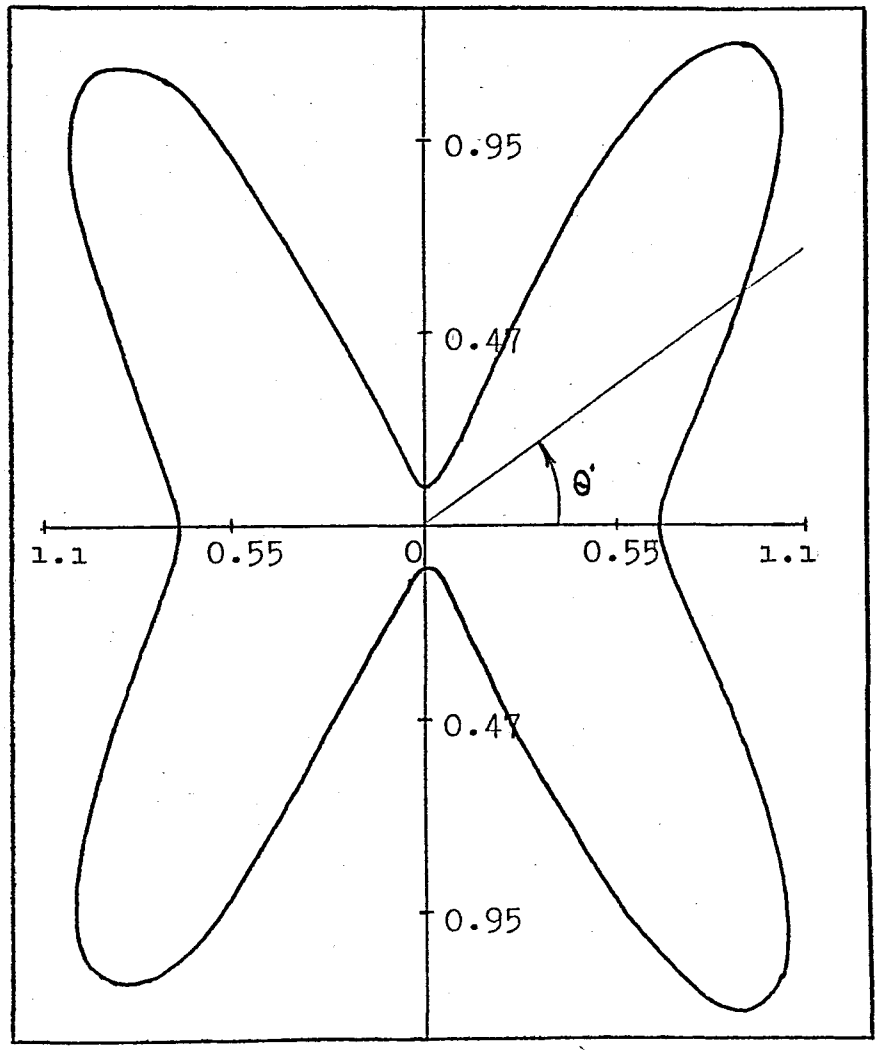

Fig. 10-j a = 2.0, b = 1.0, k = 5.0

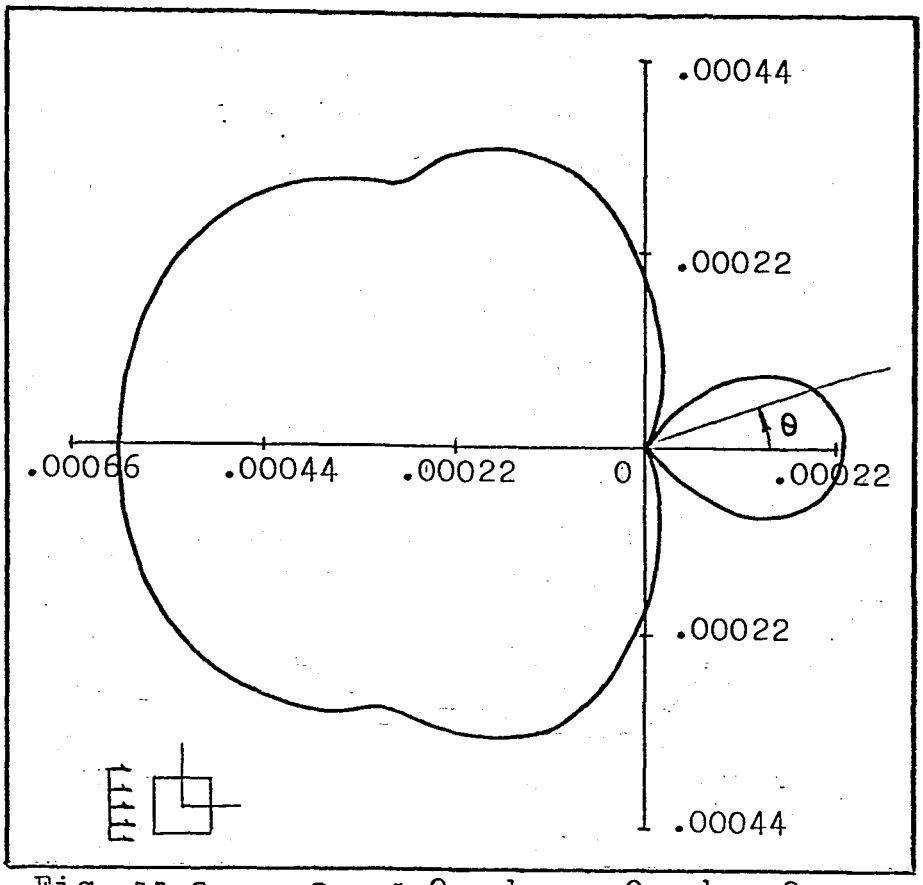

Fig. 11-a a = 1.0, b = 1.0, k = 0.1

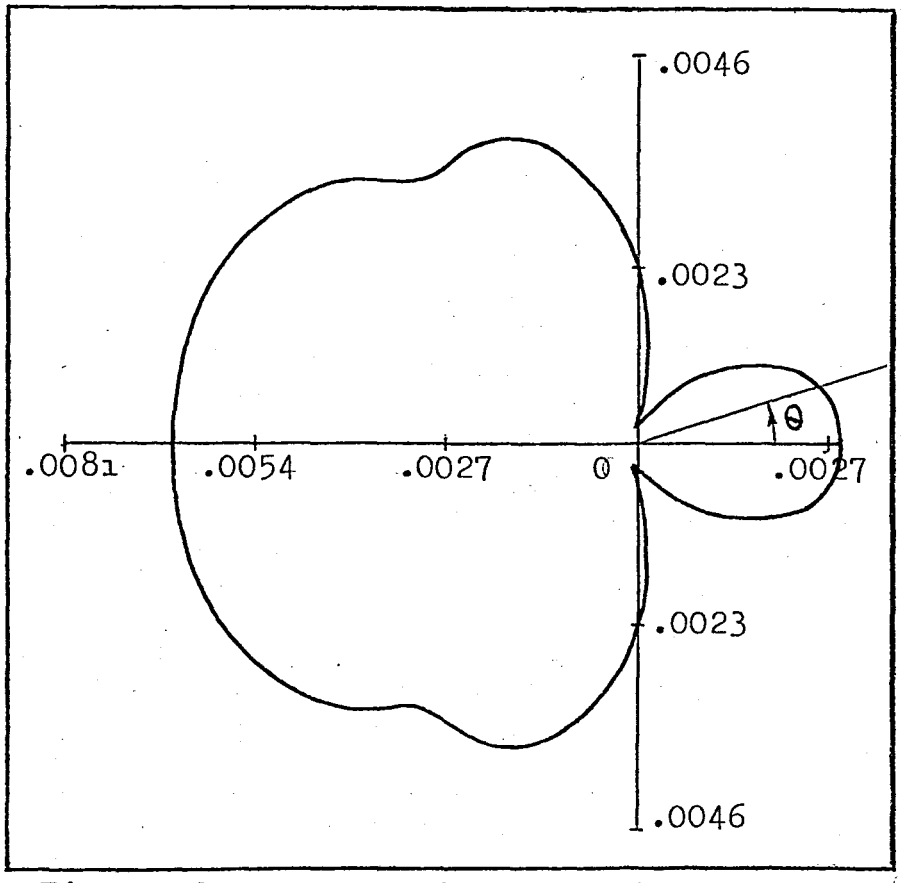

Fig. 11-b a = 1.0, b = 1.0, k = 0.5

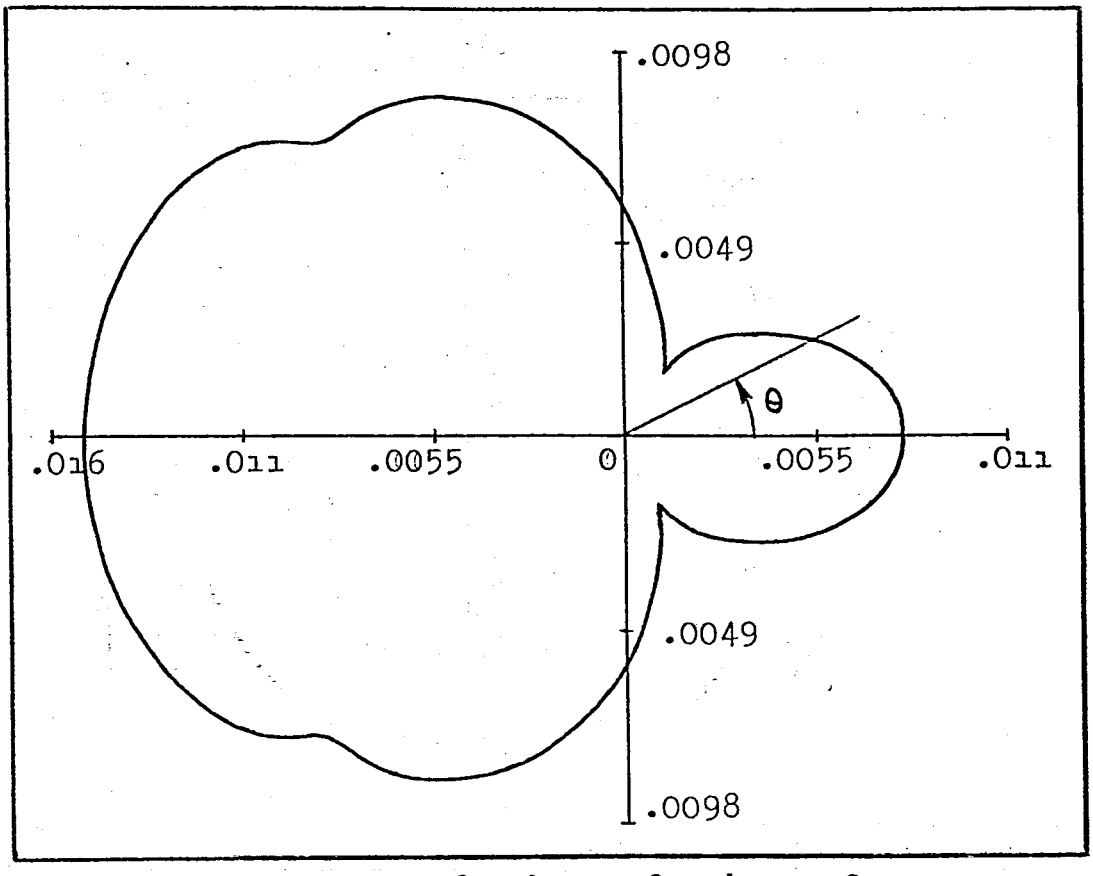

Fig. 11-c a = 1.0, b = 1.0, k = 1.0

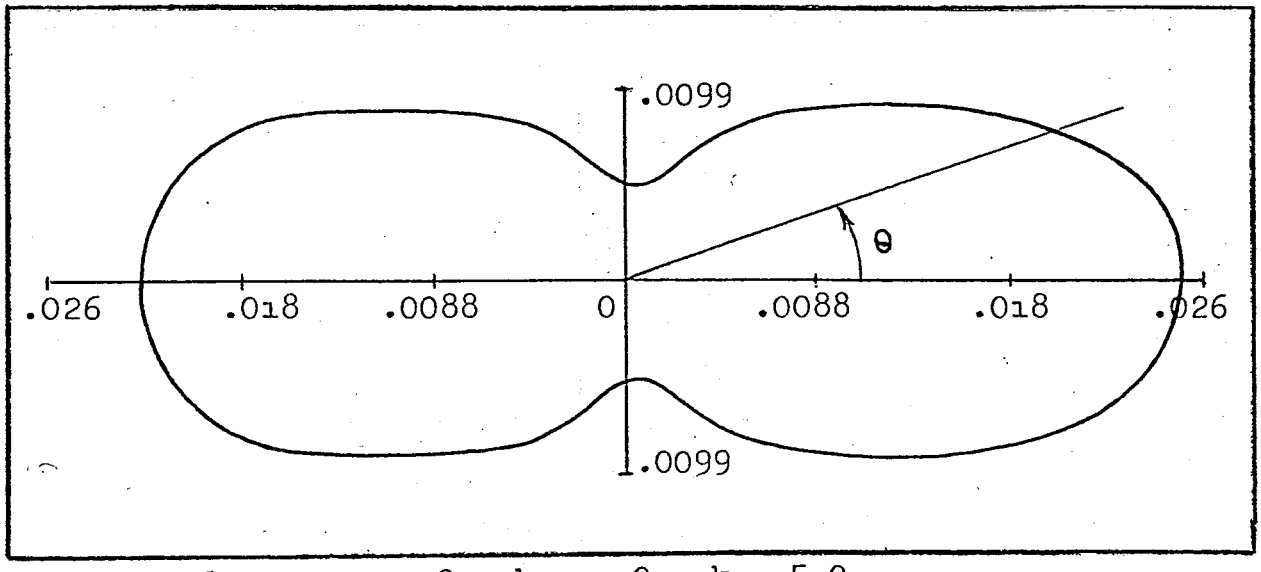

Fig. 11-d a = 1.0, b = 1.0, k = 5.0

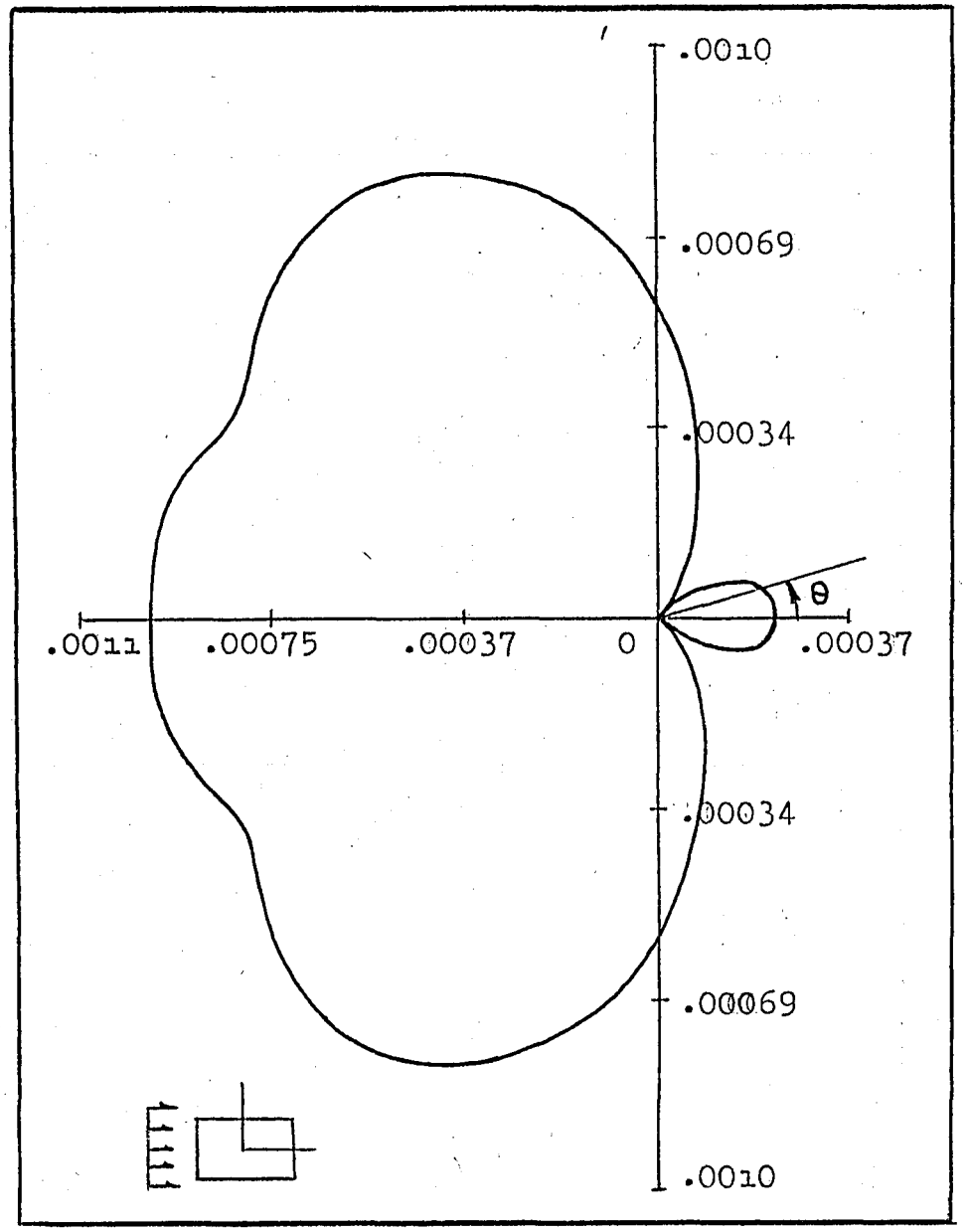

Fig. 11-e a = 1.0, b = 2.0, k = 0.1

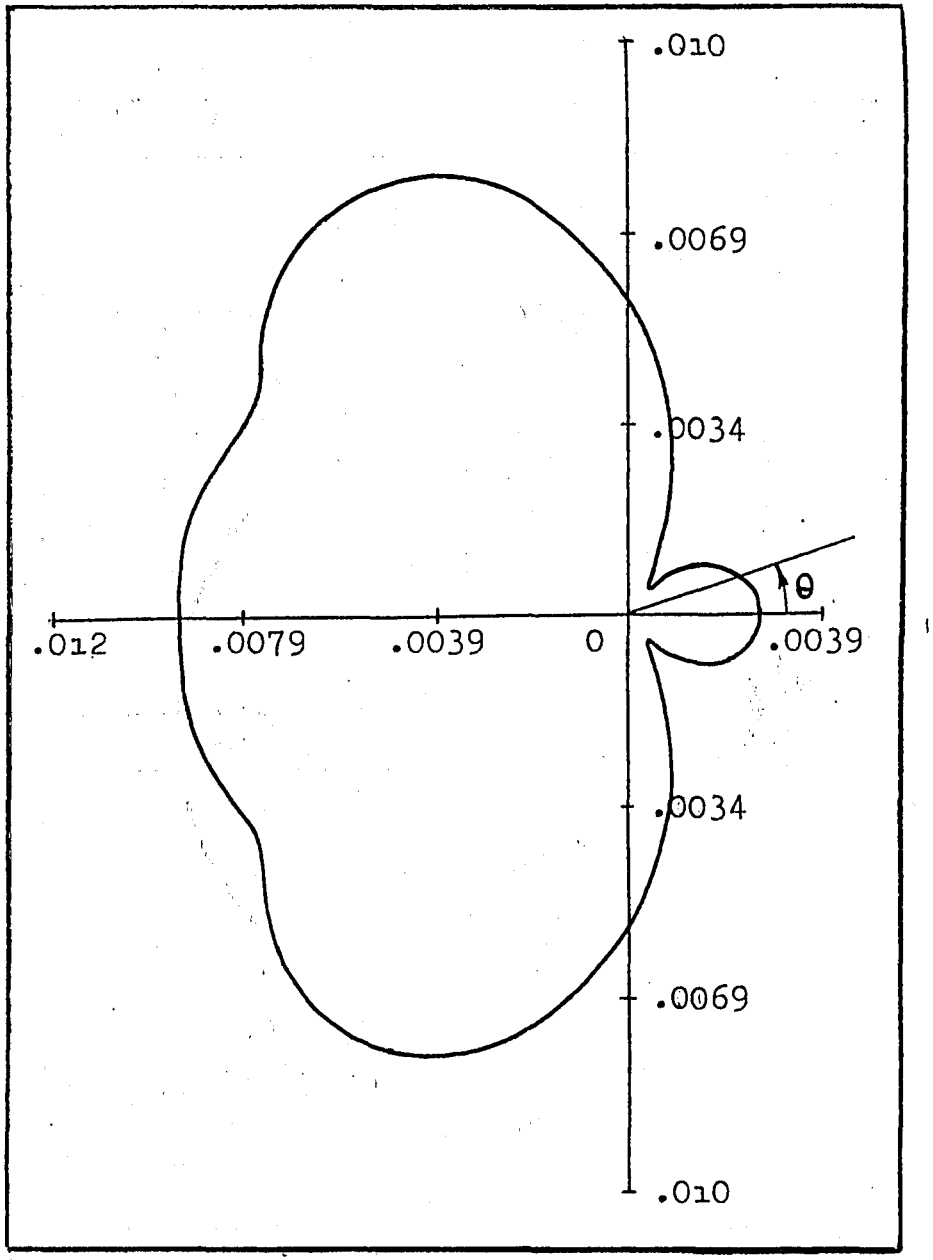

Fig. 11-f a = 1.0, b = 2.0, k = 0.5

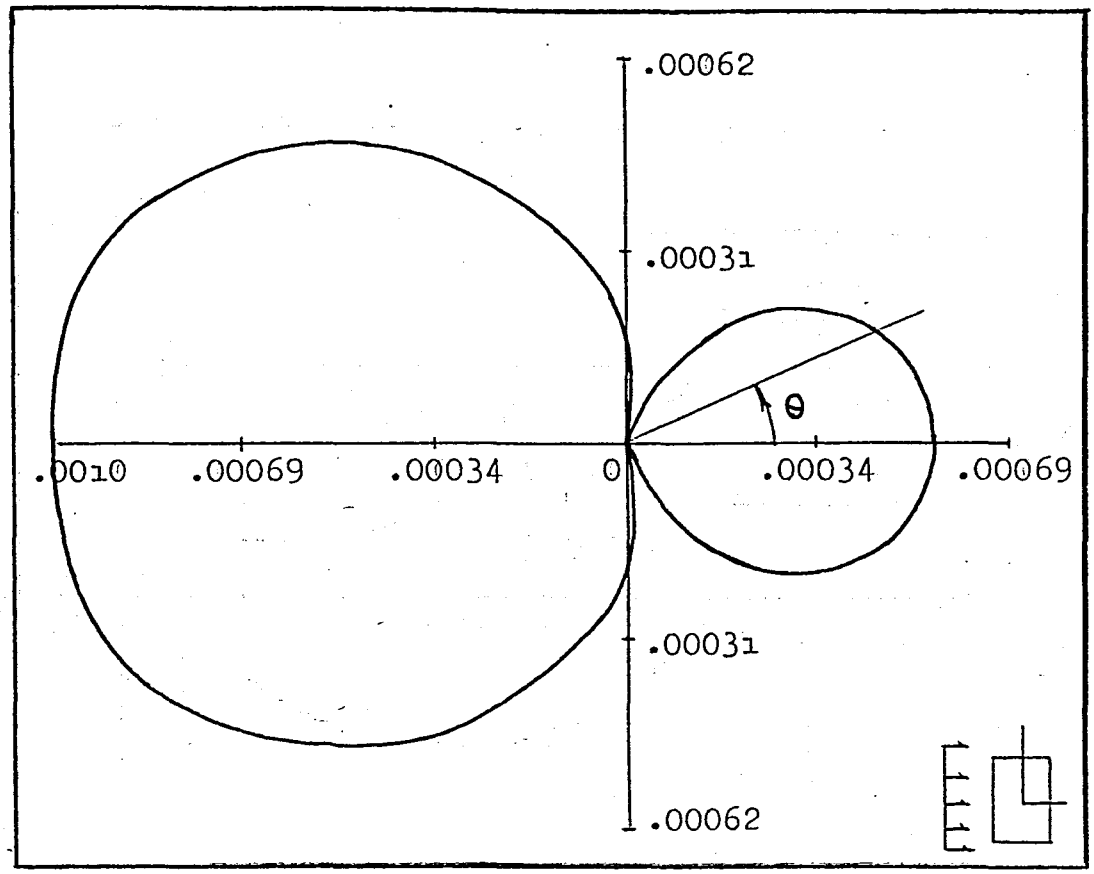

Fig. 11-g a = 2.0, b = 1.0, k = 0.1

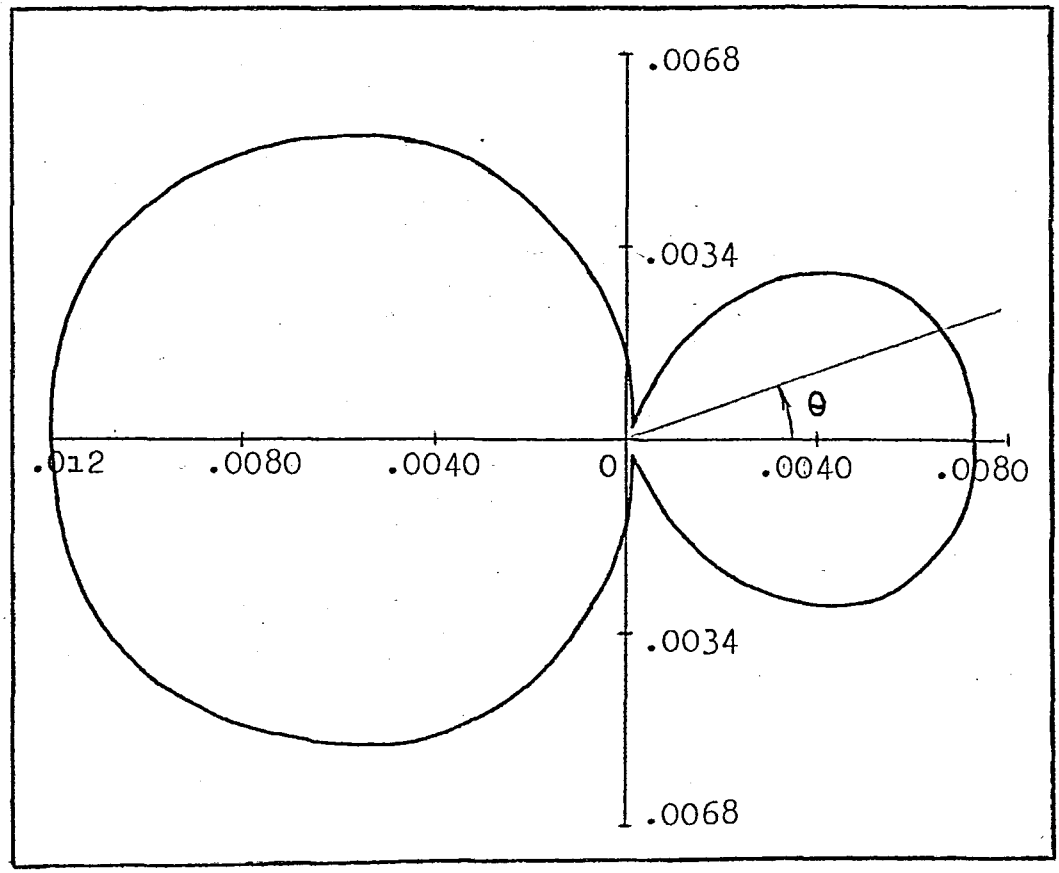

Fig. 11-h a = 2.0, b = 1.0, k = 0.5

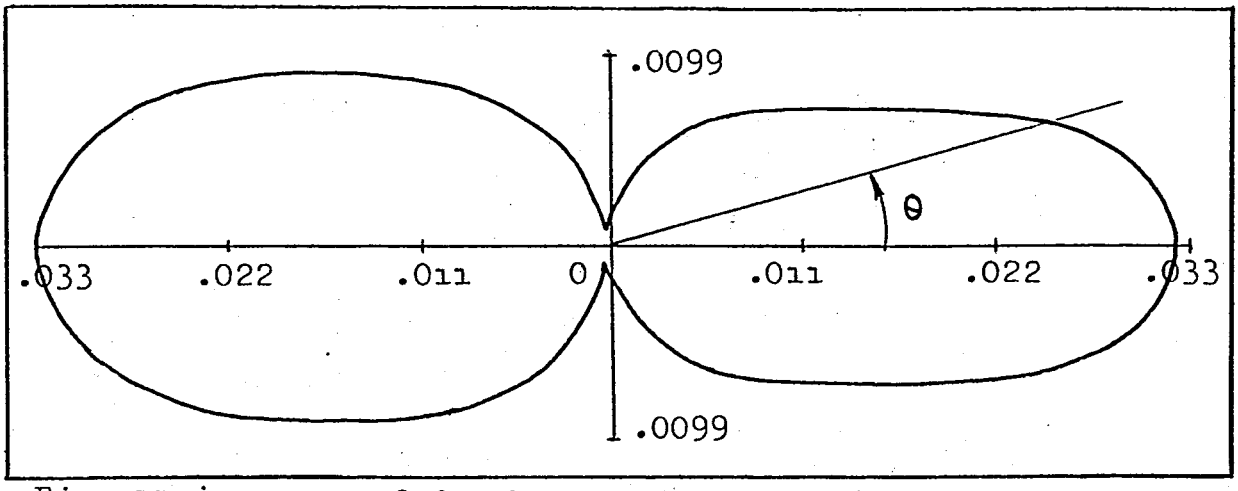

Fig. 11-i $a = 2.0, \quad b = 1.0, \quad k = 5.0$

APPENDIX A

Evaluation of $\lim\limits_{\underline{r}\to\underline{r}'} \dfrac{\partial G(\underline{r},\underline{r}')}{\partial n'}$

For generality, express Eq.(3.15) in its three-dimensional analog

$$\iint_A \left[U^{(s)}(\underline{r}') \frac{\partial G(\underline{r},\underline{r}')}{\partial n'} - G(\underline{r},\underline{r}') \frac{\partial U^{(s)}(\underline{r}')}{\partial n'} \right] dA' = U^{(s)}(\underline{r}), \quad \underline{r} \text{ in } V . \tag{A.1}$$

where G is now $\dfrac{e^{ik|\underline{r}-\underline{r}'|}}{4\pi|\underline{r}-\underline{r}'|}$.

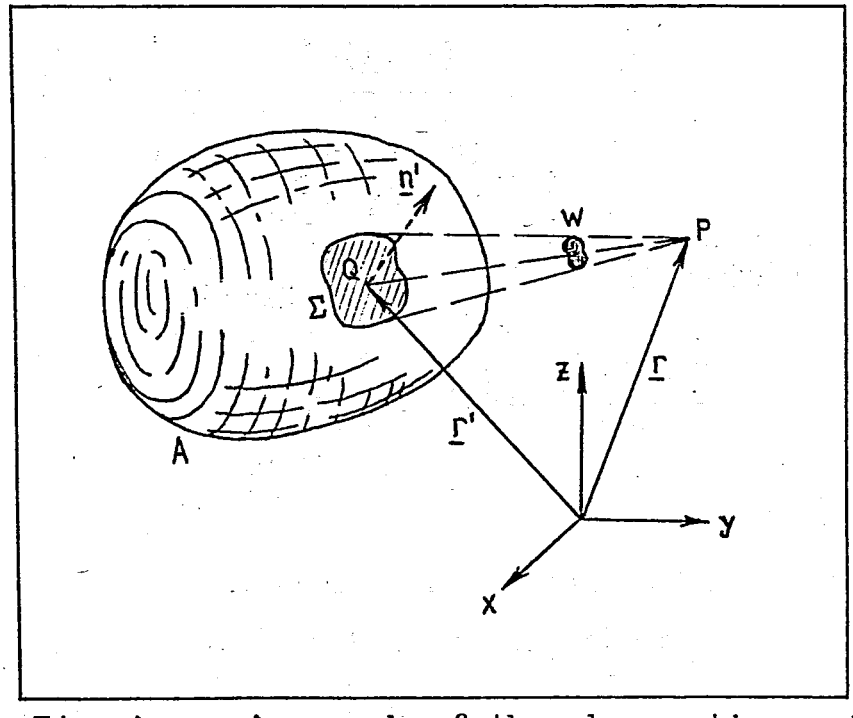

Fig. A-1 Approach of the observation point $P(\underline{r})$ to the source point $Q(\underline{r}')$ on the surface of a scatterer with volume V_A and bounding surface A

Consider now the limit of the leading term on the left-hand side of Eq.(A.1)

$$\lim_{\underline{r}\to\underline{r}'_+} \iint_A U^{(s)}(\underline{r}') \frac{\partial G(\underline{r},\underline{r}')}{\partial n'} dA'$$

where $\underline{r}'_+$ indicates that the limit is approached from the positive side of the normal $\underline{n}'$ (Fig.A-1). Since $\partial G(\underline{r},\underline{r}')/\partial n'$ is singular at $\underline{r} = \underline{r}'$, we exclude the source point from the surface integral by encircling it with a small area Σ. In the neighborhood of $Q(\underline{r}')$, the Green's function for the wave equation can be approximated as

$$\lim_{\underline{r}\to\underline{r}'_+} G(\underline{r},\underline{r}') = \lim_{\underline{r}\to\underline{r}'_+} \frac{e^{ik|\underline{r}-\underline{r}'|}}{4\pi|\underline{r}-\underline{r}'|} \doteq \frac{1}{4\pi|\underline{r}-\underline{r}'|} .$$

Hence,

$$\lim_{\underline{r}\to\underline{r}'_+} \iint_A U^{(s)}(\underline{r}') \frac{\partial G(\underline{r},\underline{r}')}{\partial n'} dA' =$$

$$\frac{1}{4\pi} \lim_{\underline{r}\to\underline{r}'_+} \iint_\Sigma U^{(s)}(\underline{r}') \frac{\partial}{\partial n'} \frac{dA'}{|\underline{r}-\underline{r}'|} +$$

$$\lim_{\underline{r}\to\underline{r}'_+} \iint_{A-\Sigma} U^{(s)}(\underline{r}') \frac{\partial G(\underline{r},\underline{r}')}{\partial n'} dA' .$$

The limit of the second term on the right can be evaluated directly because $\partial G/\partial n'$ is continuous at $A-\Sigma$. For the first term, one notes that

$$\frac{\partial}{\partial n'} \frac{1}{|\underline{r}-\underline{r}'|} dA' = \frac{\underline{n}'\cdot(\underline{r} - \underline{r}')}{|\underline{r} - \underline{r}'|^3} dA' = dw(\underline{r},\underline{r}')$$

where dw is the solid angle subtended by the surface dA'. With a smooth surface at $\underline{r}'$, we then obtain

$$\lim_{\underline{r}\to\underline{r}'_+} \iint_{\Sigma} U^{(s)}(\underline{r}') \frac{\partial}{\partial n'} \frac{1}{|\underline{r}-\underline{r}'|} dA' = U^{(s)}(\underline{r}') \lim_{\underline{r}\to\underline{r}'_+} \iint_{\Sigma} dw$$

$$2\pi U^{(s)}(\underline{r}') .$$

The final answer is

$$\lim_{\underline{r}\to\underline{r}'_+} \iint_{A} U^{(s)}(\underline{r}') \frac{\partial G(\underline{r},\underline{r}')}{\partial n'} dA' = \frac{1}{2} U^{(s)}(\underline{r}') + \text{PV.} \iint_{A} U^{(s)}(\underline{r}') \frac{\partial G(\underline{r},\underline{r}')}{\partial n'} \tag{A.2}$$

where PV. designates the value of the integral as defined by

$$\text{PV.} \iint_{A} F(x,y)\,dx\,dy = \lim_{\Sigma\to 0} \iint_{A-\Sigma} F(x,y)\,dx\,dy .$$

In view of Eq.(A.2), Eq.(A.1) may be expressed as

$$\frac{1}{2} U^{(s)}(\underline{r}') = \iint_{A} \left[U^{(s)}(\underline{r}') \frac{\partial G(\underline{r},\underline{r}')}{\partial n'} - G(\underline{r},\underline{r}') \frac{\partial U^{(s)}(\underline{r}')}{\partial n'} \right] dA'.$$

With $G(\underline{r},\underline{r}') = \frac{i}{4} H_0^{(1)}(k|\underline{r} - \underline{r}'|)$, one obtains Eq.(3.16).

APPENDIX B

4-POINT GAUSSIAN INTEGRATION FORMULA

$$\int_{-1}^{1} y(x)\ dx \simeq \sum_{i=1}^{4} w_i y(x_i) \tag{B.1}$$

where

x_i	w_i
0.86113631	0.34785485
- 0.86113631	0.34785485
0.33998104	0.65214515
- 0.33998104	0.65214515

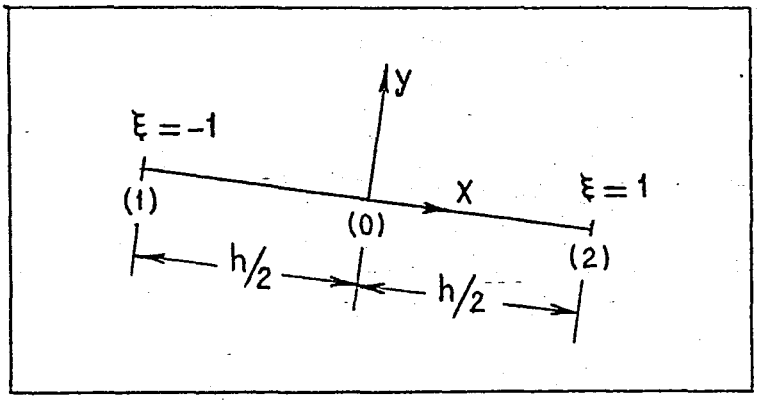

Transforming the coordinates from x-y to the dimensionless coordinate ξ ,

$$x = \xi \frac{h}{2} \quad \text{,and}$$

$$\int_{(1)}^{(2)} y(x)\ dx = \int_{-1}^{1} y(\xi \frac{h}{2})\ d\xi \tag{B.2}$$

where () that the number in parantheses corresponds to the point number,not the distance.Using Eq.(B.1),Eq.(B.2) may be approximated as

$$y(\xi \frac{h}{2})\, d\xi \simeq \sum_{i=1}^{4} w_i y(\xi \frac{h}{2})$$

$$\simeq w_1 y(0.86113631 \frac{h}{2}) + w_2 y(-0.86113631 \frac{h}{2}) +$$

$$w_3 y(0.33998104 \frac{h}{2}) + w_4 y(-0.33998104 \frac{h}{2}) \ .$$

Thus, on the interval (1)-(2), integration points are determined as shown in the figure below.

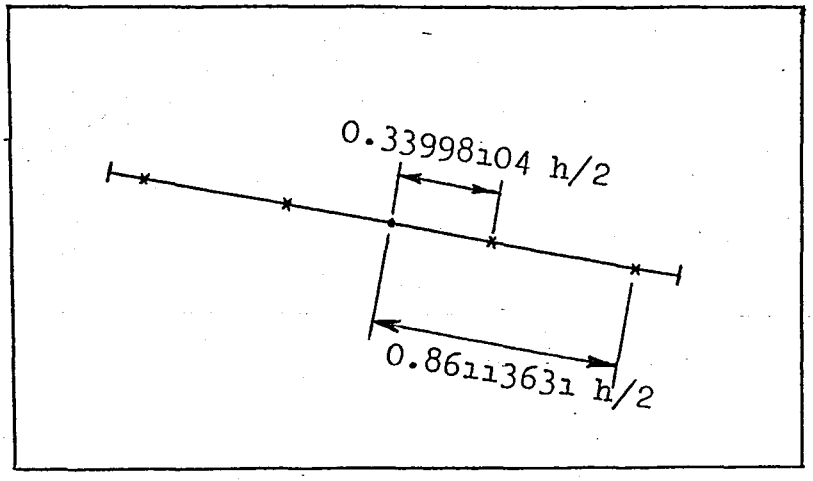

APPENDIX C

Computation of $\dfrac{\partial \hat{r}}{\partial n'}$

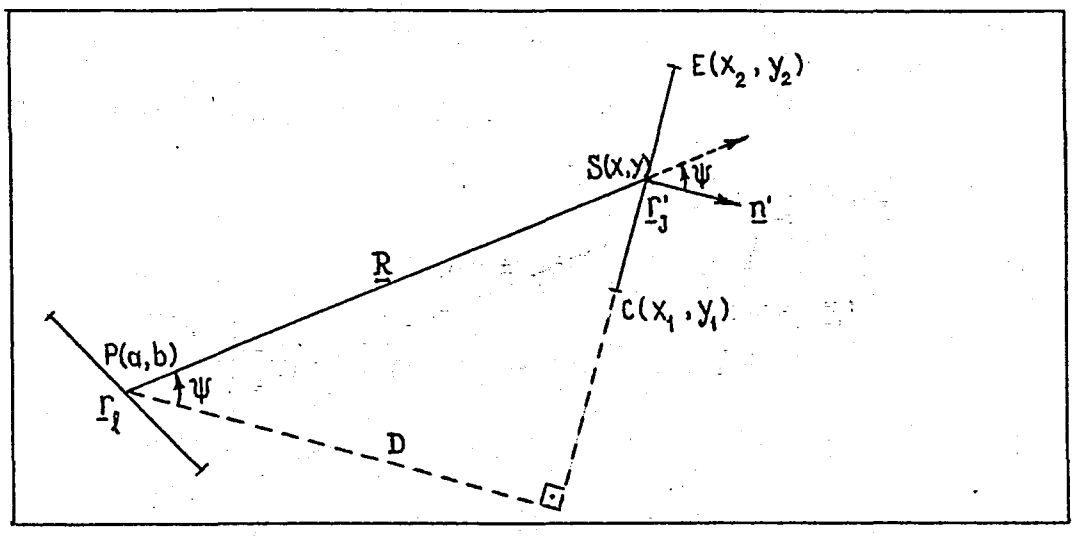

Fig. C-1

$$\frac{\partial R}{\partial n'} = \underline{n}' \cdot \nabla R \,, \qquad \text{where} \quad R = |\underline{R}|$$

Since $\underline{r}_\ell$ and $\underline{r}_j$ are the position vectors $a\underline{e}_1 + b\underline{e}_2$ and $x\underline{e}_1 + y\underline{e}_2$ of P and S respectively (Fig.C-1), then

$$\underline{R} = \underline{r}_j - \underline{r}_\ell = (x-a)\underline{e}_1 + (y-b)\underline{e}_2$$

so that

$$R = |\underline{R}| = \sqrt{(x-a)^2 + (y-b)^2} \quad .$$

Then $$\nabla R = \nabla\left[\sqrt{(x-a)^2 + (y-b)^2}\right]$$

$$= \frac{(x-a)\underline{e}_1 + (y-b)\underline{e}_2}{\sqrt{(x-a)^2 + (y-b)^2}} = \frac{\underline{R}}{|\underline{R}|} = \frac{\underline{R}}{R}$$

is a unit vector in the direction of $\underline{R}$.

Hence,

$$\frac{\partial R}{\partial \underline{n}'} = \underline{n}' \cdot \nabla R = \underline{n}' \cdot \frac{\underline{R}}{R} = \frac{|\underline{R}|\,|\underline{n}'| \cos\psi}{R}$$

$$= \frac{R \cdot 1 \cdot \cos}{R} = \cos\psi \qquad (C.1)$$

but also $\cos\psi = \frac{D}{R}$, where D is the distance from the line CE to the point P.(Fig.C-1)

Let C and E respectively have the coordinates (x_1, y_1) and (x_2, y_2). Then the equation of the line CE is given by

$$y = mx + \left(y_1 - mx_1\right) = mx + d \quad .$$

From analytic geometry, the distance from point (x_o, y_o) to line $Ax + By + D = 0$ is given by

$$\frac{Ax_o + By_o + D}{\pm\sqrt{A^2 + B^2}} \quad .$$

Thus, from P(a,b) to CE, defined by $y = mx + d$ $(mx - y + d = 0)$, the distance D is

$$D = \frac{ma - b + d}{\pm\sqrt{m^2 + 1}} = \frac{ma - b + y_1 - mx_1}{\pm\sqrt{m^2 + 1}} \quad .$$

Since x_1 and y_1 are known through a knowledge of the coordinates of the interval points, D and hence $\cos\psi$ are completely determined.

APPENDIX D

Evaluation of

$$\frac{i}{4}\left(\frac{\partial U'^{(t)}}{\partial n'}\right)_J \int_{\Delta_J} \left[J_o(k\hat{r}) + iY_o(k\hat{r})\right] ds' \qquad \text{when } J = \ell .$$

Since $J_o(k\hat{r}) \rightarrow 1$ as $\hat{r} \rightarrow 0$, the real part of $H_o(k\hat{r})$ causes no difficulty. For the $Y_o(k\hat{r})$ part, using the series representation

$$Y_o(z) = \frac{2}{\pi}\left[\gamma + \ln\frac{z}{2}\right] J_o(z) - \frac{\pi}{2}\sum_{m=1}^{\infty} \frac{(-1)^m (z/2)^{2m}}{(m!)^2}\left(1 + \frac{1}{2} + \cdots \frac{1}{m}\right)$$

we see that the predominant contribution comes from the first term. Therefore the problem reduces to the evaluation of

$$\left(\frac{\partial U'^{(t)}}{\partial n'}\right)_J \frac{i}{4}\int_{\Delta_J}\left\{1 + i\frac{2}{\pi}\left[\gamma + \ln\frac{k\hat{r}}{2}\right]\right\} ds'$$

which can be expressed as

$$\left(\frac{\partial U'^{(t)}}{\partial n'}\right)_\ell \frac{i}{4}\int_{\Delta_\ell}\left\{1 + i\frac{2}{\pi}\left[\gamma + \ln\frac{kr}{2}\right]\right\} ds'$$

where r is measured from the point ℓ .

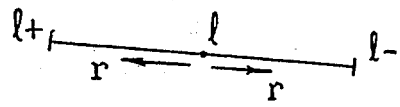

We now use the ξ coordinate (Fig. D-1, below) and have

$$\frac{i}{4}\int_{(1)}^{(2)}\left\{1 + i\frac{2}{\pi}\left[\gamma + \ln\frac{kr}{2}\right]\right\} ds' = \frac{i}{4}\int_{(1)}^{(2)}\left\{1 + i\frac{2}{\pi}\left[\gamma + \ln\frac{kr}{2}\right]\right\} dr$$

where () indicates that the number between them corresponds to the point number not the distance.

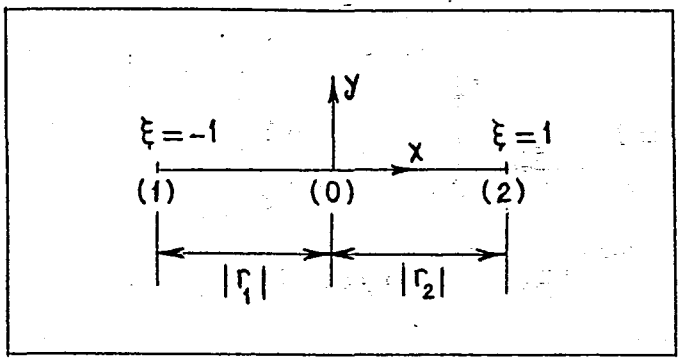

Fig. D-1 ξ coordinates

Transforming coordinates and noting $r = \xi|r_1|$, where $|r_1| = |r_2| = \frac{h_\ell}{2}$, one obtains

$$\frac{i}{4}\int_{(1)}^{(2)} \left\{1 + i\frac{2}{\pi}\left[\gamma + \ln\frac{kr}{2}\right]\right\} dr = \frac{i}{4}2\int_{(0)}^{(2)} \left\{1 + i\frac{2}{\pi}\left[\gamma + \ln\frac{kr}{2}\right]\right\} dr$$

$$= \frac{i}{2}\int_0^1 \left[1 + i\frac{2}{\pi}\gamma + i\frac{2}{\pi}\ln\frac{k(h_\ell/2)\xi}{2}\right]\frac{h_\ell}{2}\,d\xi$$

$$= \frac{i}{2}\frac{h_\ell}{2} - \frac{1}{\pi}\left[\ln\frac{k(h_\ell/2)}{2} - 0.4228\right]\frac{h_\ell}{2}$$

Thus, when $J = \ell$

$$\frac{i}{4}\left(\frac{\partial U'^{(t)}}{\partial n'}\right)_J \int_{\Delta_J} \left[J_o(k\hat{r}_{J\ell}) + iY_o(k\hat{r}_{J\ell})\right] ds'$$

may be approximated as

$$\left(\frac{\partial U'^{(t)}}{\partial n'}\right)_\ell \left\{-\frac{1}{\pi}\left[\ln\frac{k(h_\ell/2)}{2} - 0.4228\right]\frac{h_\ell}{2} + \frac{i}{2}\frac{h_\ell}{2}\right\} .$$

A similar procedure is also given in [4] .

ACKNOWLEDGMENTS

I would like to thank Dr. Ahmet Ceranoğlu, Prof. Dr. Akın Tezel, Doç. Dr. Başar Civelek and Prof. Dr. Atilla Aşkar for their sincere cooperation and excellent support throughout this work.

REFERENCES

I. Pao,Y.-H.,and Mow,C.C.,"Diffraction of Elastic Waves and Dynamic Stress Concentrations",Crane Russak, New-York,I973

2. Brebbia,C.A.,"The Boundary Element Method for Engineers",Pentech Press,I978

3. Jaswon,M.A.,and Symm,G.T.,"Integral Equation Methods in Potential Theory and Elastostatics",Academic Press, New-York,I977

4. Banaugh,R.P.,and Goldsmith,W.,"Diffraction of Steady Acoustic Waves by Surfaces of Arbitrary Shape", J.Acoustical Soc. Amer.,Vol.35,I963,p.I590

5. Chu,L.L.,Çakmak,A.S.,and Aşkar,A.,"Born Approximation for Wave Scattering in Elastodynamics",ASME paper,I980

6. Chu,L.L.,"An Approximate Method for Scattering in Elastodynamics:the Born Approximation",Ph.D. thesis, Dept. of CE,Princeton University,I980

7. Eringen,A.C.,and Şuhubi,E.S.,"Elastodynamics II:Linear Theory",Academic Press,New-York,I975

8. Morse,P.M.,and Feshbach,H.,"Methods of Theoretical Physics",McGraw-Hill,New-York,I953

9. Pao,Y.-H.,and Varatharajulu,V.,"Huygen's Principles, Radiation Conditions and Integral Formulas for the Scattering of Elastic Waves",J.Acoustical Soc. Amer., Vol.59,I976,p.I36I